

Doctoral thesis / Dissertation

for the doctoral degree / *zur Erlangung des Doktorgrads*

Doctor rerum naturalium (Dr. rer. nat.)

Synthesis, solubility and optical activity of chiral poly(2,4-
disubstituted-2-oxazoline)s

*Synthese, Löslichkeit und optische Aktivität von chiralen Poly(2,4-
disubstituierten-2-oxazolin)en*



Submitted by / *Vorgelegt von*

M.Sc. Mengshi Yang

from / *aus*

Zhejiang, China

Würzburg: 2023

Submitted on / *Eingereicht am*:

.....

Stamp / *Stempel* Graduate School

Members of thesis committee / *Mitglieder des Promotionskomitees*

Chairperson / *Vorsitz*:

.....

1. Reviewer and Examiner / *1. Gutachter und Prüfer*: Robert Luxenhofer

2. Reviewer and Examiner / *2. Gutachter und Prüfer*: Paul Dalton

3. Examiner / *3. Prüfer*: Dirk G. Kurth

Additional Examiners / *Weitere Prüfer*:

.....

.....

.....

Day of thesis defense / *Tag des Promotionskolloquiums*:

.....

Better go home and weave a net than to stand by the pond longing for fish. (Chinese idiom)

The present work was carried out from October 2017 to May 2023 at the Chair for Chemical Technology of Materials Synthesis at the Julius-Maximilians-Universität of Würzburg (JMU) under the supervision of Prof. Dr. Robert Luxenhofer.

Acknowledgement

At this point, I would like to thank all those who have helped me and encouraged me to complete this work.

I would like to express sincere appreciation to Prof. Dr. Robert Luxenhofer for the opportunity to study in his lab, the guidance during the research process, and the encouragement when writing this thesis. I also thank the other two advisors of my dissertation committee, Prof. Dr. Paul Dalton and Prof. Dr. Dirk G. Kurth, for attending my annual doctoral student meeting and giving valuable insights and suggestions.

I would also like to thank Dr. Stephan Schröder-Köhne, the head of office, University of Würzburg Graduate Schools, for caring about my study and helping me advance the development of my thesis. I am grateful to all my colleagues at Functional Polymer Materials Group for the friendly atmosphere. Among them especially, Malik Salman Haider, Chen Hu, Stefan Forster, Jochen Löblein shared experimental experiences and solved experimental problems with me. Guntram Schwarz, technician Christian May and secretary Sandra Stockman were very helpful in accessing the equipment and processing the necessary information.

I thank the China Scholarship Council for the four years of financial support, and also thank the DAAD STIBET scholarship offered by the German Academic Exchange Service (DAAD) during my thesis writing.

I thank my roommates and my friends, Meiqi Ding, Chunchu Deng and Kunkun Li, whose kind, patient and accompany were extremely helpful during times of stress and uncertainty.

Finally, I thank my mother and father for their understanding and support.

List of Publications

“Synthesis and investigation of chiral poly(2,4-disubstituted-2-oxazoline) based triblock copolymers, their self-assembly and formulation with chiral and achiral drugs”

Yang, M.; Haider, M; Forster, S; Hu, C.; Luxenhofer, R.

Macromolecules **2022**, 55 (14), 6176-6190.

“Development of a 3D printable and highly stretchable ternary organic-inorganic nanocomposite hydrogel”

Hu, C.; Haider, M.; Hahn, L.; Yang, M.; Luxenhofer, R.

Journal of Materials Chemistry B **2021**, 9, 4535-4545.

“Improving printability of a thermoresponsive hydrogel biomaterial ink by nanoclay addition”

Hu, C.; Hahn, L.; Yang, M.; Altmann, A.; Stahlhut, P.; Groll, J.; Luxenhofer, R.

Journal of Materials Science **2021**, 56 (1), 691-705.

“Tuning the thermogelation and rheology of poly (2-oxazoline)/poly (2-oxazine) s based thermosensitive hydrogels for 3D bioprinting”

Haider, M. S.; Ahmad, T.; Yang, M.; Hu, C.; Hahn, L.; Stahlhut, P.; Groll, J.; Luxenhofer, R.

Gels **2021**, 7 (3), 78.

Contents

Abbreviations and Symbols.....	III
1 Introduction	1
2 State of Knowledge	3
2.1 Drug Delivery	3
2.1.1 Applications of polymer in drug delivery	3
2.1.2 Chiral drug delivery system	6
2.1.3 Summary	7
2.2 Poly(2-oxazoline)s.....	8
2.2.1 2-Oxazolines	8
2.2.2 Living cationic ring-opening polymerization of 2-oxazolines.....	10
2.2.3 Biocompatibility of poly(2-oxazoline)s	11
2.2.4 Chiral poly(2-oxazoline)s.....	14
2.2.5 Summary	16
3 Motivation	17
4 Results and Discussion	19
4.1 Synthesis of chiral/racemic poly(2,4-disubstituted-2-oxazoline) homopolymers	19
4.1.1 Synthesis of chiral/racemic 2-oxazolines monomers.....	19
4.1.2 Synthesis of chiral/racemic homopolymers	22
4.1.3 Conclusion	28
4.2 Physicochemical properties of homopolymers	29
4.2.1 Thermal properties of homopolymers.....	29
4.2.2 X-ray diffraction of homopolymers	33
4.2.3 Optical activity of homopolymers.....	35
4.2.4 Conclusion	36
4.3 Synthesis and characterization of chiral/racemic triblock copolymers	37
4.3.1 Synthesis of pMeOx- <i>block</i> -pEtEtOx- <i>block</i> -pMeOx and pMeOx- <i>block</i> -pPrMeOx- <i>block</i> -pMeOx.....	37
4.3.2 Thermal properties of triblock copolymers.....	44
4.3.3 X-ray diffraction of triblock copolymers	47
4.3.4 Optical activity of triblock copolymers	48
4.3.5 Conclusion	49

4.4	Applicability of chiral/racemic triblock copolymers based micelles as a drug delivery system.....	51
4.4.1	Fluorescence spectroscopy-critical micelle concentration	51
4.4.2	Drug formulation	52
4.4.3	Dynamic light scattering.....	60
4.4.4	Long-term stability studies	66
4.4.5	Conclusion	71
5	Summary	73
6	Zusammenfassung.....	79
7	Experimental	85
7.1	Reagents and solvents	85
7.2	Equipment & methods of measurement	86
7.2.1	Equipment.....	86
7.2.2	Methods of measurement.....	89
7.3	Methods	91
7.3.1	Monomer synthesis, general synthetic procedure, GSP 1	91
7.3.2	Polymer synthesis, LCROP of 2-oxazolines	93
7.3.2.1	Homopolymers, general synthetic procedure, GSP 2	93
7.3.2.2	Triblock copolymer, general synthetic procedure, GSP 3	102
	Bibliography.....	113

Abbreviations and Symbols

Abbreviations

ACN	acetonitrile
Ar	Argon
Boc	tert-butyloxycarbonyl
BocPip	N-tert-butyloxycarbonylpiperazine
bp	boiling point
CMC	critical micelle concentration
CP	cloud point
CUR	curcumin
DLS	dynamic light scattering
DNA	deoxyribonucleic acid
DP	degree of polymerization
DSC	dynamic scanning calorimetry
FDA	U.S. Food and Drug Administration
GPC	gel permeation chromatography
HFIP	hexafluoroisopropanol
IR	infrared
IBU	ibuprofen
LC	loading capacity
LE	loading efficiency
LCROP	living cationic ring opening polymerization
MeOTf	methyl trifluoromethylsulfonate, methyltriflat
NMR	nuclear magnetic resonance
PBS	phosphate-buffered saline
PEG	poly(ethylene glycol)
pEtOx	poly(2-ethyl-2-oxazoline)
PLA	poly(lactic acid)
pMeOx	poly(2-methyl-2-oxazoline)

POx	poly(2-oxazoline)
POzi	poly(2-oxazine)
PS	polystyrene
pEtEtOx	poly(2-ethyl-4-ethyl-2-oxazoline)
pPrMeOx	poly(2-propyl-4-methyl-2-oxazoline)
PTX	pacliaxel
rcf	relative centrifugal force
RT	room temperature
SD	standard deviation
SEM	scanning electron microscopy
SEC	size exclusion chromatography
TGA	thermogravimetric Analysis
UV	ultraviolet
XRD	X-ray diffraction

Symbols

a.u.	arbitrary units
°C	degree Celsius
cm	centimeter
δ	chemical shift
d	day
\bar{D}	dispersity ($\bar{D} = M_w/M_n$)
(k)Da	(kilo)Dalton
D_h	hydrodynamic diameter
eq	equivalent
(k)g	(kilo)gram
h	hour
(k)Hz	(kilo)hertz
K	Kelvin
L	liter
λ	wavelength
m	meter
m	milli, 10^{-3}
M	molar
M	mol/L
μ	micro, 10^{-6}
min	minute
M_n	number-average molar mass
mol	amount of substance: $6.02214076 \times 10^{23}$ (the Avogadro number) substance
M_w	weight-average molar mass
n	nano, 10^{-9}
(k)Pa	(kilo)pascal
ppm	parts per million
rpm	revolutions per minute
s	second
t	time

Abbreviations and Symbols

T	temperature
TFA	trifluoroacetic acid
T _g	glass transition temperature
T _m	melting temperature
v/v	volume ratio
w/w	weight ratio
wt%	weight percent

1 Introduction

Chirality is an important property for many biologically active molecules. Many natural compounds show chirality, including biomacromolecules like polysaccharides, proteins, nucleic acids (DNA and RNA), *etc.* In contrast to natural compounds, their synthetic analogues and many synthetic chiral molecules are obtained as crude products with a mixture of two enantiomers. Enantiomers have the same chemical structure but a different stereostructure and many enantiomers of racemic drugs exhibit differences in biological activities such as pharmacokinetics, pharmacodynamics, toxicology, metabolism *etc.*¹ When one isomer is able to produce the desired therapeutic activities, the other one might be similarly active, inactive, or even produce undesired or toxic effects. For example, thalidomide was marketed as a sedative to relieve pregnancy reactions in Germany in 1957, but it was taken off the market because of the severe teratogenic effects (phocomelia, amelia, urinary tract and heart problem) caused by its S-isomer. Therefore, the chiral resolution is very important and can be achieved, *inter alia*, by chiral chromatography in which a chiral compound is used as the stationary phase.² It is reasonable to think of chiral drug delivery systems that enhance the aqueous solubility of a target chiral drug. Consequently, synthetic stereoactive polymers bearing chiral centers in the repeating units attract increasing attention. Some research of poly(lactide) (PLA)³, poly(glutamic acid)⁴, poly(leucine) based block copolymers⁵ reported the effect of polymer stereoregularity on the physicochemical and functional properties of their self-assembled nanostructures⁶. However, the effect of polymer stereoregular blocks on the properties (such as micellar size, micellar thermodynamic stability, drug loading and cell interaction) are generally not broadly investigated and understood.

Poly(2-oxazoline) (POx) is a synthetic polymer that contains *N*-acyl ethylene imine units in its chemical structure, and is also a member of the so-called pseudo-polypeptides. As more features (*e.g.*, biocompatible and thermoresponsive) are discovered, POx has recently gained increasing interest in a wide range of applications, especially in the biomedical field, *e.g.*, drug (protein or gene) delivery, tissue engineering, 3D bioprinting, *etc.*⁷⁻⁹ A diverse array of POx have been synthesized via cationic ring-opening polymerization (CROP) from the substituted 2-oxazoline monomers that can be tailored relatively easily and synthesized straightforwardly.⁸⁻¹⁴ While the list of 2-substituted 2-oxazolines and their corresponding polymers has been

expanding rapidly, the work on the 4- and 5-substituted monomers and corresponding polymers is quite limited¹⁵. Since Saegusa *et al.* synthesized optically active poly(ethylenimine) derivative by ring-opening polymerization of 4-substituted-2-oxazoline and 4,5-disubstituted-2-oxazoline for the first time,¹⁶⁻¹⁷ the synthesis and properties of more main chain chiral POx were discussed only much later, such as chiral poly(2-R-4-ethyl-2-oxazoline)s (R = ethyl, butyl, octyl, nonyl, undecyl)¹⁸⁻²², chiral poly(2-R-4-methyl-2-oxazoline)s (R = methyl, ethyl)²³, poly(4(S)-4-ethyl-2-phenyl-2-oxazoline)²⁴.

Considering that many drugs are chiral (including hydrophobic ones) and a drug delivery system based on main chain chiral POx has not been studied before, it is interesting to study the effect of chirality on POx based drug formulations. The aim of this work was to improve the understanding of stereoregular polymers as drug carriers in general and to enlarge the toolbox of POx based drug formulations in particular.

2 State of Knowledge

2.1 Drug Delivery

Drug delivery is a technology that presents pharmaceutical compounds to the desired body site for therapeutic purposes²⁵. Many drug delivery systems (DDS) (*e.g.* micelles, liposomes, nanoparticles, hydrogels) have been developed for better control of the drug dose, side effects, drug half-life, drug release, pharmacokinetics, *etc.*²⁶⁻²⁹

2.1.1 Applications of polymer in drug delivery

In many cases, it is difficult to administer free drugs directly through oral, injection, or epidermal methods to achieve the appropriate dosage, effectiveness, and minimize side effects. The most common challenge of many drugs is poor water solubility which hinders their application in clinical treatment. Therefore, DDS (such as micelles, liposomes, nanoparticles and hydrogels) are intensively investigated in order to improve the drug solubility, bioavailability, body distribution, circulation time, *etc.* Various natural and synthetic polymers that meet the most basic requirements (*e.g.*, biocompatible, hemocompatible and non-immunogenic) have the potential to be used in drug delivery systems. Considering biodegradable and bio-reducible, natural polymers such as chitosan, albumin, cyclodextrin, and hyaluronic acid are investigated as a choice for encapsulation and delivery of drugs³⁰⁻³². Because of the high customizability and well-controlled production process, synthetic polymers such as poly(lactic acid) (PLA), poly(glycolic acid) (PGA), poly(ethylene glycol) (PEG), poly(ϵ -caprolactone) (PCL), POx are also often used for drug delivery^{9, 30, 33-35}. Either natural polymers or synthetic polymers exhibit their characteristics, unique advantages and disadvantages. Therefore, the choice of a polymer for DDS depends on the specific requirements of the application and the desired properties of the final product. Combining synthetic polymers with natural polymers is also a common way to modify the morphology, surface charge, surface chemistry, *etc.*, as well as to functionalize the

delivery systems^{31, 36}. There are also inorganic materials which can be used in DDS³⁷⁻³⁸, but this work focuses more on synthetic polymers.

The field of synthetic polymers has experienced rapid growth in the last 40 years, and it plays a leading role in the biomedical field nowadays.^{33, 39-41} Due to the advantage of easy-tailored structure, controlled product quality, and facile functionalization, the DDS based on synthetic polymers can be designed to be biodegradable⁴², porous⁴³, thermoresponsive⁴⁴, pH-responsive or other environmentally responsive⁴⁵. For example, PLA is a hydrophobic aliphatic polyester that was discovered in 1700s for the first time, then was first used for medical application in the repair of mandibular fractures in dogs⁴⁶. PLA has been approved by US Food and Drug Administration (FDA) for clinical use. With the properties of biocompatibility, biodegradability by hydrolysis and enzymatic activity, low levels of immunogenicity and toxicity, PLA and its copolymers (*e.g.*, poly(lactic-co-glycolic acid) (PLGA)) have been used as drug-loaded nanoparticle drug carriers (such as liposomes, dendrimers, and micelles) for a long time⁴⁷. The drug release of PLA microparticles can be varied from a few days to a year by altering the molecular weight, particle size, drug loading, solubility, and diffusion ability⁴⁸. Xu *et al.* prepared an injectable microsphere via the o/w emulsification-solvent evaporation method, using PLA and PLGA as matrix material and bupivacaine as loaded drug⁴⁹. The microsphere structures were figured as a porous core shell structure, consisting of a dense shell of PLA layer and a core of PLA material and form II bupivacaine crystals. After testing the *in vitro* drug release, plasma drug concentration and sciatic nerve blockade post-injection, it was found that the drug release is directly dependent on particle size and drug feed ratios. Compared to PLGA microspheres, which released 80% of the loaded drug within one day, the PLA microspheres with the same drug feed ratios showed prolonged drug release over 5 days.

PEG is the most used non-ionic hydrophilic polymer and also the gold standard for stealth polymers in the field of polymeric DDS³⁴. The process of modifying proteins, drugs and other polymers with PEG is known as PEGylation. The PEGylated protein, drugs, and other polymers are characterized by reduced renal filtration, decreased uptake by the reticuloendothelial system (RES), and diminished enzymatic degradation. A large number of PEGylated DDS have been reported and several of them have been marketed as commercial products. Gref *et al.* first reported the effect of PEG modification on the pharmacokinetics of PLGA microspheres in 1994.⁵⁰ The non-coated microspheres were removed by the liver only 5 minutes after injection, while the PEGylated microspheres were cleaned by the liver 2 h after injection. Several PEG conjugates have entered clinical phase studies, and a few of them have been available in the

market.⁵¹ For example, Pegasys[®] is a conjugate of PEG (40 kDa) and protein interferon- α 2a (IFN- α)⁵² that was granted a marketing authorisation by European Commission in 2002 as an antiviral medicine for the treatment of hepatitis. IFN- α has a short *in vivo* elimination half-life of 3-8 h following intravenous administration⁵², and it only remains in the circulation within 24 h after subcutaneous administration⁵³. After being linked to a branched PEG (40 kDa), the half-life of IFN- α is extended to 65 h (Pegasys[®], intravenous administration).⁵² Although the PEGylation reduce the *in vitro* activity of the native interferon, its ability to prolong the *in vivo* half-life counterbalances this limitation. Pegasys[®] has also been evaluated as adjuvant therapy for melanomas⁵⁴, and in phase II for the treatment of chronic myelogenous leukaemia⁵⁵.

In addition, due to the good designability of polymers, the DDS can be given multiple functions for personalized theranostics. For instance, Li *et al.*⁵⁶ synthesized amino-terminal poly(N-vinylcaprolactam)-based nanogels (PVCL-NH₂ NGs) with core/shell structure using precipitation polymerization approach. The PVCL-NH₂ NGs showed pH/thermal dual-mode responsive behavior in the range of 5-50 °C and pH 3-10, and it was also biodegradable. Based on the PVCL-NH₂ NGs, various functional agents were employed to create a multipurpose nanoplatform in a modular manner. In order to apply them in cell imaging and tracing, the NGs were connected with the fluorescent molecules fluorescein isothiocyanate (FI) via the isothiocyanate-amine coupling reaction. To improve targeting capacity and biocompatibility, the NGs were functionalized with the targeted molecules lactobionic acid (LA) via EDC chemistry to obtain NGs-LA. The NGs-LA with reserved amino groups were bound with Cu(II) through the carbonyl and amino groups, and were further mixed with a Na₂S 9H₂O solution to form CuS@NGs-LA *in situ*. The CuS@NGs-LA had strong near-infrared (NIR) absorption, which can be used in photothermal therapy. With the encapsulation of doxorubicin (DOX), the hybrid CuS@NGs-LA/DOX were used to treat mice bearing tumors and were found to have good antitumor efficacy with the combinational photothermal therapy and chemotherapy.

These examples of applications suggest the importance of synthetic polymers for DDS. Apart from the main material, other factors also influence the drug loading, blood circulation time, biodistribution and excretion, such as particle size, geometric morphology, surface charge and modification, as well as mechanical properties, which should be discussed specifically.

2.1.2 Chiral drug delivery system

Chiral polymer and polymeric particles have attracted attention in recent years mainly because of their potential application in chiral chemistry, such as chiral templates for further synthesizing of chiral mesoporous materials, enantioselective crystallization, enantioseparation⁵⁷. As more chiral polymers are developed, new applications are found for them in the field, *e.g.*, chiral drug delivery systems, enantioselective catalysis.

Recent studies on PLA³, poly(glutamic acid)⁴ and poly(leucine) based block copolymers⁵ have reported the effect of polymer stereoregularity on the physicochemical and functional properties of their self-assembled nanostructures.⁶ For instance, Abyaneh *et al.* synthesized diblock copolymers composed of methoxy poly(ethylene oxide) (mPEG) and PLA with different chirality and investigated the influence of PLA crystallinity on the micelle stability and also evaluated the release profile of a model hydrophobic drug nimodipine at different drug loading levels³. The diblock copolymer mPEG-PLA with stereo-regular PLA showed crystallization of the PLA block, while the mPEG-PLA made from meso-lactide and L-/D-lactid 50/50 (w/w) ratio did not. Furthermore, the mPEG-PLA with crystalline cores formed kinetically more stable micelles than those without. The polymeric micelles with crystalline cores showed more rapid drug release at high drug loading, while at low drug loading level, the drug release was independent of the stereochemistry of the core.

Not satisfied with using achiral model drugs, Feng *et al.* investigated micelles formed by methoxy-poly(ethylene glycol)-b-poly(L-lactide) (mPEG-*b*-PLLA, L-micelles) and mPEG-*b*-PDLA (D-micelles) to solubilize the glycosylated antibiotic nocathiacin I (containing multiple chiral centres) and other chiral compounds (containing D- or L-sugars)⁵⁸. They found that the nocathiacin I loaded D-micelles exhibited better loading efficiency and smaller particle size than that of L-micelles. Also, for other chiral compounds, D- and L-micelles showed a marked difference in particle size, even though the loading efficiency between D- and L-micelles was not significantly different. The difference in stereostructure, either in the polymer or the drug, is not always reflected in the behavior of the formulations. Radwan *et al.* investigated the *in vitro* drug release of R-/S-/RS- flurbiprofen (R-/S-/RS-FL) loaded Poly(D, L-lactide-*co*-glycolide) nanoparticles, finally did not find the significant difference of the initial drug loading and *in vitro* drug release between three formulations⁵⁹. Using more complex hormones insulin as a model drug, Hu *et al.* investigated the influence of stereoregularity degree on the stereo multiblock

copoly(lactide)s (smb-PLAs) ⁶⁰. They found that smb-PLAs with a high stereoregularity degree showed much higher insulin loading efficiency than the atactic PLA.

Apart from the stereoregularity, the rigidity of the chiral chain also has an effect on the polymer properties. Nguyen *et al.* synthesized sets of chiral bottlebrush polymers (CBPs) with different stereochemistry and rigidity, based on unimolecular norbornene-terminated macromonomers (MMs) ⁶¹. The stereoregularity affected the CBPs which had flexible chiral side-chains remarkably in cytotoxicity, cell uptake, blood pharmacokinetics and liver clearance. In contrast, the CBPs with relatively rigid chiral side-chains did not show the obvious difference between isomers. Clearly, the bigger conformational flexibility amplifies the diastereomeric interactions.

Generally speaking, the influence of stereoregular blocks on the properties of polymers has not been broadly investigated and understood. These properties include micellar size, micellar thermodynamic stability, drug loading and release, cell interaction, and more.

2.1.3 Summary

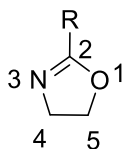
Many natural bio(macro)molecules are already monochiral when they are produced, such as sugars, amino acids and their polymers (proteins, polysaccharides, DNA/RNA). However, it is common for synthetic substances to be produced as racemic mixtures in scientific research and industrial applications. Enantiomers of drugs can exhibit significant differences in their biological activity, therefore studying the separation of therapeutically active enantiomers is very important. Fortunately, chirality is not only commonly seen in nature, but also can be created in synthetic polymers. As mentioned above, the stereostructure of the synthetic polymers can affect the corresponding drug delivery system under certain conditions. Although the application of chiral polymers in drug delivery is just emerging, and many areas are yet to be discovered, it might be logical to think about using chiral drug delivery systems to preferentially interact/solubilize a drug enantiomer of interest.

2.2 Poly(2-oxazoline)s

Poly(2-oxazoline)s (POx) were first reported in 1966^{11, 62-64}, and since then various POx have been obtained via the cationic ring-opening polymerization (CROP) of corresponding 2-alkyl/aryl-2-oxazolines^{8-9, 65}. As the monomers can be tailor-made and synthesized in relatively easy and straightforward ways, diverse POx with different solution, thermal and surface properties can be developed^{8, 15, 66}. Apart from the monomers, the initiators and terminating agents applied in the polymerization can also be used to functionalize POx for subsequent modifications or special applications⁶⁷. Based on this adjustability, POx can also be designed into a variety of different geometry structures, such as linear⁶⁸, branched⁶⁹, cyclic⁷⁰, brush-shaped⁷¹⁻⁷², and star-shaped structures⁷³⁻⁷⁴. As POx have been gradually discovered the properties of biocompatibility, smart-behavior properties (*e.g.*, thermo-, pH-responsivity), antimicrobial, low ionic conductivity, *etc.*, POx are widely investigated in the field of fouling release coating⁷⁵, polymer electrolyte⁷⁶, dipole layers of solar cells⁷⁷, especially in the biomedical area such as drug (or protein, gene) delivery, tissue engineering, 3D bioprinting and biofabrication^{7, 9, 78-79}.

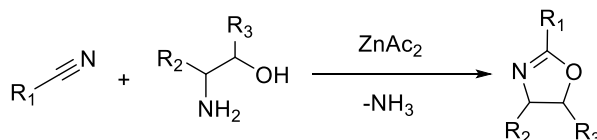
2.2.1 2-Oxazolines

The diversity of 2-oxazolines benefits the wide variety of POx. Some versatile, straightforward and practical methods are commonly used to synthesize 2-oxazolines (**Fig. 2.1**)^{8, 15, 66}, including some 4- and 5-substituted 2-oxazolines^{12, 16, 20, 80-82}. However, due to the reactivity and large steric hindrance of the substituents, and potential racemization during the polymerization, the polymerization of 4- and 5-substituted 2-oxazolines is limited.

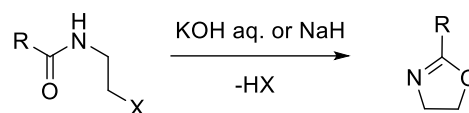


Method 1, ring formation by the reaction of nitriles and aminoalcohols was reported by Witte and Seeliger¹⁰. A moderate Lewis acid such as zinc acetate or cadmium acetate is used as catalyst. Method 2, cyclization of haloamide (Wenker method⁸³) is useful to prepare unsubstituted 2-oxazoline which is accomplished with a strong base (KOH aq.). Later, Franco *et al.*⁸⁴ modified the method with sodium hydride as a base in anhydrous 1-methyl-2-pyrrolidone, and also prepared 2-methyl-2-oxazoline. Method 3, cyclization of hydroxyamides is carried out under mild and neutral conditions, and using triphenylphosphine and diethyl azodicarboxylate as dehydrating agent⁸¹. It can be used to prepare some 2-oxazolines which could not be easily prepared by other methods, such as 2-trifluoromethyl- and 2-trichloromethyloxazolines. Method 4, the reaction of isocyanides and aminoalcohols is only suitable for preparing 2-unsubstituted 2-oxazolines with transition metal catalyst, *e.g.* silver cyanide⁸⁵. Method 5, the reaction of imidates with aminoalcohols can be used to synthesize chiral 2-oxazolines such as L-serine ester hydrochloride¹².⁸⁰ There are also some less common synthesis routes that can be used to synthesize 2-oxazolines with complex structures, *e.g.*, α -deprotonation of 2-methyl-2-oxazoline followed by alkylation⁸⁶⁻⁸⁷.

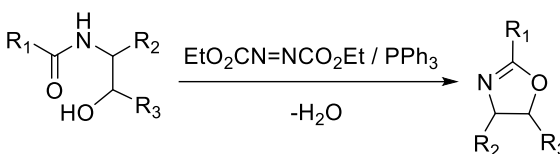
Method 1: Reaction of nitriles with aminoalcohols



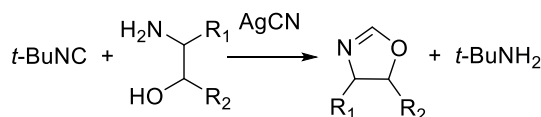
Method 2: Cyclization of haloamides



Method 3: Cyclization of hydroxyamides



Method 4: Reaction of isocyanides with aminoalcohols



Method 5: Reaction of imidates with aminoalcohols

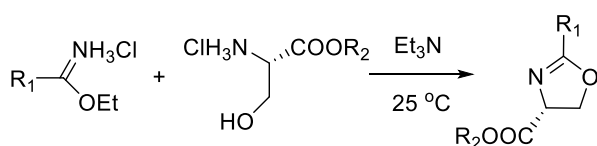


Figure 2.1 Common methods for synthesizing 2-oxazolines

2.2.2 Living cationic ring-opening polymerization of 2-oxazolines

The LCROP of 2-oxazolines was first reported by four independent research groups in 1966^{11, 62-64}. The LCROP mechanism generally consists of initiation, propagation, and termination steps (**Fig. 2.2**)^{8, 88}.

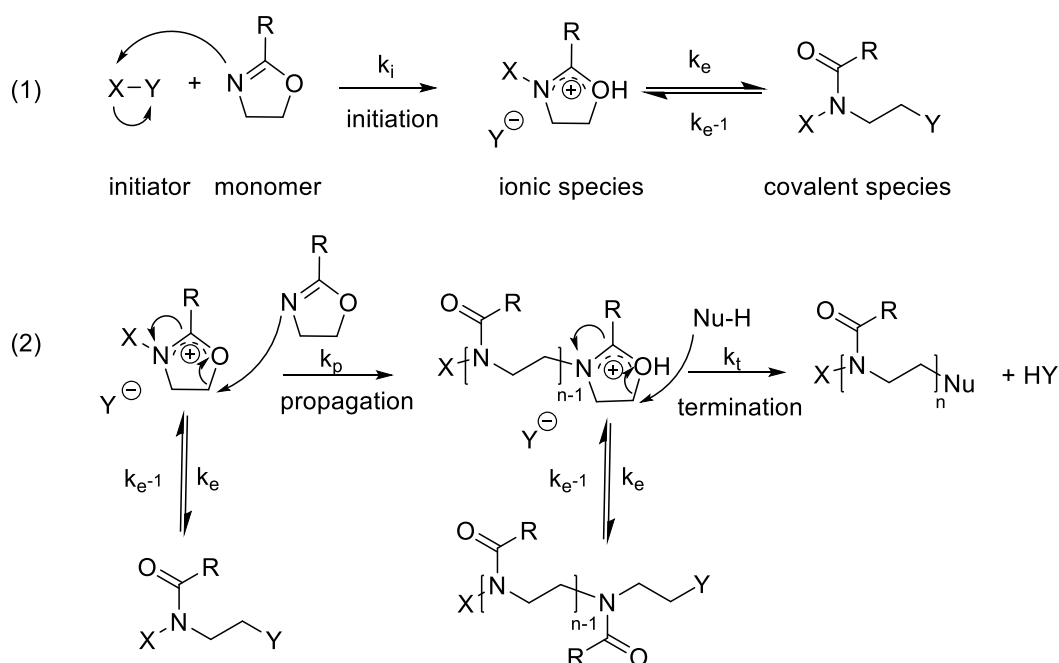


Figure 2.2 The cationic ring-opening polymerization of 2-oxazolines

Commonly used initiators are Lewis acids, strong protic acids and their esters and alkyl halides⁶⁶. In the initiation step, a nucleophilic attack of the nitrogen atom of the 2-oxazoline monomer onto the initiator forms a propagating species. The propagating species are in equilibrium between the oxazolinium cation and its covalent species. This equilibrium can be influenced by the stability (nucleophilicity) of the counter ion from initiator¹⁵. However, because the reactivity of the ionic species is much higher than that of covalent species, the propagation mainly occurs via the ionic species.⁸⁹⁻⁹¹ For example, the initiator methyl trifluoromethanesulfonate (MeOTf) contributes the most stable (least nucleophilic) triflate anion, and the corresponding propagation species are reported to be ionic type for all type of 2-oxazolines.^{15, 92-94} The nitrogen atom of 2-oxazoline attacks the C(5) carbon of the propagating 2-oxazolinium species, leading to the bond cleavage of O(1)-C(5), isomerization of the

oxazolinium ion and chain growth with a living oxazolinium chain-end.⁹²⁻⁹⁴ In an ideal polymerization process each chain-end will keep living growth, but chain transfer reactions such as β -elimination and coupling reactions have been found in practice which influence the degree of polymerization (DP) and dispersity (\mathcal{D})⁹⁵. The termination may occur at the 2- and 5-position of the propagating 2-oxazolinium species⁹⁶⁻⁹⁷, while the termination on the 5-position attracts more attention. Nucleophiles can be used as the terminator, such as water, amines, carboxylates, and thiolates. The polymerization should proceed under an anhydrous and inert gas atmosphere. Extremely pure and dry reagents are very important to prepare POx with narrow molecular weight distributions. Any unexpected nucleophile could terminate the reaction early leading to low DP and wide \mathcal{D} .

2.2.3 Biocompatibility of poly(2-oxazoline)s

PEG is the most frequently-used polymer and the gold standard in the biomaterial field which has many advantages such as cytocompatibility, stealth behavior, good solubility in organic solvents and water, among others³⁴. However, PEG is also reported some drawbacks, *e.g.*, toxicity of impurities³⁴. Recently, it is reported the rise of anti-PEG IgM and IgG in experimental and clinical research with different PEGylated drugs⁹⁸⁻⁹⁹, which is also related to undesired accelerated blood clearance phenomenon and hypersensitivity reactions¹⁰⁰⁻¹⁰¹. The hydrophilic POx, poly(2-methyl-2-oxazoline) (pMeOx) and poly(2-ethyl-2-oxazoline) (pEtOx), are considered as one of the alternative polymers to PEG, which were introduced as food additives at the beginning and found to exhibit stealth/protein repellent effects after being intensively studied^{9, 34, 102-108}. pMeOx is more hydrophilic than pEtOx and PEG, while the conformational rigidity of pEtOx is similar to PEG¹⁰⁹. Therefore, pMeOx and pEtOx are widely used as hydrophilic polymer components, such as in micelles (in combination with other hydrophobic POx¹¹⁰) and polymer nanoparticles¹¹¹, polymer-peptide conjugates,¹¹²⁻¹¹³ polymer-protein conjugates,¹¹⁴ lipopolymers for liposome stabilization,¹⁰³ polymer-drug conjugates,¹¹⁵ as well as antimicrobial polymers¹¹⁶. Apart from the pMeOx and pEtOx, more POx have been developing which have different hydrophobicity (*e.g.*, poly(2-alkyl/aryl -2-oxazoline)s (alkyl: butyl, nonyl¹¹⁰; aryl: phenyl, benzyl¹¹⁷)), thermoresponsive behaviour (*e.g.*, poly(2-n-propyl-2-oxazoline)¹¹⁸, poly(2-isopropyl-2-oxazoline)¹¹⁹), chemical (*e.g.*, functional groups/moieties aldehyde⁸⁶, amine¹²⁰) or structural (*e.g.*, brush-shaped⁷²) functionality. When

they are used in the biological field, biocompatibility must be investigated. The following are some general descriptions of the biocompatibility of POx, while specific POx should be investigated individually.

For both POx and PEG, the cytotoxicity was found to be strongly dependent on the incubation time, polymer concentration, molar masses, and purity of the polymers. The molar mass of PEG used for biomedical applications is commonly above 0.4 kDa, because the PEG below this range could degrade into toxic diacid and hydroxyacid metabolites in the presence of alcohol and aldehyde dehydrogenase in humans ¹²¹. Fischer and co-workers compared the cytotoxicity and hemocompatibility of PEG and pEtOx in the molar masses range of 0.4-200 kDa *in vitro* ¹²². When the incubation time was short (3 h), none of the PEG and pEtOx caused negative effects on cell viability (>70%, L929 mouse fibroblasts), even at a very high concentration of 80 g/L. After 24 h, the PEG remained non-toxic up to 40 g/L. The pEtOx showed moderate cytotoxic effects at 20-40 g/L only after treatment of 12 and 24h, but the high molar mass pEtOx (50 and 200 kDa) remained non-cytotoxic. The cytotoxicity was strongly correlated with the molar mass. The low molar mass PEG (up to 10 kDa) and pEtOx (20 and 40 kDa) affected the cell viability more profoundly than that of high molar mass. In their experiment, no hemolytic activity was observed for PEG and pEtOx at 0.4-200 kDa up to 80 g/L, and also no erythrocyte aggregation was found for PEG. The concentration and molar mass of pEtOx affected the erythrocytes, the erythrocyte aggregation of pEtOx up to 40 kDa and 80 g/L was similar to PEG, while the 40 kDa pEtOx started to result in moderate aggregates at 80 g/L. The same group also investigated the cytotoxicity and hemocompatibility of pMeOx (2-20 kDa) *in vitro* ¹²³. All the pMeOx did not cause the release of hemoglobin, even at a high concentration of 80 g/L. It was also confirmed that the pMeOx was generally highly cytocompatible, except that the low molar mass pMeOx (2 kDa) reduced the cell viability <70% after 3 h and 12 h incubation at 80 g/L. It is worth noting that the maximum dose and molar mass of polymers used in the cytotoxicity and hemocompatibility experiments are far more than the therapeutic dose and required molar mass. In the therapeutic range, PEG, pEtOx and pMeOx were all well tolerated by mouse fibroblasts cells, and also the red blood cells. In contrast to the pEtOx and pMeOx, the poly(2-iso-propenyl-2-oxazoline) (piPrOx) obtained from LCROP was found to be highly cytotoxic for NIH 3T3 mouse fibroblasts (24 h incubation), and should be handled carefully ¹²⁴.

Apart from the toxicity investigation, POx has also been studied with respect to its immunogenicity. The pEtOx and poly[2-(4-aminophenyl)-2-oxazoline-co-2-ethyl-2-oxazoline]

have been found the immunomodulatory effects in activation of mouse lymphoid macrophage line P388.D1 (clone 3124) by Kronek *et al.*¹²⁵⁻¹²⁷ mPEG has been utilized for the immunocamouflage of cells.¹²⁸⁻¹³⁰ Kyliuk-Price *et al.* covalently grafted pEtOx on the surface of red blood cells (RBC) and leukocytes to compare the capability of immunoprotection to that of mPEG¹³¹. The pEtOx showed the capability of mediating immunocamouflage of both RBC and leukocytes similarly to the grafted mPEG. At similar membrane grafting, the mPEG had superior immunocamouflage efficacy to pEtOx, while pEtOx showed improved RBC morphology. pEtOx is still a useful addition for the immunocamouflage of allogeneic cells.

The pharmacokinetic behavior and biodistribution of POx, such as pEtOx and pMeOx, have been investigated very early¹³²⁻¹³³. More recently, Wyffels *et al.* investigated the influence of the molar mass of pEtOx (20-110 kDa) on the pharmacokinetic profile¹³⁴. The polymers were injected *i.v.* into mice with the labeling of ⁸⁹Zr, and detected by the micro positron emission tomography (μ PET) molecular imaging. The pEtOx 20 kDa can be rapidly excreted via renal clearance and had low accumulation in the rest of the body. The 40 kDa was likely to be the cut off molar mass for glomerular filtration of pEtOx, therefore pEtOx 40 kDa had longer blood circulation times than that of 20 kDa. When the molar mass was above 70 kDa, the pEtOx was scavenged by RES, and moderately accumulated in the pancreas, lungs, fat and skin at one-week post-injection. Such research contributed to further designing of POx for regulation of the circulation time, accumulation, and metabolic pathways. Besides, similar to PEGylation which is the process of attaching the PEG chain to molecules and macrostructures, POxylation also attracts more attention as an alternative to PEGylation. The POx has been connected with the liposomes^{103, 135}, nanoparticles¹³⁶⁻¹³⁷, proteins¹³⁸, drugs¹³⁹, and other bioactive molecules¹⁴⁰ to provide stealth properties and regulate their blood circulation^{7, 141-142}.

As many POx are studied for biological application, the degradability also needs to be considered. Although PEG and POx are normally regarded as non-biodegradable, PEG was found to be sensitive to oxidative degradation¹⁴³⁻¹⁴⁴, and also mentioned above, the PEG with 200 Da molar mass could degrade in the presence of alcohol and aldehyde dehydrogenase and results in a clastogenic effect and genotoxic effect¹²¹. In certain circumstances, acidic and basic hydrolysis, and oxidative degradation might also happen on POx. Van Kuringen *et al.* studied the hydrolysis of pEtOx in the presence of digestive enzymes of gastric and intestinal and 5.8 M hydrochloric acid¹⁴⁵. The hydrolysis of pEtOx at 37 °C was negligible. Up to 10% hydrolysis level, the thermal and solution properties were not significantly changed, and no mucosal irritation and cytotoxicity were found. Konradi *et al.* grafted the pMeOx (2-5 kDa) and PEG (4-

8 kDa) onto poly(L-Lysine) (PLL), then compared the stability of pMeOx and PEG in a simple model of oxidative environments (10×10^{-3} M H_2O_2 solution)¹⁴⁶. Up to 7 days' exposure to the oxidative test solution, the PLL-g-PEG monolayers were degraded to below 50% of their initial thickness, while the PLL-g-pMeOx monolayers lost less than 20%. Moreover, the degraded PLL-g-PEG appeared strong protein adsorption when being exposed to full human serum, but the degraded PLL-g-pMeOx did not strongly adsorb proteins. In their research, the pMeOx was more stable in oxidative environments. Pidhatika *et al.* also reported similar results¹⁰⁸. Instead of using plain H_2O_2 solution to mimic the complex situation of reactive oxygen species (ROS) *in vivo*, Luxenhofer and co-workers reported the degradation of PEG, Poly(N-ethylglycine) (POI) and pEtOx (molar masses of 2-11 kDa) after being incubated with the system $\text{H}_2\text{O}_2/\text{Cu(II)}$ at concentration of 50 μM CuSO_4 and 50, 5 and 0.5 mM H_2O_2 , respectively.¹⁴⁷ Under the catalysis of Cu(II), H_2O_2 can be decomposed into more reactive ROS, such as hydroperoxide radical and hydroxyl radical. At defined times, the incubated samples were lyophilized and analyzed with SEC. Interestingly, at the concentration of 0.5 mM H_2O_2 , polymers were degraded to 50% of initial M_w in a range of 10 days (pEtOx and POI) to about 50 days (PEG). The PEG showed to be more stable than pEtOx and the most stable of the three. In addition, the degradation of polymers with higher molar mass was higher than corresponding low molar mass polymers. The degradation of more POx under various conditions (*e.g.*, acidic/alkaline condition, ROS, enzyme) deserves further study.

POx is being rapidly developed as an alternative to PEG in the field of polymer therapeutics. With various composition, POx show more functions that PEG does not have.

2.2.4 Chiral poly(2-oxazoline)s

POx are considered as so-called pseudo-polypeptides because of the similarities in chemical structure to polypeptides. If some chiral carbon atoms can be introduced into the polymer backbone, the structure of POx could be even closer to polypeptides, which are inherently chiral. The chiral POx in the following text specifically refers to the POx with chiral carbon atoms on the main chain.

The proof-of-principle that such chiral POx are accessible was provided by Saegusa *et al.*, who synthesized optically active poly(ethylenimine) derivatives by CROP of 4-disubstituted-

2-oxazoline and 4,5-disubstituted-2-oxazoline for the first time¹⁶⁻¹⁷. Though many chiral 4- and 5-substituted 2-oxazolines have been synthesized^{12, 16, 20, 80-82}, their polymerizations via LCROP are limited due to the reactive substituents, large steric hindrance of the substituents, and potential racemization during the polymerization. For example, Hermes *et al.* synthesized polymers by the CROP of 4(S)-2-propyl-4-methoxycarbonyl-2-oxazoline with dimethyl sulfate as initiator¹⁴⁸. Although the monomer had a rotation of +152°, the polymers obtained under different reaction conditions either had different values of negative rotation or zero optical activity. The racemization during the CROP might be caused by the deprotonation and reprotonation on the C(4) of a growing chain end or the formation of dehydroalanine derivative. Hermes did not mention the difference between those reaction conditions, but Chengpei *et al.* repeated Hermes's experiment using monomer 4(S)-2-methyl-4-methoxycarbonyl-2-oxazoline and got similar results¹⁴⁹. Chengpei reported that the obtained polymer had no optical activity when the reaction temperature was 120 °C, while had negative rotation when the temperature was below 100 °C. Both Hermes and Chengpei got polymers with only low DP (Hermes: 8-10 DP; Chengpei: 10-20 DP) even when the monomers were excessive. Such polymers were not further developed for applications because of the uncontrollable chain length, side reactions, and unstable chirality.

Fortunately, researchers have been able to obtain main chain chiral POx with well-controlled molar mass and narrow molar mass distributions from the polymerization of some other monomers. Schubert, Hoogenboom *et al.* reported the synthesis and properties of chiral poly(2-alkyl-4-ethyl-2-oxazoline)s (alkyl = ethyl, butyl, octyl, nonyl, undecyl)¹⁸⁻²¹, and further discussed the self-assembly of chiral amphiphilic block copolymers composed of a hydrophilic block of pEtOx and a hydrophobic block of poly((R)-2-butyl-4-ethyl-2-oxazoline) (p^RBuEtOx) or racemic p^{RS}BuEtOx²². They found that varying the hydrophobic/hydrophilic ratio in the copolymers could control the type of self-assembled structures from spherical and cylindrical micelles to sheets and vesicles. However, the direct comparison of chiral and racemic polymers with the same composition was not provided in this contribution²².

Some relatively hydrophilic chiral POx have also been studied. Jordan *et al.* investigated the influence of chirality on the lower critical solution temperature (LCST) behavior of water soluble poly(2-alkyl-4-methyl-2-oxazoline)s (alkyl: methyl, ethyl)²³. Introduction of chirality via the alkyl substituents in the main chain of poly(2,4-disubstituted-2-oxazoline)s allows for the formation of secondary structure in aqueous and non-aqueous environments as well as in bulk^{20, 23}. As for the secondary structure of chiral POx, Oh *et al.* carried out a molecular mechanics

calculations for pMeMeOx with DP=20 and a corresponding tetramer in 1992¹⁵⁰. The calculated structures were defined by a left-handed helices containing 14 residues/3 turns with an identity period of 17.8 Å. Afterwards, more chiral POx were found to form secondary structures in solution, p^RBuEtOx and p^REtEtOx as well^{19-21, 23}. The conformation of chiral pBuEtOx was considered similar to the polyproline type II helix.

In 1985, Schmidt and Bott proposed a possible application of poly(4(S)-4-ethyl-2-phenyl-2-oxazoline) in the separation of enantiomeric mixtures of D,L-2-chloro-4-methylphenoxy-propionic acid methylester²⁴. However, the application of chiral POx in the biomedical area is still in its early stages.

2.2.5 Summary

Due to the tunable properties, relative ease of preparation and excellent biocompatibility, POx are currently re-emerging and have application value in many fields, especially in the biomedical area. POx are regarded as analogues of poly(amino acid)s, *i.e.* pseudo-polypeptides that have aliphatic polyamide backbone with substitution on the nitrogen atoms. When chiral centers are introduced into the backbone, chiral POx may exhibit optical activity and form secondary structures. These properties make them potentially useful in the areas of polymeric chiral catalysts, specific drug delivery system, and as a separation and purification medium for racemic mixture.

3 Motivation

Synthesizing more chiral/racemic poly(2,4-disubstituted-2-oxazoline)

Some 2,4- and 2,5- substituted POx have been described in **Chapter 2.2.4**, but a drug formulation based on main chain chiral POx has not been studied before. In order to improve the understanding of stereoregular polymers as drug carriers in general and to enlarge the toolbox of POx based drug formulations in particular, some 2,4-disubstituted POx with the chiral center in the main chain and reasonable hydrophobicity are considered as a good starting point to investigate. In this work, chiral and racemic poly(2-ethyl-4-ethyl-2-oxazoline) (pEtEtOx) and poly(2-propyl-4-methyl-2-oxazoline) (pPrMeOx) are synthesized. Using them as hydrophobic B block and the pMeOx as hydrophilic A block, ABA-type triblock copolymer A-pEtEtOx-A and A- pPrMeOx-A series are synthesized.

Characterizing the homopolymers and triblock copolymers

The stereoregularity and rigidity of the chiral chain potentially influence the micellar size, micellar thermodynamic stability, drug loading and cell interaction. In order to explore the potential applications, the solubility, thermal properties and optical activity of the synthesized homopolymers and triblock copolymers are characterized. In the meantime, the pEtEtOx and pPrMeOx with different chirality can be compared together, as well as the structure isomer pBuOx and pPrOzi.

Exploring the application of synthesized triblock copolymers in drug delivery system

As one group of pseudo-polypeptides, POx have been widely investigated in the biomedical field. Since it is relatively straightforward to synthesize the 2-oxazolines by changing the substituents in the 2-position, many poly(2-oxazoline)s (POx) with different side-chains have been easily obtained by polymerizing the corresponding 2-alkyl/aryl-2-oxazolines. However, the knowledge on monomers and polymers with the 4-/5- position substituents are quite limited.

When the novel chiral POx based ABA amphiphilic triblock copolymers are obtained, it is interesting to explore the application in the biomedical field, *e.g.*, drug delivery. In order to explore the possibility of the new triblock copolymers as drug delivery systems, common hydrophobic drugs (*e.g.* curcumin and paclitaxel) and chiral/racemic drugs (R-, S-, RS-ibuprofen) are applied as model drugs to formulated with the triblock copolymers. Afterwards, the drug loading capacity, particle size and long-term stability of the formulation are investigated. The influence of stereoregularity and rigidity of the chiral chain on drug loading should be partly shown in this work.

4 Results and Discussion

4.1 Synthesis of chiral/racemic poly(2,4-disubstituted-2-oxazoline) homopolymers

4.1.1 Synthesis of chiral/racemic 2-oxazolines monomers

^REtEtOx has been synthesized by Bloksma *et al.* through the reaction of nitriles and aminoalcohols²⁰. Lambert *et al.* initially reported the discovery of PrMeOx in a decomposition product¹⁵¹, but no information is available regarding its synthesis process. In this work, the one step synthesis of chiral or achiral EtEtOx and PrMeOx monomers from nitrile and alkanolamine was successfully performed according to the procedure of Witte and Seeliger *et al.*¹⁰⁻¹¹ The chiral or achiral alkanolamine (enantiomeric or racemic 2-amino-1-butanol, 2-amino-1-propanol) were used as purchased with purity 98%. In order to consume the alkanolamine completely, 1 eq alkanolamine and 1.2 eq nitrile (propionitrile, butyronitrile) were heated at 130 °C for 2-6 d under the catalysis of zinc acetate (**Fig. 4.1**) until the signal of alkanolamine was not detected by ¹H-NMR spectroscopy.

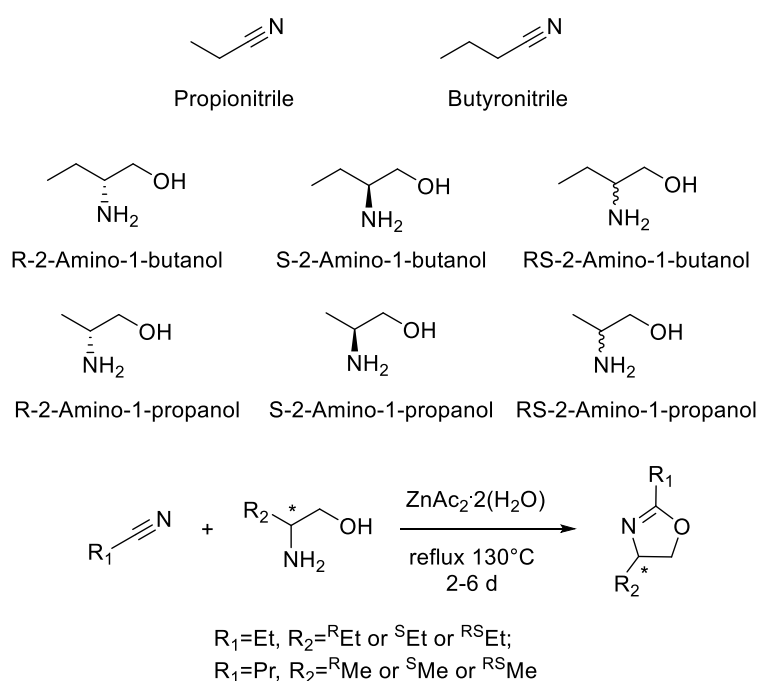


Figure 4.1 Reaction schemes for the monomer synthesis.

After drying and vacuum distillation, colorless liquid products were obtained, which were characterized via NMR spectroscopy. No signals that can be attributed to nitrile, alkanolamine residues or moistures in the ^1H and ^{13}C -NMR spectra (**Fig. 4.2, 4.3**), all the EtEtOx and PrMeOx monomers were considered pure enough for the following polymerization. In these small-scale reactions, the yields of monomers showed no clear difference related to the stereostructure (yield 40-55%, 14-23 g) (**Tab. 4.1**).

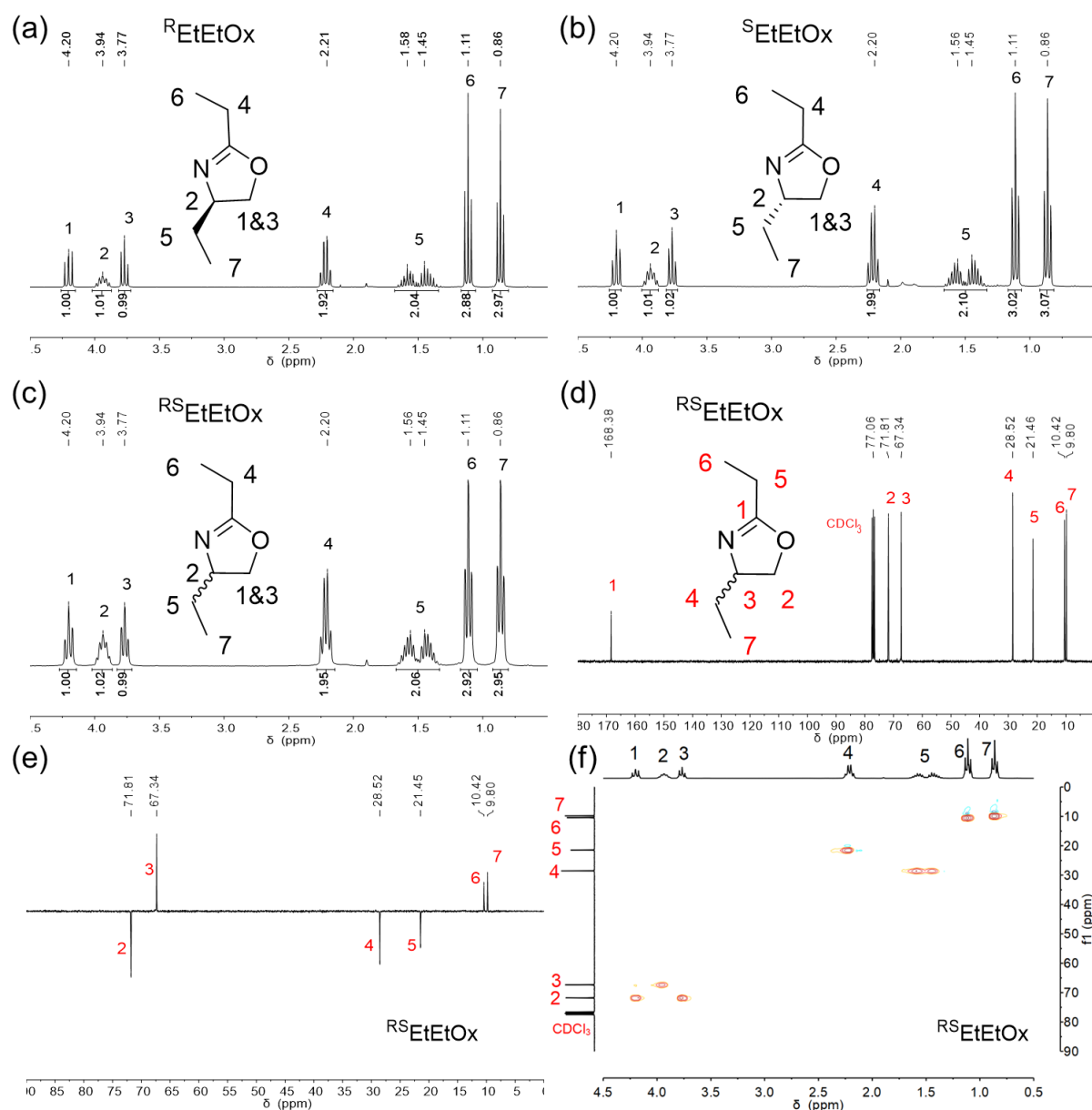


Figure 4.2 ^1H -NMR (CDCl₃; 300 MHz; 298 K) of monomers (a) $R\text{-EtEtOx}$, (b) $S\text{-EtEtOx}$ and (c) $RS\text{-EtEtOx}$ with signal assignment of all major signals. (d) ^{13}C -NMR, (e) DEPT-135, (f) HSQC (CDCl₃; 75 MHz; 298 K) of monomers $RS\text{-EtEtOx}$ with signal assignment of all major signals.

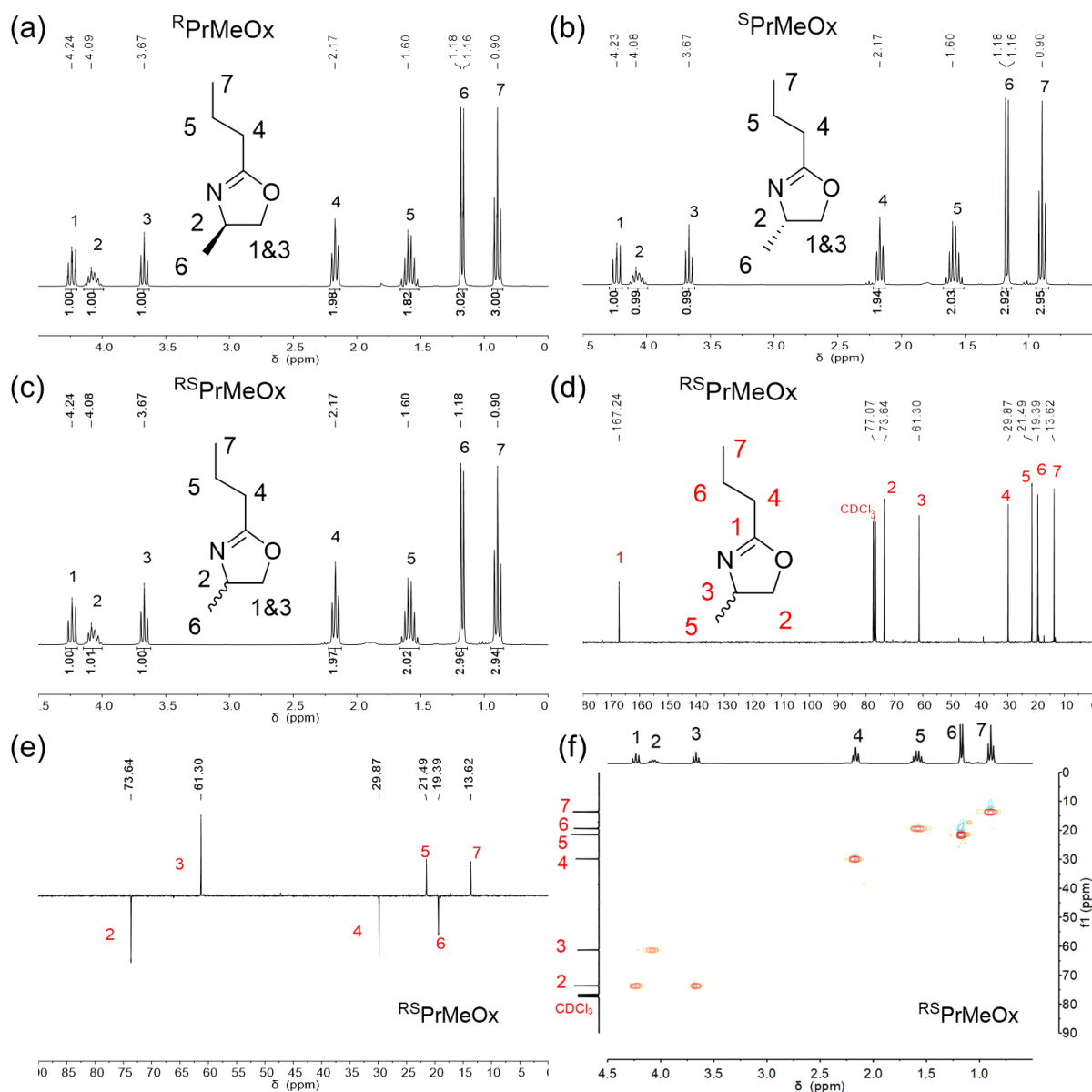


Figure 4.3 1H -NMR (CDCl₃; 300 MHz; 298 K) of monomers (a) $RPrMeOx$, (b) $SPrMeOx$ and (c) $RSPrMeOx$ with signal assignment of all major signals. (d) ^{13}C -NMR, (e) DEPT-135, (f) HSQC (CDCl₃; 75 MHz; 298 K) of monomers $RSPrMeOx$ with signal assignment of all major signals.

Table 4.1 Yields and boiling points (bp) of the synthesized monomers

Monomer	Abbrev.	Yield [%]	bp [°C]
(R)-2-ethyl-4-ethyl-2-oxazoline	^R EtEtOx	43	37 °C (10 mbar)
(S)-2-ethyl-4-ethyl-2-oxazoline	^S EtEtOx	40	37 °C (9 mbar)
(RS)-2-ethyl-4-ethyl-2-oxazoline	^{RS} EtEtOx	48	39 °C (11 mbar)
(R)-2-propyl-4-methyl-2-oxazoline	^R PrMeOx	46	36 °C (10 mbar)
(S)-2-propyl-4-methyl-2-oxazoline	^S PrMeOx	55	39 °C (10 mbar)
(RS)-2-propyl-4-methyl-2-oxazoline	^{RS} PrMeOx	53	43 °C (14 mbar)

The monomer 2-methyl-2-oxazoline (MeOx) is readily commercially available. The purchased MeOx was dried, distilled and stored under argon for further use.

4.1.2 Synthesis of chiral/racemic homopolymers

In 2011, Bloksma *et al.* synthesized poly((R)-2-ethyl-4-ethyl-2-oxazoline) under microwave-assisted conditions (180 °C), using methyl tosylate (MeOTs) as initiator and acetonitrile as solvent,²⁰ while the synthesis and characteristics of poly(2-propyl-4-methyl-2-oxazoline) (pPrMeOx) were not reported so far. Therefore, the polymerization of pEtEtOx and pPrMeOx were carried out in this work to compare the properties with each other as isomers, and also support the investigation of corresponding polymer amphiphiles.

In this work, the polymerization was performed similar to Lübtow *et al.*,¹⁵² summarized in **Fig. 4.4**. The reagents used for polymerization were all stored under argon. The initiator methyl trifluoromethylsulfonate (MeOTf), the monomers and the solvent sulfolane were all dried, and distilled under reduced pressure. The monomer preparation and polymerization procedure was conducted with glovebox and Schlenk line under inert atmosphere. MeOTf was dissolved in sulfolane in a dried and argon flushed Schlenk flask, followed by monomer addition. Afterwards, the mixture was heated at 130 °C until the monomer was completely consumed (24-72 h). Though higher reaction temperature (180 °C) can accelerate the reaction, the dispersity of obtained polymer was wider. The reaction was monitored with ¹H-NMR spectroscopy. When the monomer was consumed, the reaction mixture was cooled to room temperature to add the terminating agent 1-Boc-piperazine (PipBoc), and incubated at 50 °C for 4 h. Subsequently,

K_2CO_3 was added as neutralizing agent and stirred at 50 °C for another 4 h. The crude product was purified by dialysis. For polymer synthesis details and characterization, see experimental part in **Chapter 7.3.2**.

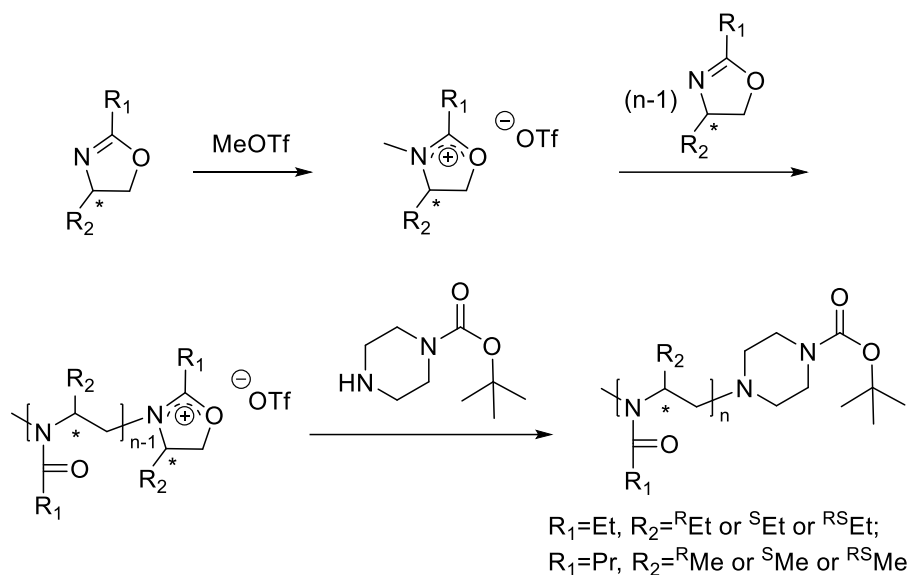


Figure 4.4 Reaction scheme for the synthesis of homopolymers.

The pEtEtOx homopolymer with $[M]/[I]$ of 50-60 has been synthesized previously²⁰, however, pEtEtOx with lower molar mass and pPrMeOx have not been investigated previously. Therefore, homopolymers of pEtEtOx and pPrMeOx with different molar mass and chirality were synthesized, using $[M]_0/[I]_0 = 10, 20, 30, 40$ for the R-isomers and $[M]_0/[I]_0 = 10, 20$ for the S- and RS-isomers. The solubility of obtained polymers in solvent used in following experiment was tested under shaking for 30 min at RT. The polymers were soluble in HFIP (≥ 5 g/L), well soluble in methanol, ethanol and chloroform (≥ 200 g/L), but poorly soluble in water (< 0.5 g/L).

pMeOx and pEtOx are normally considered as hydrophilic polymers. With the increasing length of the *N*-substituting side-chain, the POx become more hydrophobic. When the *N*-substituting side-chain is butyl, the poly(2-butyl-2-oxazoline) (pBuOx) is considered insoluble in water.¹⁵³ The limited solubility of pEtEtOx in water indicates that the additional alky group branch on the backbone also increases the hydrophobicity similar to the *N*-substituting alky group. However, it was found that both pEtEtOx and pPrMeOx are thermoresponsive. The saturated aqueous solutions of polymers were stored at 4 °C overnight for equilibration. When brought to RT, the formerly transparent solutions turned turbid. The clear saturated aqueous solutions of H2, H6, H8, H10, H14 and H16 (all $[M]_0/[I]_0 = 20$ of pEtEtOx and pPrMeOx) were sampled after equilibrating at 4 °C and lyophilized to determine the polymer mass. Accordingly,

the concentration of the saturated aqueous solutions was 8-10 g/L at 4 °C (**Tab. 4.2**), much higher than their solubility at RT. pMeOx is very hydrophilic and does not show thermoresponsive behavior, but pEtOx, pPrOx, poly(2-isopropyl-2-oxazoline) (piPrOx) and some POzi (*e.g.*, poly(2-propyl-2-oxazine) (pPrOzi) and poly(2-isopropyl-2-oxazine) (piPrOzi)) were determined to be thermoresponsive.^{119, 154-157} Thus, while the thermoresponsive behavior of pEtEtOx and pPrMeOx is within the expected range as constitutional isomers of pPrOzi, this is the first time C4 substituted POx have been found to be thermoresponsive.

Table 4.2 Polymer composition, yield, number average molecular weight M_n , dispersity \mathcal{D} , water solubility of synthesized homopolymers.

No.	Polymer composition	Abbrev.	Yield [%]	M_n [kg mol ⁻¹]			\mathcal{D} ^{c)}	Solubility ^{d)} [g/L]
				M_n ^{a)}	M_n ^{b)}	M_n ^{c)}		
H1	Me- ^R EtEtOx ₁₂ -PipBoc	/	77.4	1.5	1.7	1.0 [#]	1.05 [#]	n.d.
H2	Me- ^R EtEtOx ₂₁ -PipBoc	p ^R EtEtOx	69.3	2.7	2.9	1.5 [#]	1.07 [#]	7.8
H3	Me- ^R EtEtOx ₂₉ -PipBoc	/	84.9	4.0	3.9	1.6 [#]	1.15 [#]	n.d.
H4	Me- ^R EtEtOx ₄₁ -PipBoc	/	61.0	5.3	5.4	2.0 [#]	1.18 [#]	n.d.
H5	Me- ^S EtEtOx ₁₂ -PipBoc	/	59.9	1.5	1.7	0.9 [#]	1.13 [#]	n.d.
H6	Me- ^S EtEtOx ₂₃ -PipBoc	p ^S EtEtOx	83.2	2.7	3.1	1.1 [#]	1.22 [#]	7.8
H7	Me- ^{RS} EtEtOx ₁₁ -PipBoc	/	65.7	1.5	1.6	0.8 [#]	1.17 [#]	n.d.
H8	Me- ^{RS} EtEtOx ₂₁ -PipBoc	p ^{RS} EtEtOx	57.7	2.8	2.9	1.7 [#]	1.11 [#]	9.4
H9	Me- ^R PrMeOx ₁₂ -PipBoc	/	60.2	1.5	1.7	1.2 [#]	1.05 [#]	n.d.
H10	Me- ^R PrMeOx ₂₂ -PipBoc	p ^R PrMeOx	76.0	2.8	3.0	1.6 [#] 3.5 ^{###}	1.07 [#] 1.13 ^{###}	9.3
H11	Me- ^R PrMeOx ₃₂ -PipBoc	/	79.7	4.0	4.3	1.8 [#]	1.11 [#]	n.d.
H12	Me- ^R PrMeOx ₃₈ -PipBoc	/	79.6	5.1	5.0	2.1 [#]	1.11 [#]	n.d.
H13	Me- ^S PrMeOx ₁₂ -PipBoc	/	69.9	1.5	1.7	1.2 [#]	1.06 [#]	n.d.
H14	Me- ^S PrMeOx ₂₂ -PipBoc	p ^S PrMeOx	86.6	2.8	3.0	1.7 [#] 3.2 ^{###}	1.06 [#] 1.10 ^{###}	8.9
H15	Me- ^{RS} PrMeOx ₁₂ -PipBoc	/	77.1	1.5	1.7	1.1 [#]	1.02 [#]	n.d.
H16	Me- ^{RS} PrMeOx ₂₃ -PipBoc	p ^{RS} PrMeOx	87.1	2.8	3.1	1.4 [#] 3.0 ^{###}	1.03 [#] 1.09 ^{###}	9.9

^{a)} theoretical molar mass from $[M]_0/[I]_0$; ^{b)} as obtained by ¹H-NMR (CDCl₃; 300 MHz) evaluated as mean of all relevant integral ratios; ^{c)} as obtained by SEC ([#] eluent: HFIP, PSS PFG linear M column, calibrated with PEG standards; ^{###} eluent: chloroform, Malvern LC4000L column, calibrated with polystyrene); ^{d)} solubility in water at 4 °C in g/L. n.d.: not determined. /: no Abbrev.

The polymer composition was characterized by ¹H-NMR spectroscopy. The Boc moiety from the *N*-Boc-piperazine (PipBoc) forms a sharp and intense singlet in ¹H-NMR spectrum, which assists the end-group analysis. The ¹H-NMR spectra of pEtEtOx and pPrMeOx (DP ≈20) are showed as examples in **Fig. 4.5** with signal assignment of all major signals. Please note, it is

difficult to get precise end-group analysis because all the signals of the polymers are in part extremely broad and overlapping. Therefore, the relatively isolated peaks from the proton of $\text{-CO-CH}_2\text{-}$ (signal number 4, 2.30 ppm) and $\text{CH}_3\text{-}$ (signal number 7 and 8, 1.33-0.87 ppm) were considered as reference to calculate the degree of polymerization (DP) of obtained pEtEtOx (H1-H8) and pPrMeOx (H9-H16). The determined DP of all the synthesized polymers were close to the theoretical polymer composition (**Tab. 4.2**).

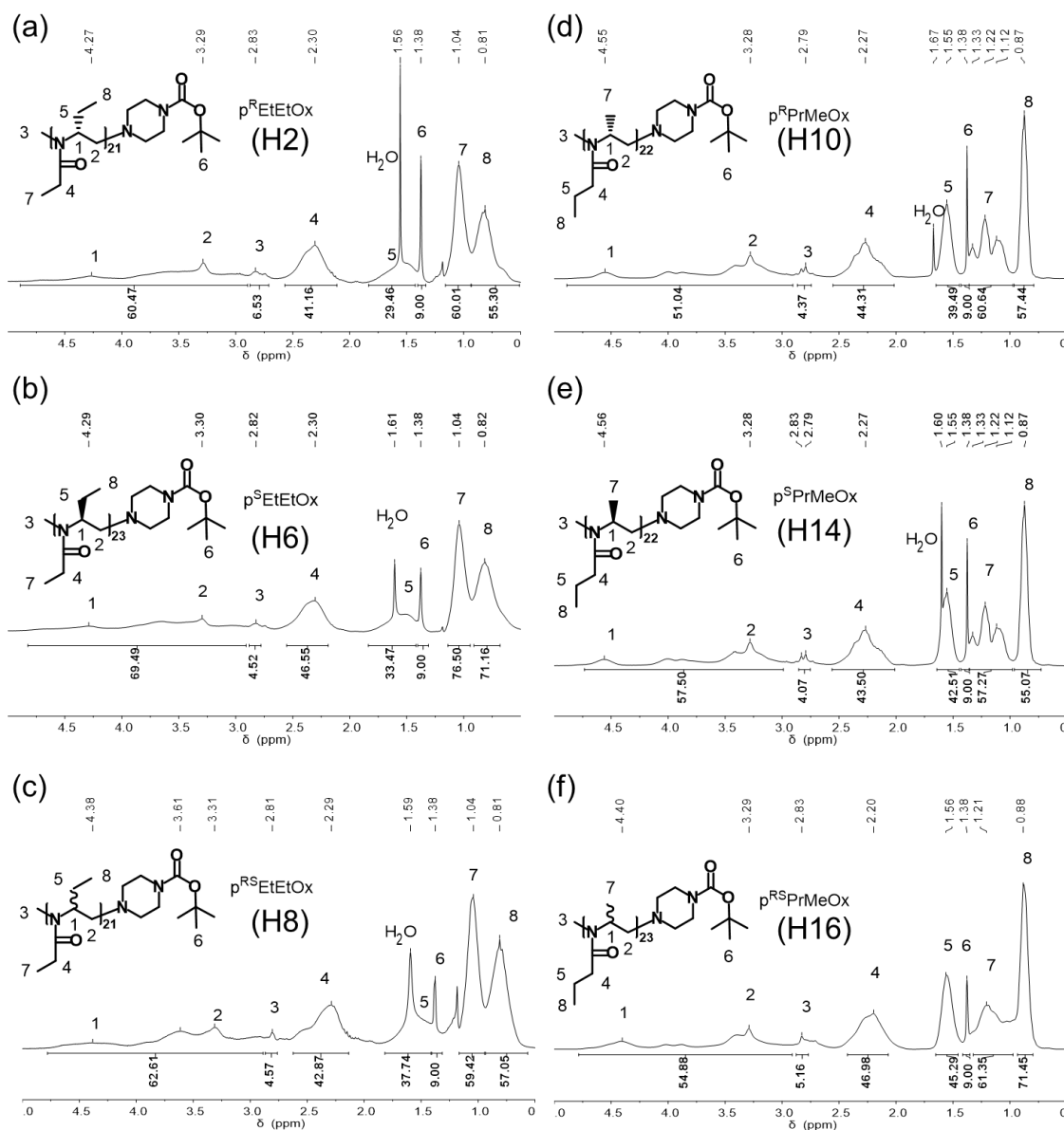


Figure 4.5 $^1\text{H-NMR}$ (CDCl_3 ; 300 MHz; 298 K) of homopolymers (a) $\text{p}^{\text{R}}\text{EtEtOx}$ (H2), (b) $\text{p}^{\text{S}}\text{EtEtOx}$ (H6), (c) $\text{p}^{\text{RS}}\text{EtEtOx}$ (H8), (d) $\text{p}^{\text{R}}\text{PrMeOx}$ (H10), (e) $\text{p}^{\text{S}}\text{PrMeOx}$ (H14) and (f) $\text{p}^{\text{RS}}\text{PrMeOx}$ (H16) with signal assignment of all major signals.

The $^1\text{H-NMR}$ spectra of polymers are compared to investigate the influence of the DP and chirality in **Fig. 4.6**. The pEtEtOx polymers with R, S and RS stereostructure (H1-H4, H5-

H6 and H7-H8, respectively) have similar peak shape in spectra. When the integral values of the end groups Boc were normalized to 9, the integral values of other peaks, *e.g.* peaks from the proton of $-\text{CO}-\text{CH}_2-$, increased with the DP increase. (**Fig. 4.6a, b**). The differentiation of enantiomeric molecules can be facilitated by NMR analysis in a chiral environment,¹⁵⁸ but in the achiral solvent environment, it is very difficult. Here in this achiral chloroform-d environment, the stereostructural differences between these pEtEtOx homopolymers were not observed in the spectra. At the same time, the pPrMeOx polymers with R and S chirality (H9-H12 and H13-H14) did not exhibit difference in peak shape (**Fig. 4.6c, d**). However, comparing to the spectra of R- and S-isomers, both of RS structure pPrMeOx (H15-H16) showed a broad signal in the chemical shift range of 1.33-1.12 ppm instead of three signals observed for R- and S-isomers, which was attributed to the proton of methyl branched on the backbone. NMR can be applied in determination of precise protein secondary structure with more validation from other experiments which was not available here.¹⁵⁹⁻¹⁶⁰ From the obtained spectra of pPrMeOx, it was supposed that even in the solvent chloroform-d, the pPrMeOx polymers of R- and S-isomer still formed a regular secondary structure while the RS-isomer did not. But it was not clear how the pEtEtOx behaved in the chloroform.

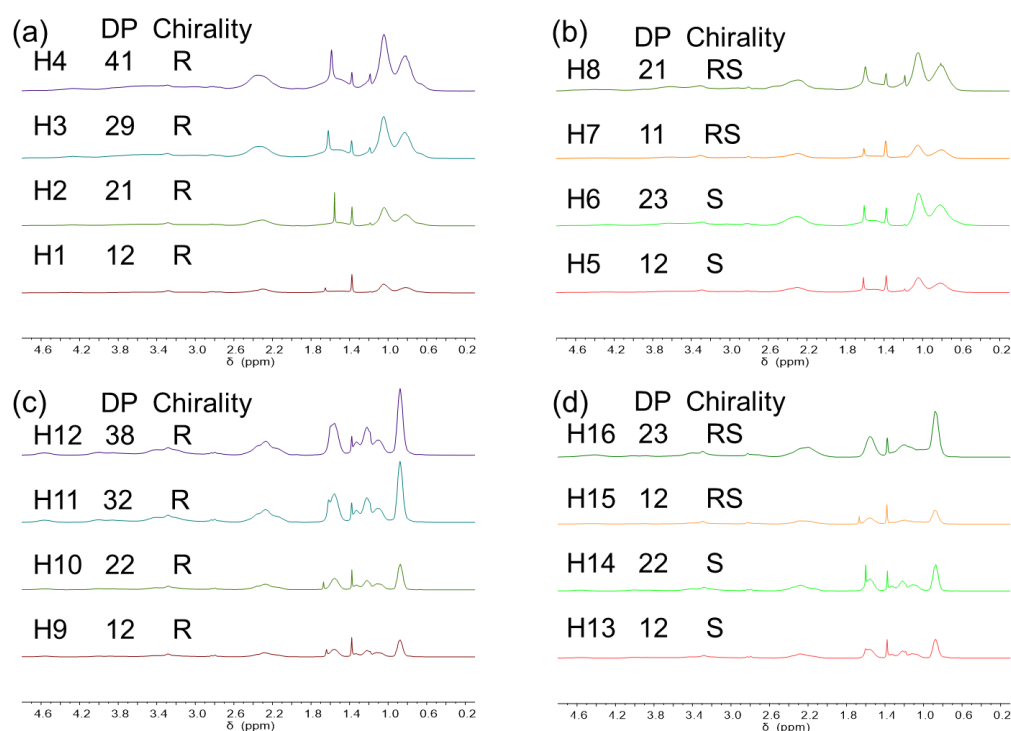


Figure 4.6 ^1H -NMR (CDCl_3 ; 300 MHz; 298 K) of homopolymers (a) H1-H4 (R-isomer of pEtEtOx, DP=12, 21, 29, 41), (b) H5-H8 (S- and RS-isomer of pEtEtOx, DP=12, 23, 11, 21), (c) H9-H12 (R-isomer of pPrMeOx, DP=12, 22, 32, 38), (d) H13-H16 (S- and RS-isomer of pPrMeOx, DP=12, 22, 12, 23).

SEC analysis was used to determine the molar mass and molar mass distribution of the synthesized polymers. The dispersity \bar{D} values of all polymers were below 1.3 (Fig. 4.7 and Tab. 4.2), which reflected the reasonable control of polymerization. The molar masses obtained from SEC ($^{\#}$ eluent: HFIP, PSS PFG linear M column, calibrated with PEG standards) was lower than the values of $[M]_0/[I]_0$ and $^1\text{H-NMR}$. Considering that the SEC results are related to the different solution behavior of polymers in the eluent, influence of stationary phase and calibration standards, the molar masses given by SEC are just a qualitative reference between polymers under same test condition. Besides, the pPrMeOx polymers of $[M]_0/[I]_0=20$ were also characterized using another SEC system ($^{\#\#\#}$ eluent: chloroform, Malvern LC4000L column, calibrated with polystyrene) (Tab. 4.2), to elucidate the effects of eluent and calibration standard.

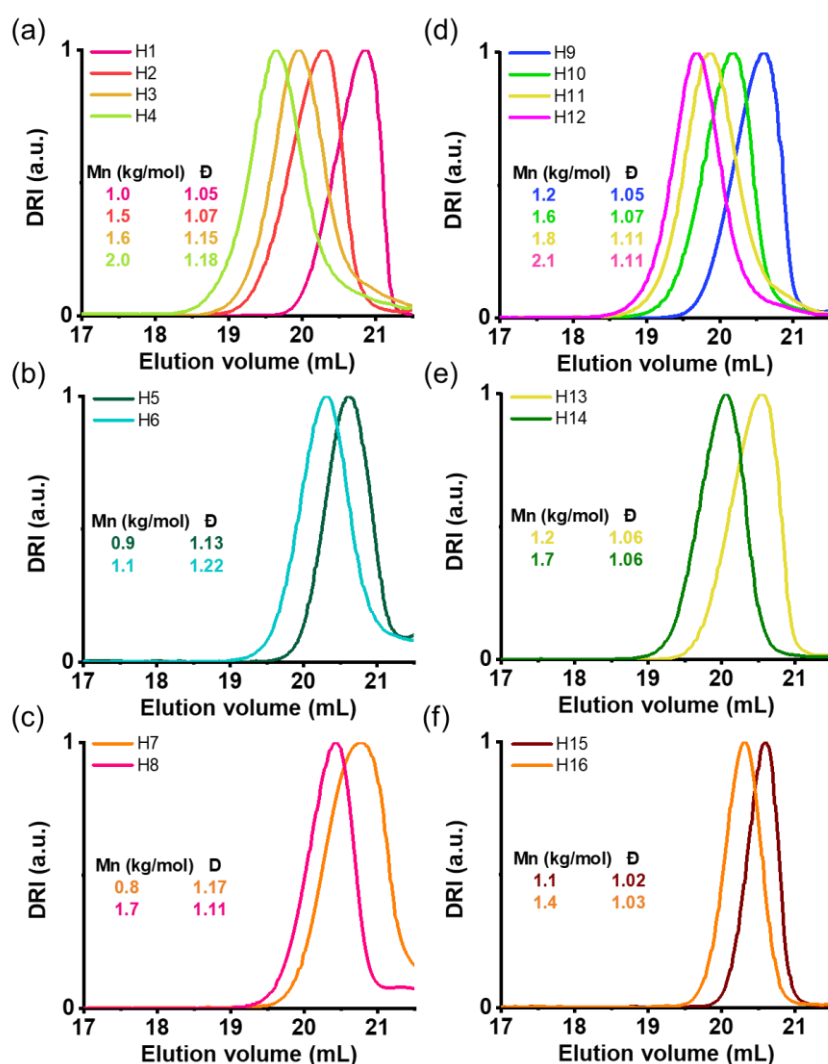


Figure 4.7 SEC elugrams of homopolymers (a) H1-H4 (R-isomer of pEtEtOx, DP=12, 21, 29, 41), (b) H5-H6 (S-isomer of pEtEtOx, DP=12, 23), (c) H7-H8 (RS-isomer of pEtEtOx, DP=11, 21), (d) H9-H12 (R-isomer of pPrMeOx, DP=12, 22, 32, 38), (e) H13-H14 (S-isomer of pPrMeOx, DP=12, 22), (f) H15-H16 (RS-isomer of pPrMeOx, DP=12, 23) before purification. $^{\#}$ Eluent: HFIP; PSS PFG linear M column.

4.1.3 Conclusion

In summary, the monomers of 2-ethyl-4-ethyl-2-oxazoline (EtEtOx) and 2-propyl-4-methyl-2-oxazoline (PrMeOx) with different chirality were successfully synthesized. Subsequently, the homopolymers of chiral and racemic poly(2,4-disubstituted-2-oxazoline)s (pEtEtOx and pPrMeOx) were synthesized via living cationic ring-opening polymerization (LCROP). The polymers were characterized by $^1\text{H-NMR}$ spectroscopy and SEC. The synthesized polymers had a DP reasonably close to the initial monomer to initiator ratio $[\text{M}]_0:[\text{I}]_0$. With the result of low dispersity ($\text{Đ} < 1.2$), the polymerization was considered as well controlled. Both pEtEtOx and pPrMeOx were of very low water solubility at RT (< 0.5 g/L) but had relative high solubility at 4 °C (8-10 g/L). The thermoresponsive behavior was observed visually.

4.2 Physicochemical properties of homopolymers

4.2.1 Thermal properties of homopolymers

The chain length, side-chain and chirality potentially influence the thermal properties of POx, such as glass transition or melting temperature.^{21, 161} In order to view the differentiation between the stereoisomers and chains with different DP, the thermal stability and transition of pEtEtOx (H1-H8) and pPrMeOx (H9-H16) were investigated by thermogravimetric analysis (TGA) and differential scanning calorimetry (DSC), respectively (**Tab. 4.3**, **Fig. 4.8** and **Fig. 4.9**).

Table 4.3 Glass transition temperatures T_g and the extrapolated onset temperature of major mass loss T_d of synthesized homopolymers.

No.	Polymer composition	Abbrev.	DP ^{a)}	T_g ^{b)} [°C]	T_d ^{c)} [°C]
H1	Me- ^R EtEtOx ₁₂ -PipBoc	/	12	65	358
H2	Me- ^R EtEtOx ₂₁ -PipBoc	p ^R EtEtOx	21	82	362
H3	Me- ^R EtEtOx ₂₉ -PipBoc	/	29	83	365
H4	Me- ^R EtEtOx ₄₁ -PipBoc	/	41	87	363
H5	Me- ^S EtEtOx ₁₂ -PipBoc	/	12	75	359
H6	Me- ^S EtEtOx ₂₃ -PipBoc	p ^S EtEtOx	23	80	345
H7	Me- ^{RS} EtEtOx ₁₁ -PipBoc	/	11	70	362
H8	Me- ^{RS} EtEtOx ₂₁ -PipBoc	p ^{RS} EtEtOx	21	79	361
H9	Me- ^R PrMeOx ₁₂ -PipBoc	/	12	46	363
H10	Me- ^R PrMeOx ₂₂ -PipBoc	p ^R PrMeOx	22	55	357
H11	Me- ^R PrMeOx ₃₂ -PipBoc	/	32	59	364
H12	Me- ^R PrMeOx ₃₈ -PipBoc	/	38	60	360
H13	Me- ^S PrMeOx ₁₂ -PipBoc	/	12	47	361
H14	Me- ^S PrMeOx ₂₂ -PipBoc	p ^S PrMeOx	22	56	344
H15	Me- ^{RS} PrMeOx ₁₂ -PipBoc	/	12	48	361
H16	Me- ^{RS} PrMeOx ₂₃ -PipBoc	p ^{RS} PrMeOx	23	55	351

^{a)} as obtained by ¹H-NMR (CDCl₃; 300 MHz) evaluated as mean of all relevant integral ratios; ^{b)} mean T_g obtained from second and third heating curve (DSC); ^{c)} Extrapolated onset temperature of major mass loss (TGA). /: no Abbrev.

TGA of pEtEtOx (**Fig. 4.8a**) and pPrMeOx (**Fig. 4.8b**) was performed for thermal stability determination by monitoring the weight change, which was in the temperature range of 30-900 °C (10 °C/min) under synthetic air. A slight mass loss occurred at ≈ 220 °C, which was attributed to the loss of the Boc group from the terminator residues.¹⁶² The 2-6% mass loss was consistent with the weight percent of Boc in the polymer, depending on the chain length. The extrapolated onset temperature T_d of major mass loss was around 350 °C and no obvious difference was found between the stereoisomers. The high thermal stability of pEtEtOx and pPrMeOx was similar to many previously reported POx, *e.g.*, poly(2-*n*-nonyl-2-oxazoline) (pNonOx, $T_d=359$ °C).¹⁶³⁻¹⁶⁴

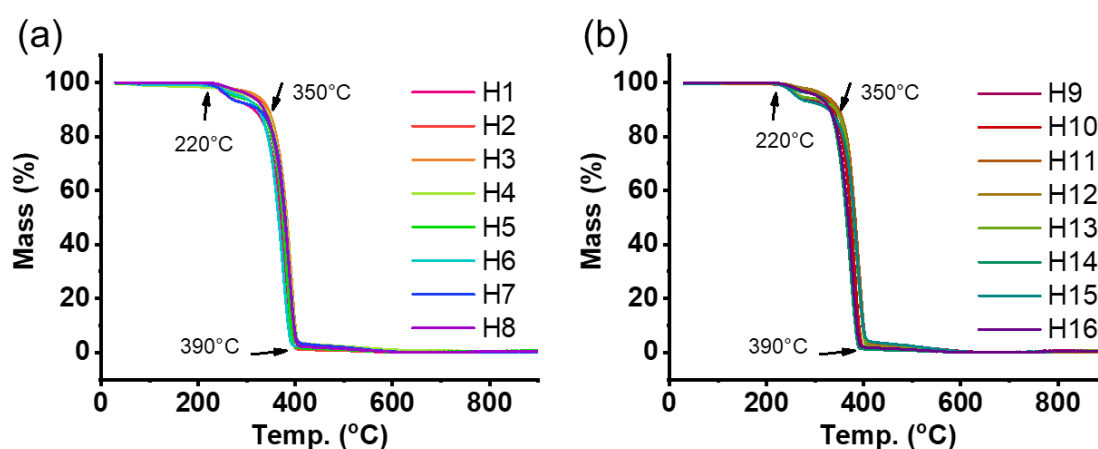


Figure 4.8 Weight loss occurring during thermogravimetric analysis (TGA) of homopolymers (a) pEtEtOx (H1-H8, DP=12, 21, 29, 41, 12, 23, 11, 21) and (b) pPrMeOx (H9-H16, DP=12, 22, 32, 38, 12, 22, 12, 23). Samples were heated from 30 to 900 °C with a heating rate of 10 °C/min.

The thermal transition were investigated using DSC measurements in the temperature range of -50-190 °C (10 °C/min) under N_2 -atmosphere (**Fig. 4.9**). Considering the degradation of Boc group in pEtEtOx and pPrMeOx, the temperature range of DSC was set only up to 190 °C. No melting peak of pEtEtOx and pPrMeOx was observed in the investigated temperature range. In the series of *N*-alkyl-substituted POx, the melting temperature (T_m) around 150 °C has been detected in the POx with butyl to nonyl side-chains (pBuOx to pNonOx), but not been detected in POx with shorter side-chain, *e.g.*, pMeOx, pEtOx and pPrOx.¹⁶⁵ The melting peak of pBuOx to pNonOx is attributed to the crystallization of long side-chain, while the short side-chains of pMeOx to pPrOx do not reach the minimum length required to induce crystallization, and as a result, remain amorphous. In addition, a structural isomer of pEtEtOx and pPrMeOx, *pi*PrOzi was investigated previously, and no melt transitions was observed in DSC.¹¹⁹ Similarly, the

pEtEtOx and pPrMeOx, bearing relative short side-chains are assumed to be amorphous, but should be further confirmed (*e.g.*, XRD, **Chapter 4.2.2**).

The glass transition temperature (T_g) is an endothermic transition that occurs in amorphous materials or amorphous region of semicrystalline materials. At this temperature, the polymer chain segments undergo a transition from hard and brittle (glassy state) to soft and flexible (rubbery state).¹⁶⁶⁻¹⁶⁷ The value of T_g relates to the mobility of the polymer chain segments. High T_g points to rigid and inflexible chain segments. In this work, the T_g of polymers was determined using the midpoint of the step in the heat curve. Comparing within respective series of pEtEtOx and pPrMeOx (**Fig. 4.9a, c**), the T_g of homopolymers increased quickly (R-isomer of pEtEtOx from 65 to 82 °C, R-isomer of pPrMeOx from 46 to 55 °C) in the range of $[M]_0/[I]_0=10-20$, afterwards increased slowly with the chain length growth. As the T_g significantly depended on the chain length, the products with $DP \approx 10$ (H1, H5, H7, H9, H13, H15) would be more accurately called “oligomer”, and had more flexible chain segments than longer polymers. However, these products will still be called “polymer” for convenience in the following text. In order to figure out the influence of chirality, the T_g of homopolymers ($DP \approx 20$) with different stereostructures were compared together. The T_g of p^REtEtOx (H2), p^SEtEtOx (H6) and p^{RS}EtEtOx (H8) were similar around 80 °C, and the T_g of p^RPrMeOx (H10), p^SPrMeOx (H14) and p^{RS}PrMeOx (H16) were close to each other around 55 °C (**Tab. 4.3** and **Fig. 4.9**). The chirality of pEtEtOx and pPrMeOx did not affect their chain mobility. However, the difference of T_g between constitutional isomers pEtEtOx (≈ 80 °C) and pPrMeOx (≈ 55 °C) was obvious. The pEtEtOx was less flexible than pPrMeOx, which can be attributed to the steric hinderance coming from the bigger ethyl substituent on the backbone.

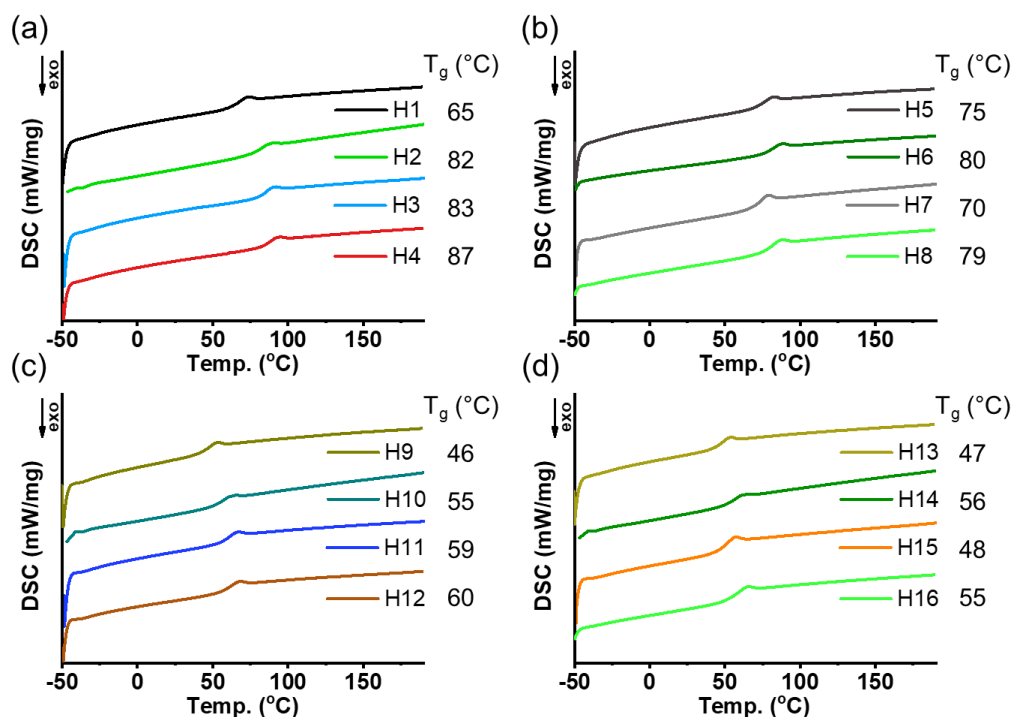


Figure 4.9 DSC heat flow of the third heating cycle of homopolymers (a) H1-H4 (R-isomer of pEtEtOx, DP=12, 21, 29, 41), (b) H5-H8 (S- and RS-isomer of pEtEtOx, DP=12, 23, 11, 21), (c) H9-H12 (R-isomer of pPrMeOx, DP=12, 22, 32, 38), (d) H13-H16 (S- and RS-isomer of pPrMeOx, DP=12, 22, 12, 23). The samples were heated 3 times and cooled two times from -50 °C to 190 °C (10 °C/min).

The T_g values of some alky substituted POx that come from literatures and this work are listed in **Tab. 4.4** for better comparison. On one hand, with same backbone branch, chiral POx $p^R\text{BuEtOx}$ has two more $-\text{CH}_2-$ on *N*-substituting side-chain than $p^R\text{EtEtOx}$ (H2), but its T_g is about 30 °C lower than $p^R\text{EtEtOx}$. The *N*-alky-substituted POx has been investigated intensively, generally when the side-chain is methyl to pentyl, longer side-chain results in lower T_g .¹⁶¹ The higher T_g of $p^R\text{EtEtOx}$ compared to $p^R\text{BuEtOx}$ is due to its shorter *N*-substituting side-chain. On the other hand, with same *N*-substituting side-chain, pEtEtOx has two more carbon atoms on the backbone branch than pEtOx, and its T_g is 20 °C higher than pEtOx; pPrMeOx has one more carbon atom than pPrOx, and its T_g is 15 °C higher than pPrOx. Clearly, the longer backbone branch hinders the chain mobility, different from the *N*-substituted side-chain. However, when the additional methylene unit is in the main chain, it has been demonstrated that the T_g of *N*-alky-substituted POzi is lower than that of POx with same *N*-substituted side-chain. It is apparent that the additional carbon atom works differently at different position. Of course, it would be very interesting if POx with longer backbone branch could be synthesized in the future.

Table 4.4 Glass transition temperatures T_g of polymers reported here ($DP \approx 20$) and compared with literature values for similar polymers.

poly(2-R-4-R'-2-oxazoline)		DP	T_g [°C]
R=	R'=		
Me	H	60	≈ 80 ¹⁶¹
Me	H	35	73 ¹⁶⁸
Me	Me	10	90 ²³
Et	H	60	≈ 60 ¹⁶¹
Et	Me	25	75-80 ²³
Et	Et	≈ 20	79-82 ^{a)}
Pr	H	60	≈ 40 ¹⁶¹
Pr	Me	≈ 20	55-56 ^{a)}
CH ₃ (CH ₂) ₃ (Bu)	H	60	≈ 25 ¹⁶⁵
Bu	Et	60	≈ 52 ²¹
CH ₃ (CH ₂) ₄ (Pent)	H	60	≈ 5 ¹⁶¹

^{a)} this work, mean T_g obtained from second and third heating curve (DSC)

4.2.2 X-ray diffraction of homopolymers

The *N*-*n*-alky-substituted POx with butyl or longer side-chain are known to be semicrystalline, and the POx with shorter side-chain are amorphous.¹⁶⁵ Though pEtOx can also form crystalline fiber in aqueous solutions above the cloud point temperature,¹⁶⁹ it is normally amorphous without special treatment. Bearing an additional branch on the backbone, a set of pBuEtOx with different chirality was investigated by X-ray diffraction (XRD) previously.¹⁸ The chiral p^RBuEtOx and p^SBuEtOx were determined as semicrystalline, and the racemic p^{RS}BuEtOx was amorphous. However, the pEtEtOx and pPrMeOx have not been investigated using XRD before. Therefore, XRD of selected polymers was performed in powder at RT.

Because of the limited amount of polymers, a single crystal silicon plate (Bruker AXS, C79298-A3244-B249, Germany) was applied, which is suitable for small sample amount and had low background (**Fig. 4.10**). The XRD of selected pEtEtOx and pPrMeOx ($DP \approx 10$ and 20) are shown in **Fig. 4.11**. The R-isomer of pEtEtOx and pPrMeOx with $DP \approx 10$ showed two broad bands (**Fig. 4.11a, b**), as well as the chiral and racemic pEtEtOx and pPrMeOx with $DP \approx 20$ (**Fig. 4.11c, d**). The position of two broad bands in XRD was similar to that of amorphous p^{RS}BuEtOx.¹⁸ It indicated that both pEtEtOx and pPrMeOx were amorphous. The XRD results were consistent with the DSC results. Though the additional branch on the backbone made the

POx more hydrophobic, it did not contribute to form the crystalline domain when the POx contained short *N*-substituted side-chain like ethyl and propyl. Also, it must be mentioned that crystallization of these polymers may take place under specific condition, but so far it was not observed.

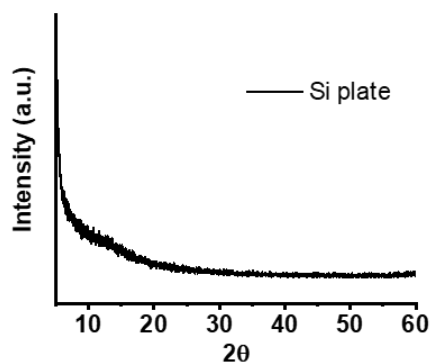


Figure 4.10 XRD patterns of the empty single crystal silicon plate (Bruker AXS, C79298-A3244-B249, Germany).

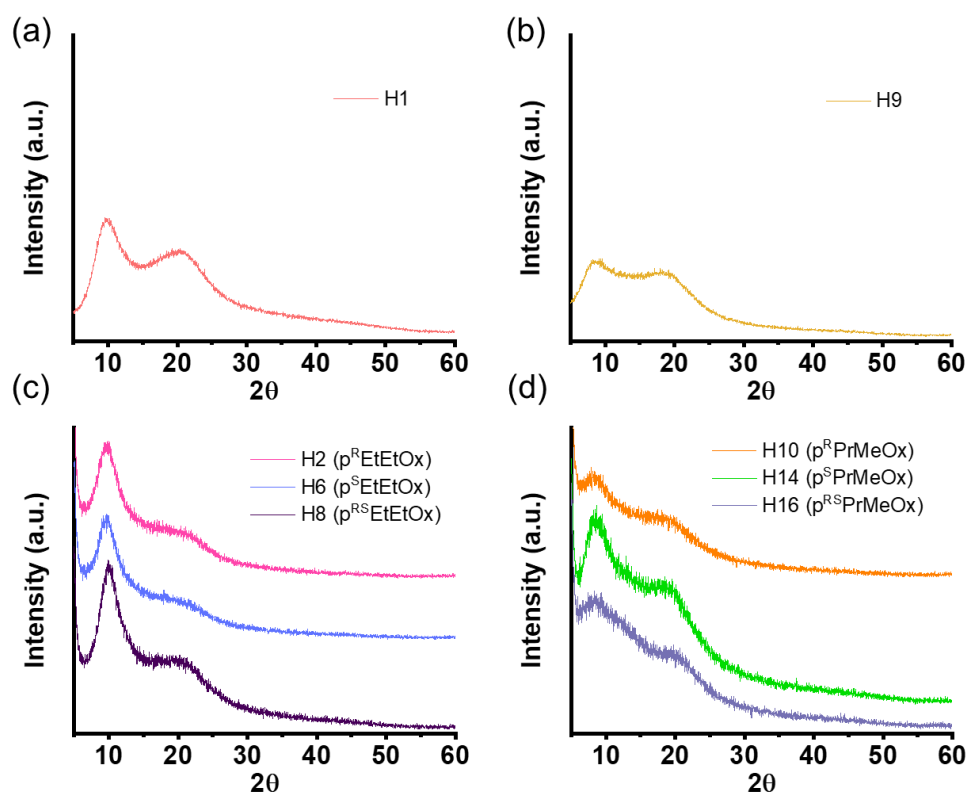


Figure 4.11 XRD patterns of homopolymers (a) H1 (R-isomer of pEtEtOx, DP=12), (b) H9 (R-isomer of pPrMeOx, DP=12), (c) H2, H6, H8 (p^REtEtOx, p^SEtEtOx, p^{RS}EtEtOx, DP=21,23,21), (d) H10, H14, H16 (p^RPrMeOx, p^SPrMeOx, p^{RS}PrMeOx, DP=22,22,23).

4.2.3 Optical activity of homopolymers

Chiroptical properties are based on the interaction of chiral substance with polarized light, which can distinguish between the enantiomers. Circular dichroism (CD) spectroscopy is one of the widely applied techniques for analyzing chiroptical properties and secondary structure of biopolymers and synthetic polymers.¹⁷⁰⁻¹⁷² Therefore, CD spectroscopy was used to study the pEtEtOx and pPrMeOx series (DP \approx 20), including their R-, S-, RS-isomers and 1/1 (w/w) mixtures of two corresponding enantiomers (simply called ^MpEtEtOx and ^MpPrMeOx). The CD measurements were performed in methanol solution (polymer concentration 0.1 g/L) at 25 °C, and the wavelength range of 200-255 nm was shown in **Fig. 4.12**. The CD value represents the difference in absorption of left and right circular polarized light. The S-isomers of both pEtEtOx and pPrMeOx showed positive Cotton effect (CE), while the R-isomers showed negative CE in the same range. The maximum CD values of all the chiral polymers were observed at 210-220 nm, which is in the n- π^* transition region of the amide chromophore. In contrast, the RS-isomers and 1/1 (w/w) ratio mixtures did not show any CE. It indicated that the R- and S-isomers formed secondary structure formation but with opposite handedness, while the RS-isomers and the mixtures either did not form secondary structure or formed secondary structure but with 50/50 mixture negate effect. Previously, the molecular mechanics calculations and CD measurements of pMeMeOx (DP=20, S- structure monomer) and corresponding tetramer were carried out by Oh *et al.*¹⁵⁰ The calculated polymer and tetramer were determined to be a kind of left-handed helix. Their CD spectra of synthesized polymer and tetramer showed positive CE at 200-238 nm in HFIP, with same shape and intensity. Afterwards, more chiral POx were found to form secondary structures in solution,^{19, 21, 23} p^REtEtOx as well.²⁰ The conformation of chiral POx was considered similar to the polyproline type II helix. Therefore, the chiral pEtEtOx and pPrMeOx are expected to form flexible helical conformation. Besides, comparing the chiral pEtEtOx and pPrMeOx, the CD value of chiral pPrMeOx (**Fig. 4.12b**) was bigger than that of pEtEtOx (**Fig. 4.12a**). It is assumed that the relatively flexible polymer chain of chiral pPrMeOx was more conducive to forming secondary structures in methanol.

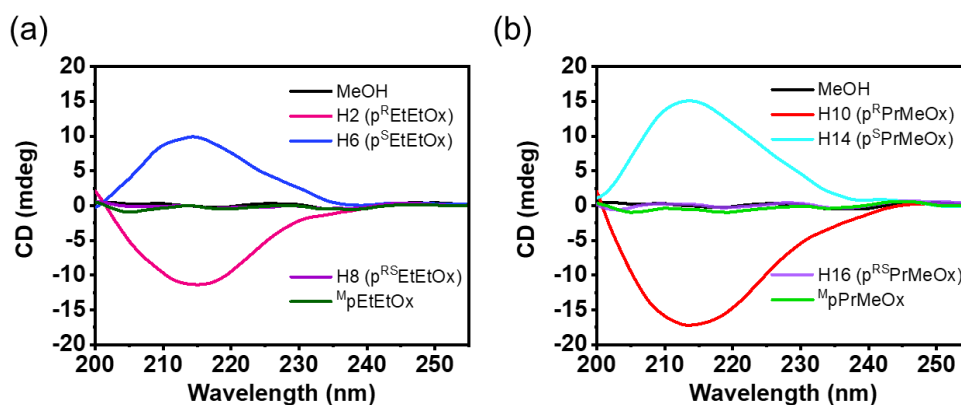


Figure 4.12 CD spectra of (a) $p^R\text{EtEtOx}$ (H2), $p^S\text{EtEtOx}$ (H6), $p^{RS}\text{EtEtOx}$ (H8), $M^p\text{EtEtOx}$ (1/1 (w/w) ratio mixture of H2 and H6) and (b) $p^R\text{PrMeOx}$ (H10), $p^S\text{PrMeOx}$ (H14), $p^{RS}\text{PrMeOx}$ (H16), $M^p\text{PrMeOx}$ (1/1 (w/w) ratio mixture of H10 and H14) in methanol at 25 °C. Polymer concentration was 0.1 g/L.

4.2.4 Conclusion

Understanding the property of homopolymer is conducive to the synthesis and characterization of the corresponding block copolymers. The TGA study of $p\text{EtEtOx}$ and $p\text{PrMeOx}$ illustrated that the thermal stability of these two constitutional isomers was quite similar and barely affected by the DP and chirality. The T_g value related to the DP of both polymer series, when the chain was short (DP=10-20), the T_g increased with the chain growth obviously. With longer chains, the T_g increased slowly and was observed $T_g = 87$ °C for $p\text{EtEtOx}$ (DP=41) and 60 °C for $p\text{PrMeOx}$ (DP=38). The difference of T_g between stereoisomers was not significant, for neither $p\text{EtEtOx}$ nor $p\text{PrMeOx}$ series. However, the T_g of $p\text{PrMeOx}$ was clearly lower than that of $p\text{EtEtOx}$ with same DP, which indicated that the polymer chain of $p\text{PrMeOx}$ was more flexible than $p\text{EtEtOx}$. From the results of DSC and XRD, it was confirmed that $p\text{EtEtOx}$ or $p\text{PrMeOx}$ were all amorphous regardless of their chirality and DP. The homopolymers were studied by CD spectroscopy in solution, which confirmed that the $p^R\text{EtEtOx}$, $p^S\text{EtEtOx}$, $p^R\text{PrMeOx}$ and $p^S\text{PrMeOx}$ maintain their chirality, *i.e.*, no racemization occurred during LCROP. These chiral polymers were able to form secondary structure in methanol, while the RS-isomer ($p^{RS}\text{EtEtOx}$ and $p^{RS}\text{PrMeOx}$) did not form. However, the mixtures ($M^p\text{EtEtOx}$ and $M^p\text{PrMeOx}$) either did not form or formed secondary structure but with 50/50 mixture negate effect.

4.3 Synthesis and characterization of chiral/racemic triblock copolymers

As mentioned previously, the purpose of this work was to investigate the synthesis of chiral poly(2,4-disubstituted-2-oxazoline) based triblock copolymers, and apply them in drug formulation. Therefore, after the synthesis and characterization of the homopolymers, the triblock copolymers were prepared. The hydrophilic pMeOx was used as A blocks and the hydrophobic pEtEtOx or pPrMeOx as B blocks to obtain the ABA triblock copolymers, which were not investigated before. In the following, the synthesis and physical properties of selected polymers were discussed.

4.3.1 Synthesis of pMeOx-*block*-pEtEtOx-*block*-pMeOx and pMeOx-*block*-pPrMeOx-*block*-pMeOx

The polymerization of triblock copolymers was also conducted via the LCROP (**Fig. 4.13**). The 10-50 eq monomer MeOx and 1 eq initiator MeOTf were heated at 100 °C until complete consumption. The second block, 10-20 eq monomer EtEtOx or PrMeOx was polymerized at 130 °C. Afterwards, another 10-50 eq MeOx was added for the third block. The detail procedure is reported in the **Chapter 7.3.2.2**.

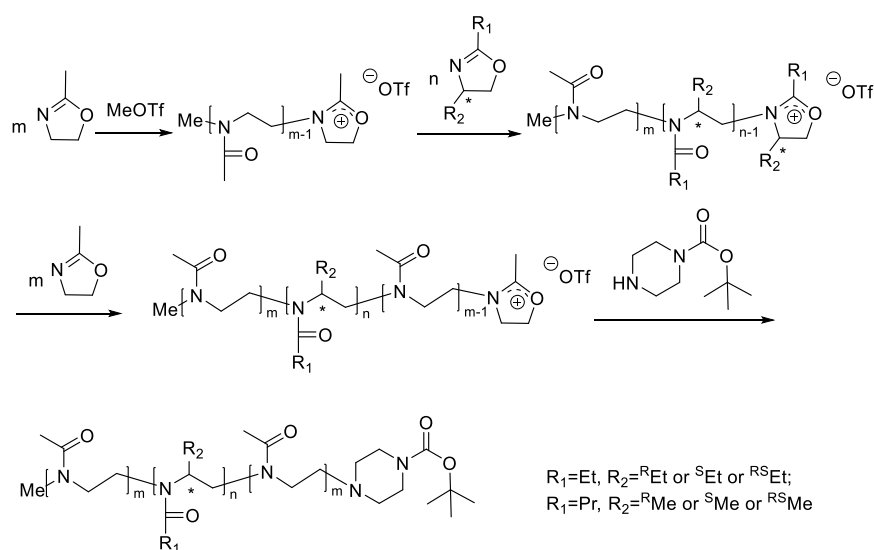


Figure 4.13 Reaction scheme for the synthesis of triblock copolymers.

Four sets of triblock copolymers with different polymer composition were designed. T1-T5 were designed as the polymers composed of 10 DP R-structure pEtEtOx (B block) and 10-50 DP pMeOx at both sides (A block), T6-T10 were 10 DP R-structure pPrMeOx (B block) and 10-50 DP pMeOx (A block). T21-23 were planned to be 20 DP R-/S-/RS- structure pEtEtOx (B block) and 35 DP pMeOx at each side (A block), T24-T26 were 20 DP R-/S-/RS- structure pPrMeOx (B block) and 35 DP pMeOx (A block). Similar to the homopolymers, the triblock copolymers were characterized by ¹H-NMR spectroscopy and SEC (see T1-T5 and T6-T10 in **Tab. 4.5** and **Fig. 4.14**, T21-T23 and T24-26 in **Tab. 4.6** and **Fig. 4.15**).

The water solubility of T1-T3 and T6-T8 were relatively poor in water and ethanol (< 20 g/L). However, the polymers T4-T5 and T9-T10 were well soluble in water and ethanol (≥20 g/L), T21-T26 were excellent soluble in water and ethanol (≥200 g/L). The chain length and ratio of hydrophobic and hydrophilic blocks related to the solubility, in the meantime the self-assembly might also be involved in this case.

Table 4.5 Polymer composition, number average molecular weight M_n and dispersity \mathcal{D} of synthesized triblock copolymers T1-T10.

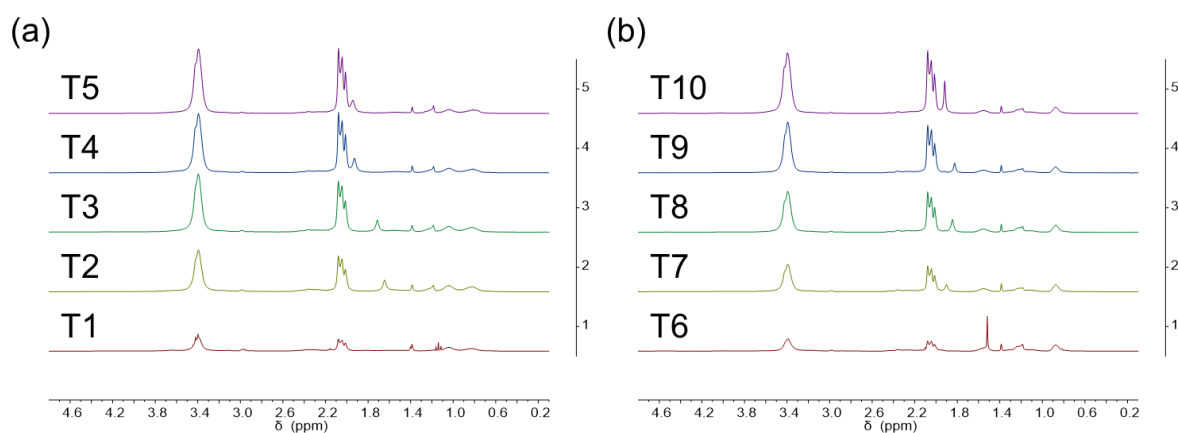
No.	Polymer composition	M_n ^{a)}	M_n ^{b)}	M_n ^{c)}	\mathcal{D} ^{c)}
		[kg mol ⁻¹]			
T1	Me-MeOx ₁₃ - <i>b</i> - ^R EtEtOx ₁₀ - <i>b</i> -MeOx ₁₃ -PipBoc	3.2	3.7	1.7	1.07
T2	Me-MeOx ₂₀ - <i>b</i> - ^R EtEtOx ₁₁ - <i>b</i> -MeOx ₂₀ -PipBoc	4.9	5.0	2.0	1.14
T3	Me-MeOx ₃₀ - <i>b</i> - ^R EtEtOx ₁₁ - <i>b</i> -MeOx ₃₀ -PipBoc	6.2	6.7	2.4	1.14
T4	Me-MeOx ₃₈ - <i>b</i> - ^R EtEtOx ₁₁ - <i>b</i> -MeOx ₃₈ -PipBoc	8.3	8.1	4.5	1.15
T5	Me-MeOx ₄₃ - <i>b</i> - ^R EtEtOx ₁₀ - <i>b</i> -MeOx ₄₃ -PipBoc	10.0	8.8	5.3	1.16
T6	Me-MeOx ₁₀ - <i>b</i> - ^R PrMeOx ₁₁ - <i>b</i> -MeOx ₁₀ -PipBoc	3.2	3.3	1.6	1.07
T7	Me-MeOx ₂₃ - <i>b</i> - ^R PrMeOx ₁₂ - <i>b</i> -MeOx ₂₃ -PipBoc	4.9	5.6	2.7	1.09
T8	Me-MeOx ₃₂ - <i>b</i> - ^R PrMeOx ₁₂ - <i>b</i> -MeOx ₃₂ -PipBoc	6.6	7.2	3.6	1.12
T9	Me-MeOx ₄₂ - <i>b</i> - ^R PrMeOx ₁₁ - <i>b</i> -MeOx ₄₂ -PipBoc	8.3	8.7	4.1	1.16
T10	Me-MeOx ₅₀ - <i>b</i> - ^R PrMeOx ₁₁ - <i>b</i> -MeOx ₅₀ -PipBoc	10.0	10.1	4.8	1.17

^{a)} theoretical molar mass from $[M]_0/[I]_0$; ^{b)} as obtained by ¹H-NMR (CDCl₃; 300 MHz) evaluated as mean of all relevant integral ratios; ^{c)} as obtained by SEC (# eluent: HFIP, PSS PFG linear M column, calibrated with PEG standards)

Table 4.6 Polymer composition, number average molecular weight M_n and dispersity \mathcal{D} of synthesized triblock copolymers T21-T26.

No.	Polymer composition	Abbrev.	M_n [kg mol ⁻¹]			\mathcal{D} ^{c)}
			M_n ^{a)}	M_n ^{b)}	M_n ^{c)}	
T21	Me-MeOx ₃₅ - <i>b</i> - ^R EtEtOx ₂₀ - <i>b</i> -MeOx ₃₅ -PipBoc	A-p ^R EtEtOx-A	8.7	8.7	4.6	1.12
T22	Me-MeOx ₃₅ - <i>b</i> - ^S EtEtOx ₂₁ - <i>b</i> -MeOx ₃₅ -PipBoc	A-p ^S EtEtOx-A	8.7	8.8	4.4	1.15
T23	Me-MeOx ₃₅ - <i>b</i> - ^{RS} EtEtOx ₂₀ - <i>b</i> -MeOx ₃₅ -PipBoc	A-p ^{RS} EtEtOx-A	8.7	8.7	4.2	1.16
T24	Me-MeOx ₃₄ - <i>b</i> - ^R PrMeOx ₂₂ - <i>b</i> -MeOx ₃₄ -PipBoc	A-p ^R PrMeOx-A	8.7	8.8	4.1	1.14
T25	Me-MeOx ₃₅ - <i>b</i> - ^S PrMeOx ₂₃ - <i>b</i> -MeOx ₃₅ -PipBoc	A-p ^S PrMeOx-A	8.7	9.1	4.0	1.15
T26	Me-MeOx ₃₄ - <i>b</i> - ^{RS} PrMeOx ₂₂ - <i>b</i> -MeOx ₃₄ -PipBoc	A-p ^{RS} PrMeOx-A	8.7	8.8	4.1	1.17

^{a)} theoretical molar mass from $[M]_0/[I]_0$; ^{b)} as obtained by ¹H-NMR (CDCl₃; 300 MHz) evaluated as mean of all relevant integral ratios; ^{c)} as obtained by SEC (# eluent: HFIP, PSS PFG linear M column, calibrated with PEG standards).

**Figure 4.14** ¹H-NMR (CDCl₃; 300 MHz; 298 K) of triblock copolymers (a) T1-T5 and (b) T6-T10.

¹H-NMR spectroscopy was applied to analyze the polymer composition, using the Boc moiety as important reference. The ¹H-NMR spectra of T21-T26 are shown as an example for triblock copolymers with signal assignment of all major signals in **Fig. 4.15**. The peak from CO-CH₃ (signal number 4, 2.08-2.01 ppm) and CH₃- (signal number 7 and 8, 1.30-0.81 ppm)

were treated as reference to calculate the DP of the A block and B block, respectively. The determined DP of triblock copolymers were shown in the **Tab. 4.5 and 4.6**.

With same feed ratio $[M]_0/[I]_0=10$ of $^R\text{EtEtOx}$ or $^R\text{PrMeOx}$, the $[M]_0/[I]_0$ of MeOx (each A block) increased from 10 to 50 to build the polymer T1-T5 and T6-T10. The $^1\text{H-NMR}$ spectra of the purified polymers revealed the different length of A block, and most of the polymers had a good synthetic control (**Fig. 4.14 and Tab. 4.5**).

The T21-T26 were designed as ABA polymers with same chain length but different type of B block which can be pEtEtOx or pPrMeOx with different chirality. Since T21-T26 were discussed more often on the chirality, their abbreviations were used when mention their stereostructure (abbreviations in **Tab. 4.6**). In achiral solvent chloroform-d, the $^1\text{H-NMR}$ spectra of T21-T23 were similar in shape and integrals (**Fig. 4.15a-c**). The stereoregularity of A-p $^R\text{EtEtOx-A}$, A-p $^S\text{EtEtOx-A}$ and A-p $^{RS}\text{EtEtOx-A}$ was not shown in $^1\text{H-NMR}$ spectra, which was consistent with the homopolymers pEtEtOx. As for the T24-T26, the $^1\text{H-NMR}$ spectra of A-p $^R\text{PrMeOx-A}$ and A-p $^S\text{PrMeOx-A}$ were quite similar (**Fig. 4.15d-f**), while the spectra of A-p $^{RS}\text{PrMeOx-A}$ showed a merged broad signal at 1.30-1.00 ppm. It was same phenomenon as the spectra of p $^R\text{PrMeOx}$, p $^S\text{PrMeOx}$ and p $^{RS}\text{PrMeOx}$, which indicated that the hydrophilic block pMeOx of the A-pPrMeOx-A did not destroy the conformation formed by the hydrophobic block p $^R\text{PrMeOx}$ and p $^S\text{PrMeOx}$ in chloroform.

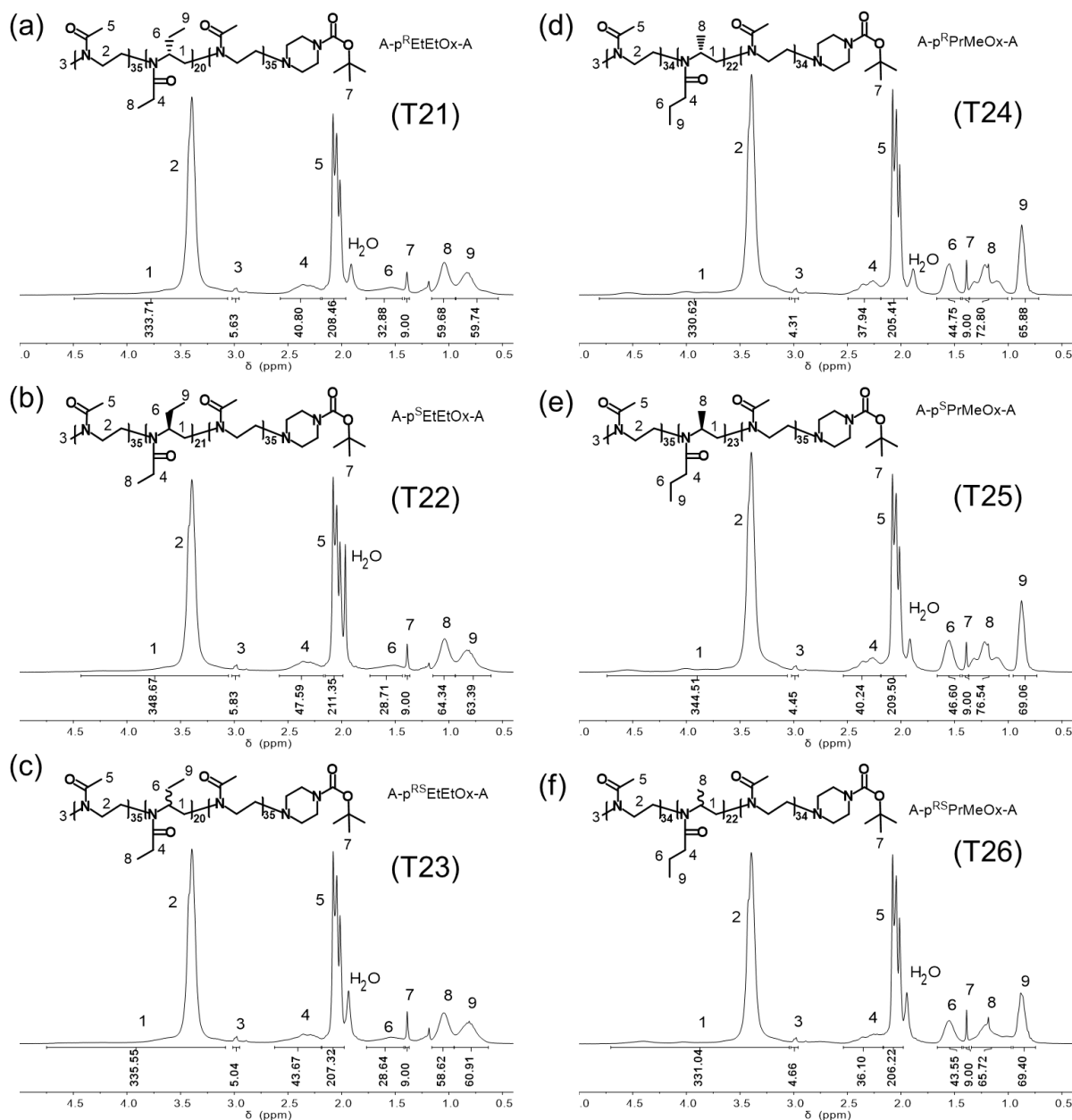


Figure 4.15 $^1\text{H-NMR}$ (CDCl_3 ; 300 MHz; 298 K) of triblock copolymers (a) $\text{A-p}^{\text{R}}\text{EtEtOx-A}$ (T21), (b) $\text{A-p}^{\text{S}}\text{EtEtOx-A}$ (T22), (c) $\text{A-p}^{\text{RS}}\text{EtEtOx-A}$ (T23), (d) $\text{A-p}^{\text{R}}\text{PrMeOx-A}$ (T24), (e) $\text{A-p}^{\text{S}}\text{PrMeOx-A}$ (T25) and (f) $\text{A-p}^{\text{RS}}\text{PrMeOx-A}$ (T26) with signal assignment of all major signals.

The SEC elugrams of T1-T10 showed narrow molar mass distribution ($\mathcal{D} < 1.2$) in **Fig. 4.16** (#eluent: HFIP; PSS PFG linear M column). The triblock copolymers with longer A block were eluted earlier, and have slightly increased dispersity \mathcal{D} (**Fig. 4.16** and **Tab. 4.5**). The purified T21-T26 and selected segment samples taken from the reaction mixture were analyzed by SEC (**Fig. 4.17** and **Tab. 4.6**), which not only showed the molar mass of the final polymers

but also reflected the control of each block over the polymerization. The monomers of three blocks were added into the reaction at equivalent quantity of 35:20:35 in succession (1 eq MeOTf initiator). The segment samples for SEC were taken after complete consumption of the current monomer. The SEC results of segment 1-3 showed peak shift from long to short elution time after consuming another segment, and the \bar{D} were all below 1.2.

According to the similar elugrams of purified polymers and the corresponding segment 3, it was clear that termination and purification process did not change the molar mass and dispersity markedly, especially the T21-23 and T26. In the case of T24-T25, the slight difference between the purified polymers and the corresponding segment 3 was suspected to be caused by the small amounts of precipitate appeared in the dialysis process, which related to self-assembly of the chiral polymers. Overall the polymerization of triblock copolymers found to be controlled well.

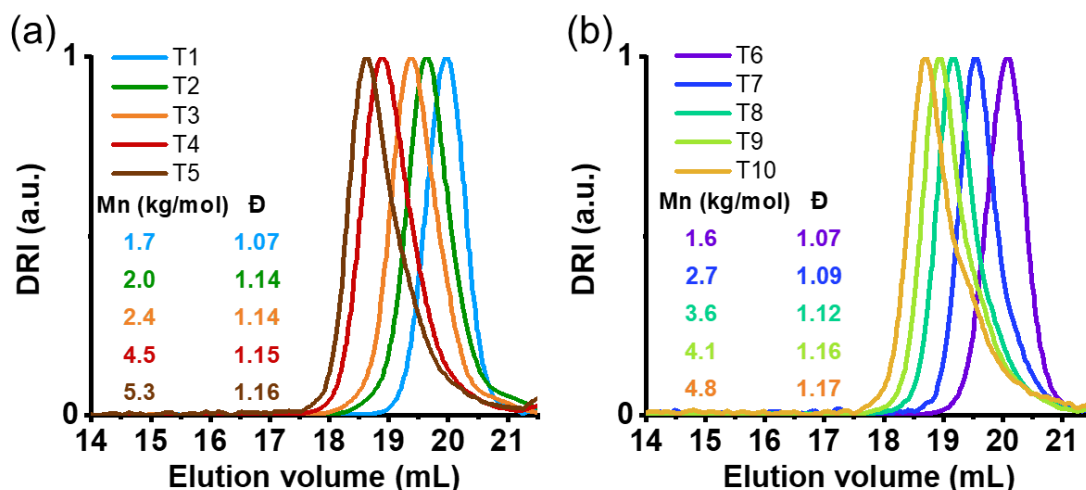


Figure 4.16 SEC elugrams of triblock copolymers (a) T1-T5 and (b) T6-T10 before purification. #Eluent: HFIP; PSS PFG linear M column.

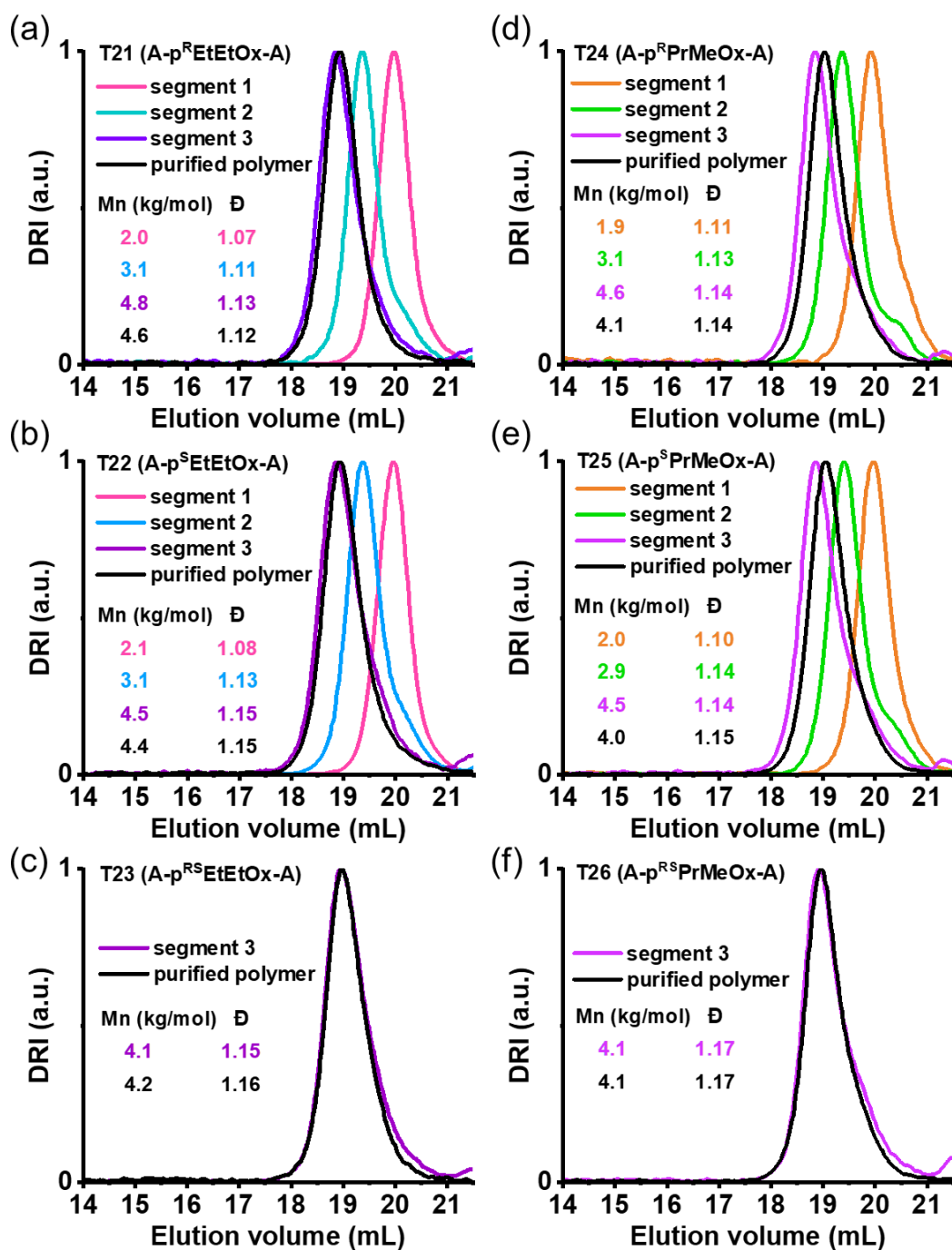


Figure 4.17 SEC elugrams of triblock copolymers (a) A-p^REtEtOx-A (T21), (b) A-p^SEtEtOx-A (T22), (c) A-p^{RS}EtEtOx-A (T23), (d) A-p^RPrMeOx-A (T24), (e) A-p^SPrMeOx-A (T25) and (f) A-p^{RS}PrMeOx-A (T26). Samples of segments were taken out of reaction, and polymers were purified. #Eluent: HFIP; PSS PFG linear M column.

4.3.2 Thermal properties of triblock copolymers

The influence of stereostructure and chains length on the thermal stability and T_g was exhibited in the **Chapter 4.2.1**. Similarly, the thermal properties of selected ABA triblock copolymers were also investigated using thermogravimetric analysis (TGA) and differential scanning calorimetry (DSC) (**Tab. 4.7** and **Fig. 4.18-21**).

Table 4.7 Glass transition temperatures T_g and the extrapolated onset temperature of major mass loss T_d of synthesized triblock copolymers.

No.	Polymer composition	Abbrev.	T_g ^{a)}	T_d ^{b)}
T1	Me-MeOx ₁₃ - <i>b</i> - ^R EtEtOx ₁₀ - <i>b</i> -MeOx ₁₃ -PipBoc	/	65	360
T2	Me-MeOx ₂₀ - <i>b</i> - ^R EtEtOx ₁₁ - <i>b</i> -MeOx ₂₀ -PipBoc	/	72	n.d.
T3	Me-MeOx ₃₀ - <i>b</i> - ^R EtEtOx ₁₁ - <i>b</i> -MeOx ₃₀ -PipBoc	/	75	n.d.
T4	Me-MeOx ₃₈ - <i>b</i> - ^R EtEtOx ₁₁ - <i>b</i> -MeOx ₃₈ -PipBoc	/	74	369
T5	Me-MeOx ₄₃ - <i>b</i> - ^R EtEtOx ₁₀ - <i>b</i> -MeOx ₄₃ -PipBoc	/	76	374
T6	Me-MeOx ₁₀ - <i>b</i> - ^R PrMeOx ₁₁ - <i>b</i> -MeOx ₁₀ -PipBoc	/	n.d.	393
T7	Me-MeOx ₂₃ - <i>b</i> - ^R PrMeOx ₁₂ - <i>b</i> -MeOx ₂₃ -PipBoc	/	n.d.	n.d.
T8	Me-MeOx ₃₂ - <i>b</i> - ^R PrMeOx ₁₂ - <i>b</i> -MeOx ₃₂ -PipBoc	/	n.d.	n.d.
T9	Me-MeOx ₄₂ - <i>b</i> - ^R PrMeOx ₁₁ - <i>b</i> -MeOx ₄₂ -PipBoc	/	72	376
T10	Me-MeOx ₅₀ - <i>b</i> - ^R PrMeOx ₁₁ - <i>b</i> -MeOx ₅₀ -PipBoc	/	74	374
T21	Me-MeOx ₃₅ - <i>b</i> - ^R EtEtOx ₂₀ - <i>b</i> -MeOx ₃₅ -PipBoc	A-p ^R EtEtOx-A	76	377
T22	Me-MeOx ₃₅ - <i>b</i> - ^S EtEtOx ₂₁ - <i>b</i> -MeOx ₃₅ -PipBoc	A-p ^S EtEtOx-A	76	377
T23	Me-MeOx ₃₅ - <i>b</i> - ^{RS} EtEtOx ₂₀ - <i>b</i> -MeOx ₃₅ -PipBoc	A-p ^{RS} EtEtOx-A	77	378
T24	Me-MeOx ₃₄ - <i>b</i> - ^R PrMeOx ₂₂ - <i>b</i> -MeOx ₃₄ -PipBoc	A-p ^R PrMeOx-A	71	374
T25	Me-MeOx ₃₅ - <i>b</i> - ^S PrMeOx ₂₃ - <i>b</i> -MeOx ₃₅ -PipBoc	A-p ^S PrMeOx-A	71	373
T26	Me-MeOx ₃₄ - <i>b</i> - ^{RS} PrMeOx ₂₂ - <i>b</i> -MeOx ₃₄ -PipBoc	A-p ^{RS} PrMeOx-A	73	380

^{a)} mean T_g obtained from second and third heating curve (DSC); ^{b)} Extrapolated onset temperature of major mass loss (TGA).
/: no Abbrev. n.d.: not determined.

The ABA triblock copolymers were comprised of pEtEtOx or pPrMeOx as hydrophobic B blocks and pMeOx as hydrophilic A blocks. Again, the weight loss of Boc was detected at ≈ 220 °C, and the loss ratio was related to the chain length. The resulting TGA curves exhibited two-step degradation pattern. The step 370-400 °C and 400-680 °C were attributed to the degradation of B blocks and A blocks, respectively (**Fig. 4.18**). When the hydrophobic B blocks were kept similar chain length ($DP \approx 10$) (T1-T4 and T6-T10), just increasing the length of hydrophilic A blocks hardly increased the T_d of major mass loss (≈ 370 °C) (**Tab. 4.7**), but

affected the plateau of second step. The length of the A block in T1 (DP=13) was much smaller compared to that of T4 (DP=38) and T5 (DP=43), which resulted in a lower second plateau of T1. The difference in A block length between T4 and T5 was not significant, which led to similar height of second plateau. Similarly, the TGA curve of T6, T9 and T10 also showed this difference in the plateau of second step. While the lengths of A blocks and B blocks were kept same (T21-T23 and T24-T26), the different stereostructure of the hydrophobic B blocks had no clear effect on the T_d (Tab. 4.7 and Fig. 4.19). Since the lengths of A blocks were quite close in the series of T21-T23 and T24-T26, the second plateaus almost coincided. In addition, comparing with the homopolymers ($T_d \approx 350$ °C), the T_d of triblock copolymers was slightly higher, which indicated that the triblock copolymers were slightly more stable than the homopolymers.

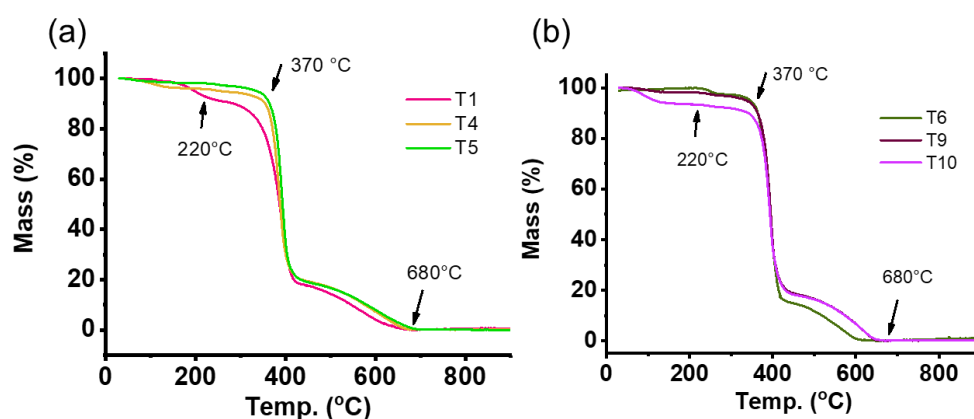


Figure 4.18 Weight loss occurring during TGA of triblock copolymers (a) T1, T4, T5 and (b) T6, T9, T10. Samples were heated from 30 to 900 °C with a heating rate of 10 °C/min.

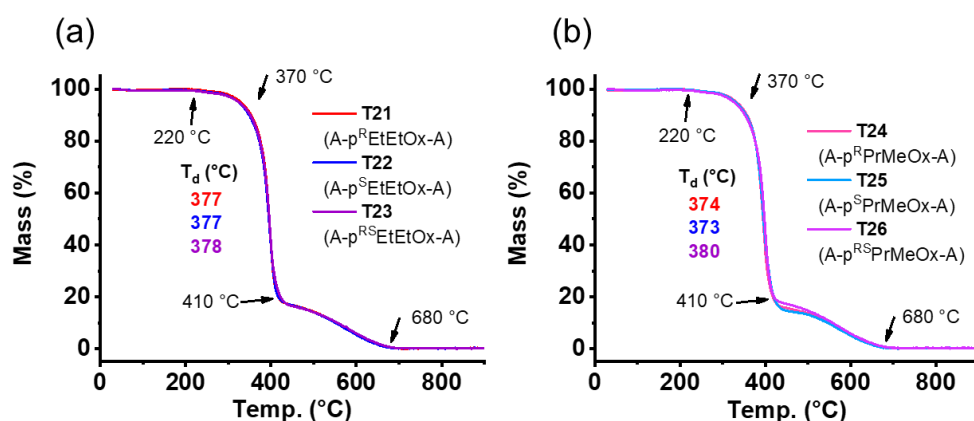


Figure 4.19 Weight loss occurring during thermogravimetric analysis of triblock copolymers (a) A-p^REtEtOx-A (T21), A-p^SEtEtOx-A (T22), A-p^{RS}EtEtOx-A (T23), (b) A-p^RPrMeOx-A (T24), A-p^SPrMeOx-A (T25) and A-p^{RS}PrMeOx-A (T26). Samples were heated from 30 to 900 °C with a heating rate of 10 °C/min.

The DSC heat flow of selected triblock copolymers were shown in **Fig. 4.20-21** (the third heating cycle). Analysis of the DSC traces of triblock copolymers showed the presence of only one T_g in each polymer measurement, and no T_m was detected in the temperature range of -50 to 190 °C. This indicated that no microphase separation or partial crystallization occurred in the triblock copolymers under the current experimental conditions.

Comparing with the triblock copolymers containing the same B block pEtEtOx, the T_g of the T1 (65 °C) was lower than T2-T5 ($T_g \approx 74$ °C) that had longer A blocks (**Fig. 4.20a**). Because the chain length of T1 was short, the DP increase still had impact on the T_g . When the polymer chains were longer than 50 DP, the T_g stabilized at around 74 °C. In the case of long triblock copolymers containing pPrMeOx, their T_g values turned to those of T9 ($T_g = 72$ °C) and T10 ($T_g = 74$ °C) (**Fig. 4.20b**). The T_g of T21-T23 was quite close ($T_g \approx 76$ °C), likewise, the T_g of T24-T26 had no big difference ($T_g \approx 71$ °C) (**Fig. 4.21**). This indicated that the stereostructure of the hydrophobic B block did not obviously influence the T_g of triblock copolymers with same chain length. Compared to the stereoisomers A-pPrOzi-A ($T_g \approx 50$ °C) and A-pBuOx-A ($T_g \approx 62$ °C)¹⁷³, the T21-T23 (A-pEtEtOx-A) and T24-T26 (A-pPrMeOx-A) had higher T_g values.

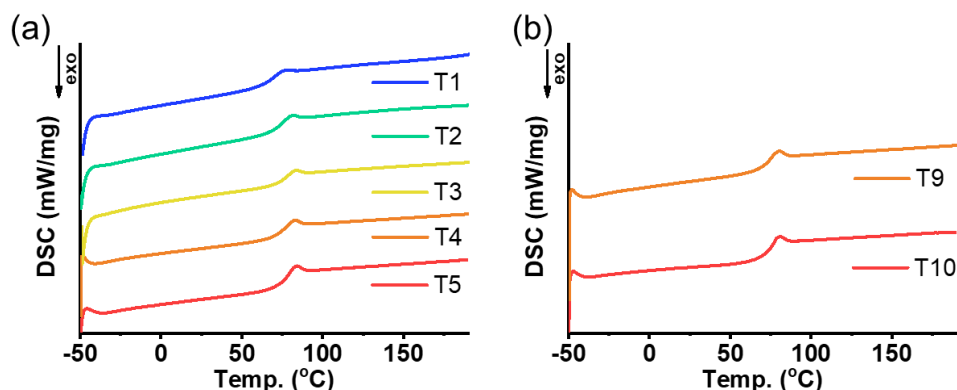


Figure 4.20 DSC heat flow of the third heating cycle of triblock copolymers (a) T1-T5 and (b) T9-T10. The samples were heated 3 times and cooled two times from -50 °C to 190 °C (10 °C/min).

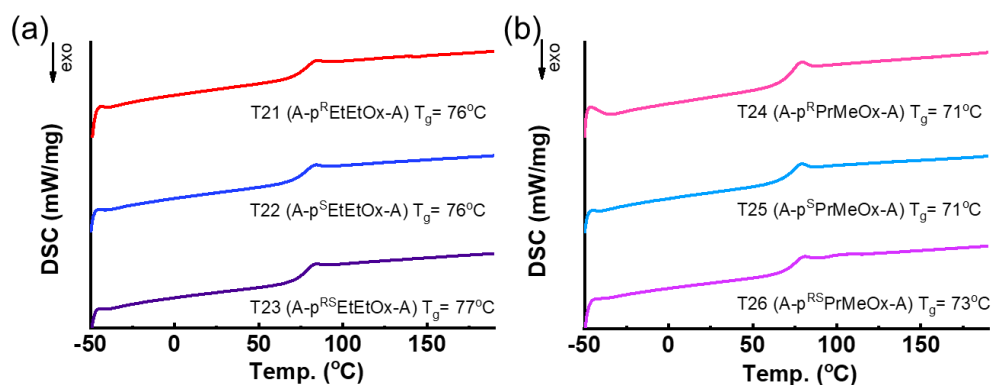


Figure 4.21 DSC heat flow of the third heating cycle of triblock copolymers (a) A-p^REtEtOx-A (T21), A-p^SEtEtOx-A (T22), A-p^{RS}EtEtOx-A (T23), (b) A-p^RPrMeOx-A (T24), A-p^SPrMeOx-A (T25) and A-p^{RS}PrMeOx-A (T26). The samples were heated 3 times and cooled two times from -50 °C to 190 °C (10 °C/min).

4.3.3 X-ray diffraction of triblock copolymers

Because of the excellent solubility in water and the potential in loading drug, the triblock copolymers T21-T26 were selected as examples be characterized with XRD at RT. Only broad bands were shown in their diffractograms (**Fig. 4.22**), which was consistent with the DSC result that the triblock copolymers were also amorphous despite the chirality of the hydrophobic block.

In the following experiment of critical micelle concentration and formulation characterization, some of polymer aqueous solutions turned cloudy after storing for some time. Therefore, XRD was applied again for the cloudy part of those samples and selected formulations, which will be shown in the **Chapter 4.4.3**.

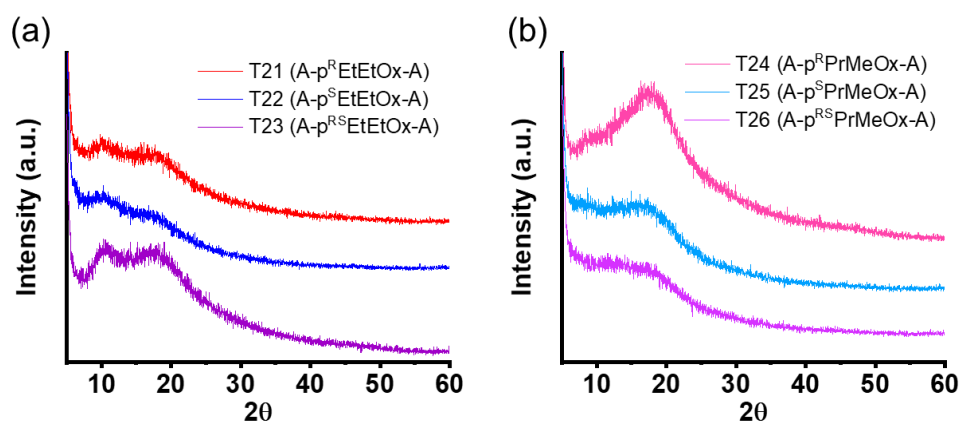


Figure 4.22 XRD patterns of triblock copolymers (a) A-p^REtEtOx-A (T21), A-p^SEtEtOx-A (T22), A-p^{RS}EtEtOx-A (T23), (b) A-p^RPrMeOx-A (T24), A-p^SPrMeOx-A (T25) and A-p^{RS}PrMeOx-A (T26).

4.3.4 Optical activity of triblock copolymers

The chiroptical activity of triblock copolymers T21-T26 and two 1/1 (w/w) mixtures of corresponding chiral triblock copolymers ($^M\text{A-pEtEtOx-A}$ and $^M\text{A-pPrMeOx-A}$) was measured by CD in both methanol and water at a polymer concentration of 0.1 g/L. In the methanol solution, the triblock copolymer $\text{A-p}^R\text{EtEtOx-A}$ (T21) and $\text{A-p}^R\text{PrMeOx-A}$ (T24) showed clear negative CE in the CD spectra, while the $\text{A-p}^S\text{EtEtOx-A}$ (T22) and $\text{A-p}^S\text{PrMeOx-A}$ (T25) showed clear positive CE (**Fig. 4.23a, b**). Apparently, the secondary structure induced by the chiral block was not prevented by the optically inactive pMeOx block. In the meantime, it should also be noticed that the CD spectra of triblock copolymers were not as smooth as those of homopolymers. The chiral block contents of triblock copolymers were lower than that of chiral homopolymers at the same polymer concentration (0.1 g/L), therefore, the CD values of triblock copolymers were smaller and more susceptible to numerical fluctuations than that of homopolymers. Considering the following hydration process in the formulation, the triblock copolymers were also investigated by CD in aqueous solution. The chiral triblock copolymers retained the CE in aqueous solution either at 25 °C or 50 °C (**Fig. 4.23c, d**). Compared with the CD spectra of chiral polymers at 25 °C, the maximum CD values of corresponding polymers at 50 °C showed a tendency to shift towards shorter wavelengths. Considering the exception, $\text{A-p}^S\text{EtEtOx-A}$ did not show this shift at 50 °C, it is hard to determine whether the shift is caused by numerical fluctuations, or if the high temperature has changed the secondary structure. In addition, the triblock copolymer $\text{A-p}^{RS}\text{EtEtOx-A}$ (T23), $\text{A-p}^{RS}\text{PrMeOx-A}$ (T26), mixture $^M\text{A-pEtEtOx-A}$ and $^M\text{A-pPrMeOx-A}$ did not show CE in methanol or aqueous solution.

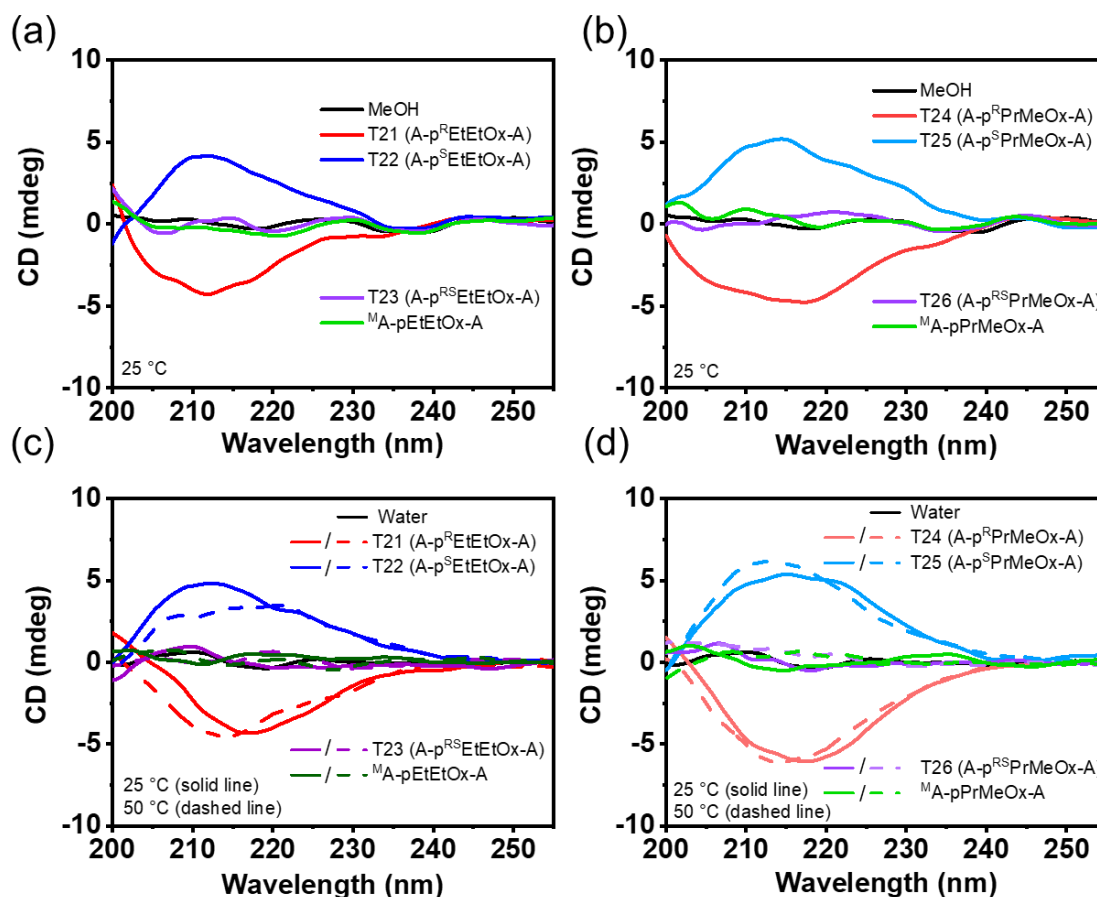


Figure 4.23 CD spectra of A-p^REtEtOx-A (T21), A-p^SEtEtOx-A (T22), A-p^{RS}EtEtOx-A (T23), ^MA-pEtEtOx-A (1/1 (w/w) ratio mixture of T21 and T22) in (a) methanol (at 25 °C) and (c) water (at 25 °C and 50 °C). CD spectra of A-p^RPrMeOx-A (T24), A-p^SPrMeOx-A (T25), A-p^{RS}PrMeOx-A (T26) and ^MA-pPrMeOx-A (1/1 (w/w) ratio mixture of T24 and T25) in (b) methanol (at 25 °C) and (d) water (at 25 °C and 50 °C). Polymer concentration was 0.1 g/L.

4.3.5 Conclusion

In summary, ABA triblock copolymers were synthesized using pMeOx as A block and chiral/racemic pEtEtOx or pPrMeOx as B block via LCROP, and subsequently characterized by ¹H-NMR spectroscopy, SEC, TGA, DSC and CD spectroscopy. The characterization of triblock copolymers can benefit the understanding of application.

The chain length, ratio of hydrophobic and hydrophilic and the chirality of the triblock copolymers had a clear effect on the solubility. The synthesized polymers T1-T3 and T6-T8 composed of 10 DP B block (R isomer of pEtEtOx and pPrMeOx) and 10-30 DP A block were

poor soluble in water and ethanol (< 20 g/L), while the polymers with longer A block (T4-T5 and T9-T10) or polymers composed of 20 DP B block and 35 DP A block (T21-T26) had better solubility. Regardless the length of the A block and the ratio of A/B block, the main chain of triblock copolymers was a little more stable than the homopolymers. In the meantime, similar to the homopolymers, the chirality hardly affected the thermal properties of the triblock copolymers. The triblock copolymers were studied by CD spectroscopy in solution. The chiral triblock copolymers showed clear CE in methanol and water, which indicated that the chiral triblock copolymers were able to form secondary structure in solution. In contrast, the triblock copolymers with racemic B block and the 1/1 (w/w) mixtures did not show CE.

4.4 Applicability of chiral/racemic triblock copolymers based micelles as a drug delivery system

Because of the large amount of chiral substances in biological systems, artificial stereoactive polymers attract increasing attention, and are potentially applied in the field of specific drug delivery, polymeric chiral catalyst, separation and purification of racemic mixture, *etc.* This research is related to the chiral drug delivery systems based on POx ABA-type triblock copolymers with chiral and racemic hydrophobic blocks for the formulation of chiral and achiral drugs. Specifically, pEtEtOx or pPrMeOx were used as hydrophobic B block and pMeOx as hydrophilic A block. Curcumin (CUR), paclitaxel (PTX), as well as chiral and racemic ibuprofen (R, S and RS-IBU) were used as model compounds for the preparation of nanoformulations. The prepared blank polymer micelles and formulations were characterized.

4.4.1 Fluorescence spectroscopy-critical micelle concentration

The critical micelle concentration (CMC) is the concentration above which micelles form. The CMC of the synthesized ABA triblock copolymers was determined by pyrene assay. When the pyrene assay was performed in summer, the data points obtained were highly scattered so that it was difficult to determine any regularity. However, with the same experiment procedure in winter time ($\approx 20\text{ }^{\circ}\text{C}$ overnight), the results in **Fig. 4.24** were obtained. It seems that the ambient temperature influences the result of pyrene assay. Although the pEtEtOx and pPrMeOx have thermoresponsive behavior, it can not explain the temperature influence on the CMC of the triblock copolymers. The CMC values of A-pEtEtOx-A and A-pPrMeOx-A series polymers were 1-4 g/L (*i.e.*, $1\text{-}4 \times 10^{-4}$ M). This is much higher than A-pBuOx-A (8 mg/L, 1×10^{-6} M), while another isomer A-PrOzi-A does not show CMC value in pyrene assay.¹⁷⁴

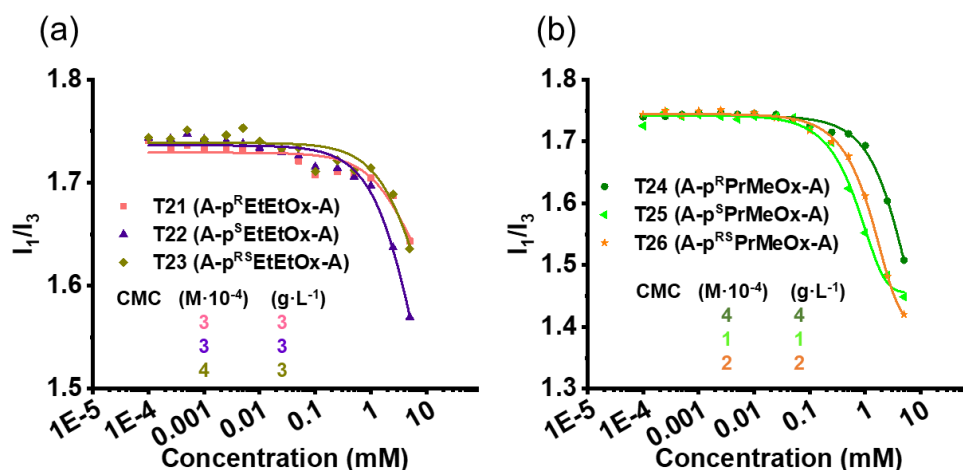


Figure 4.24 $I_1:I_3$ ratio determined from hyperfine structure of pyrene fluorescence spectra in dependence of the ABA triblock copolymer concentration with corresponding fits. (a) A-p^REtEtOx-A, A-p^SEtEtOx-A and A-p^{RS}EtEtOx-A; (b) A-p^RPrMeOx-A, A-p^SPrMeOx-A and A-p^{RS}PrMeOx-A.

4.4.2 Drug formulation

Curcumin (CUR), paclitaxel (PTX) and ibuprofen (IBU) were applied in formulation as model drugs. PTX, sold commercially as Taxol, is an anti-cancer chemotherapeutic agent in the therapy of various cancers, such as lung, ovarian and breast cancers.¹⁷⁵ PTX has with multiple chiral centers, but does not have a known enantiomer. Its water solubility is poor with about 0.4 - 4 $\mu\text{g}/\text{mL}$.¹⁷⁶ CUR is an achiral, yellow-colored polyphenol obtained from *Curcuma longa*.¹⁷⁷ It has been reported to have many biological effects such as influencing the expression of inflammatory cytokines, adhesion molecules, enzymes, the activity of several transcription factors and their signaling pathways, therefore, it has the potential to be used for the treatment of cancer, neurodegenerative disease, hepatic disorders, atherosclerosis, diabetes, *etc.*¹⁷⁸ Apart from the poor solubility of 1 - 10 $\mu\text{g}/\text{mL}$,¹⁷⁹ CUR is also considered a pan assay interference compound (PAIN) or invalid metabolic panacea (IMP), which originates from its chemical instability in aqueous media.¹⁸⁰⁻¹⁸¹ Because of these interesting issues, CUR could be an interesting compound for formulation studies. Both PTX and CUR have been investigated in different drug delivery systems to improve their aqueous solubility and thus, bioavailability.^{176, 182-184} Among them, some formulations based on POx and POzi show high overall solubilisation and extraordinary high drug loading capacity for PTX and CUR.^{152, 173, 185-187} Thus, PTX and

CUR were used as common drug model. IBU is a non-steroidal anti-inflammatory drug, has one stereogenic carbon atom which brings two types of enantiomers, R-IBU and S-IBU.¹⁸⁸ Its commercial drug is available as racemate, though the S-IBU is more potent than R-IBU as inhibitor of cyclo-oxygenase I.^{1, 189} Its enantiomers can be purchased separately. Besides, IBU is a very hydrophobic compound with water solubility of around 21 mg/L.¹⁹⁰ Therefore it was used as a chiral model drug for the formulation preparation. The model drugs were formulated with the synthesized ABA triblock copolymers by the thin film hydration method (**Fig. 4.25**)¹⁵².

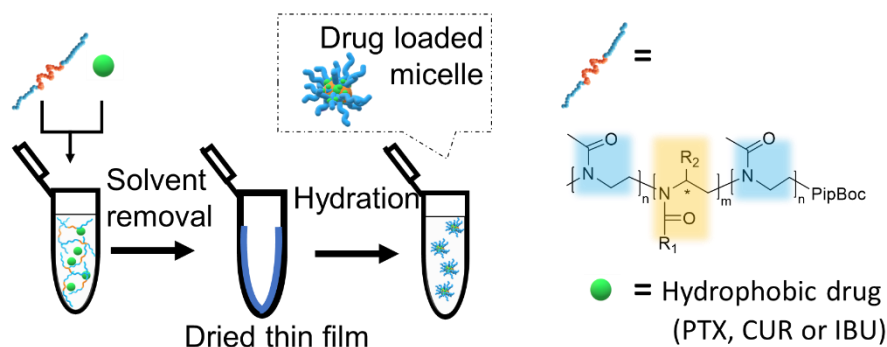


Figure 4.25 Schematic representation of the thin film hydration method.

The polymer and drug were dissolved in ethanol separately, then mixed in desired ratios. After the removal of ethanol, a thin film was left in the tube. Millipore water was added to hydrate the film. Finally, non-solubilized drug (and polymer) was removed by centrifugation, if there was any. The soluble drug concentration was analyzed by HPLC or UV spectroscopy (detail in Chapter 7.2.1). The standard curves of each drug is shown in **Fig.4.26**.

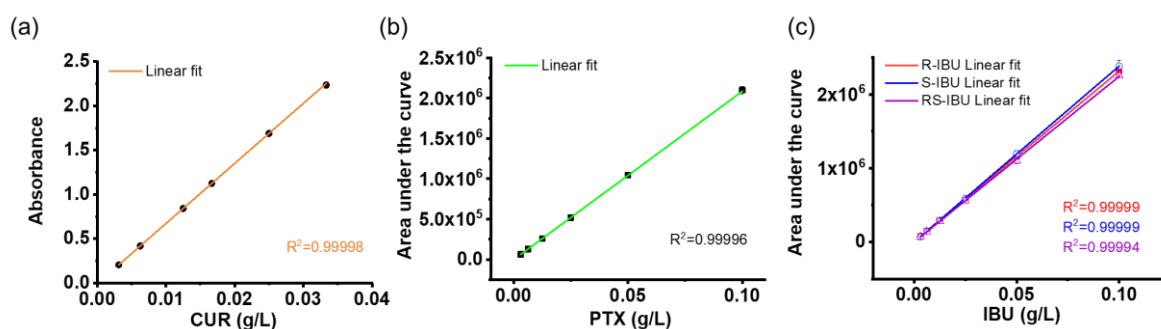


Figure 4.26 (a) Calibration curve of CUR as determined by UV-Vis absorption (on a BioTek Eon Microplate Spectrophotometer) with corresponding linear fit. Calibration curves of (b) PTX and (c) IBU were measured by HPLC with corresponding linear fit.

Many triblock copolymers were synthesized and characterized, but some of them were found not suitable for formulation after being formulated with CUR and PTX. When the triblock copolymers were formulated with CUR, T2 and T8 showed the best drug loading capacity in the series of T1-T5 and T6-10, respectively (Fig. 4.27a-b). However, their drug loading capacity were still much lower than the T21-T26 (*vide infra*). In the case of PTX loaded formulation, none of T1-T10 had usable performance even at very low PTX feed (1 g/L) (Fig. 4.27c-d).

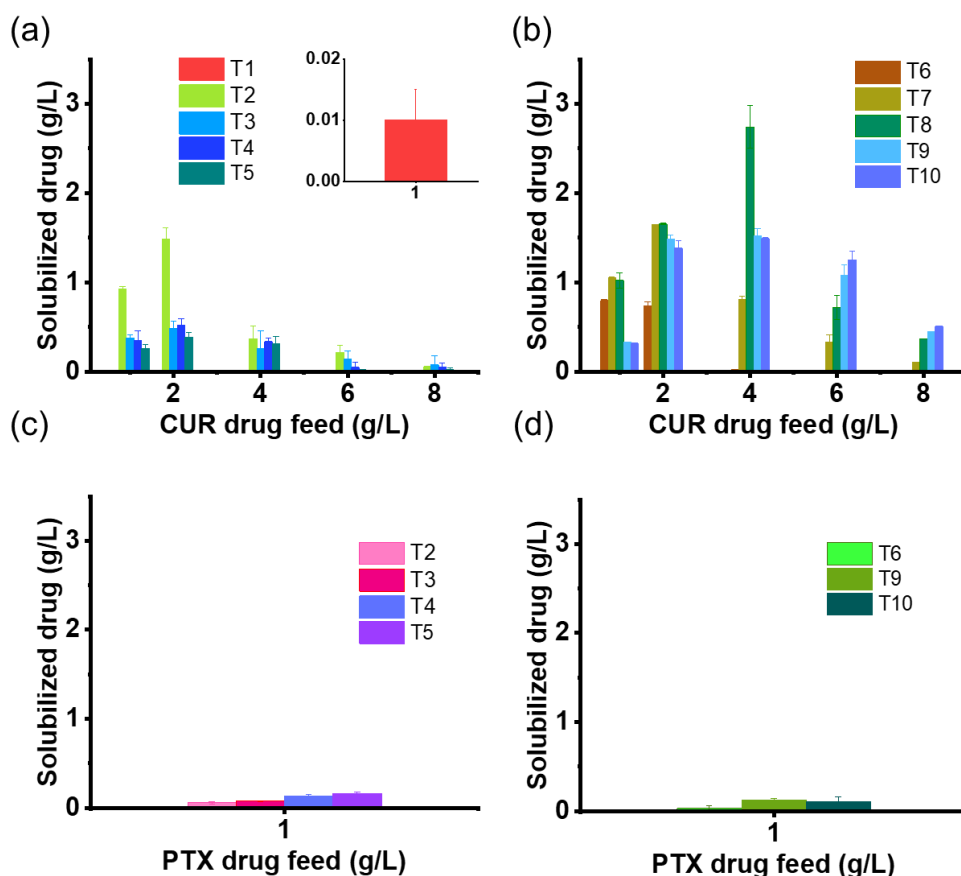


Figure 4.27 Solubilized CUR concentrations of CUR formulated (a) T1-T5, (b) T6-T10 in dependence of the CUR feed concentration. Solubilized PTX concentrations of PTX formulated (c) T2-T5, (d) T6-T10 at PTX feed of 1 g/L. The solubilized PTX concentrations of PTX formulated T1, T7 and T8 was not detected by HPLC. Polymer feed was 10 g/L. The data is given as means \pm SD ($n = 3$).

The triblock copolymer T21-T26 behaved much better than other polymers mentioned above in drug loading, therefore more attention was paid on the characterization of their solution and formulation. The abbreviations (*e.g.* A-p^REtEtOx-A) of T21-T26 are used more frequently for ease of understanding. In order to assess the drug loading capacity between different stereoisomers, 1/1 (w/w) mixtures of two corresponding chiral triblock copolymers were also

used for drug formulations apart from the triblock copolymers with chiral and racemic hydrophobic blocks. The mixtures are abbreviated as M A-pEtEtOx-A and M A-pPrMeOx-A.

The optical appearance of centrifuged formulations is shown in **Fig. 4.28**. The formulations of CUR-loaded A-p^REtEtOx-A (T21), A-p^SEtEtOx-A (T22), A-p^{RS}EtEtOx-A (T23) and M A-pEtEtOx-A were similar in appearance. Up to 4 g/L CUR feed, the formulations appeared homogenous and transparent, while a minor precipitate with transparent supernatant was observed at 6 g/L CUR feed (**Fig. 4.28a left**). In contrast, the formulation showed three layers when the CUR feed increased to 8 g/L and 10 g/L: a small amount of precipitate at the bottom of the tube, the majority of opaque layer in middle and a thin transparent layer on top (**Fig. 4.28a right, b, c and d**). The opaque layer could not be sedimented by an extra centrifugation of 5 min (rcf= 7788 g). It was also different from the gel-like agglomerate or coacervate which was reported in the formulation of A-poly(2-(3-ethylheptyl)-2-oxazoline)-A (A-pEtHepOx-A) and CUR.¹⁶³ Understanding this opaque layer would be interesting, but it is beyond the scope of present work. Accordingly, all the samples were obtained from the transparent layer for the CUR concentration analysis. The CUR-loaded A-p^RPrMeOx-A (T24), A-p^SPrMeOx-A (T25), A-p^{RS}PrMeOx-A (T26) and M A-pPrMeOx-A formulations were also transparent and homogenous up to 4 g/L CUR feed. When the CUR feed reached 6-10 g/L (except the formulation with A-p^{RS}PrMeOx-A at 10 g/L CUR feed.), a significant amount of sediment and a transparent supernatant was observed (**Fig. 4.28e, f, g left and h**). The notable exception A-p^{RS}PrMeOx-A/CUR=10/10 (g/L) (feeding ratio) was repeated extra two times to confirm. It showed different appearance from other A-pPrMeOx-A at 10 g/L CUR feed, but similar to the A-pEtEtOx-A formulations at 10 g/L CUR feed (**Fig. 4.28g right**).

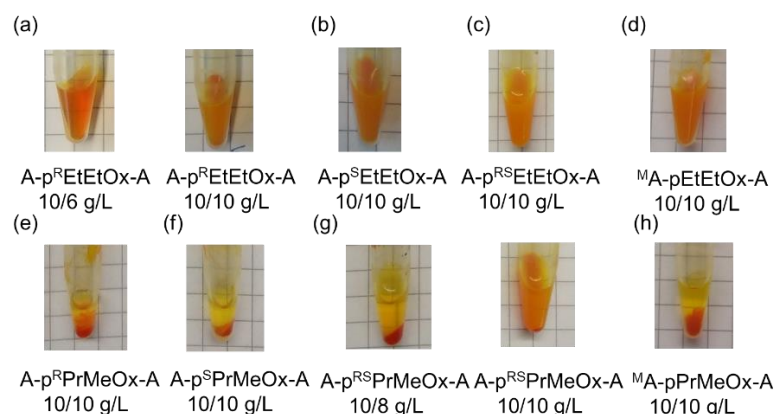


Figure 4.28 The optical appearance of CUR formulations of (a) A-pEtEtOx-A at polymer/drug-feed ratio of 10/6 and 10/10 g/L at day 0, (b) A-pPrMeOx-A at polymer/drug-feed ratios of 10/8 and 10/10 g/L.

The concentration of solubilized drug increased with the increasing of CUR and PTX feed until it reached the maximum loading capacity (LC) (**Fig. 4.29**). When the CUR or PTX

was formulated with A-pEtEtOx-A series at the same drug feed, similar CUR or PTX concentrations were obtained in the formulations of A-p^REtEtOx-A, A-p^SEtEtOx-A, A-p^{RS}EtEtOx-A, and ^MA-pEtEtOx-A formulations, respectively (**Fig. 4.29a, c**). Similarly, the CUR or PTX concentration of A-pPrMeOx-A series formulations showed no obvious difference at same CUR or PTX feed, with the exception of A-p^{RS}PrMeOx-A/CUR=10/10 (g/L) (**Fig. 4.29b, d**). As mentioned above, the optical appearance of A-p^{RS}PrMeOx-A/CUR=10/10 (g/L) was more similar to the A-pEtEtOx-A formulations at 10 g/L CUR feed, in the meantime, the solubilized CUR concentration was also similar in these and much higher than the formulation of A-p^RPrMeOx-A, A-p^SPrMeOx-A and ^MA-pPrMeOx-A. The chirality of the hydrophobic block in ABA triblock copolymers has no obvious effect in solubilizing CUR and PTX in most cases. But when A-p^{RS}PrMeOx-A was given extremely large amount of specific drug (*e.g.* CUR), the self-assembly of the polymer might affect drug loading.

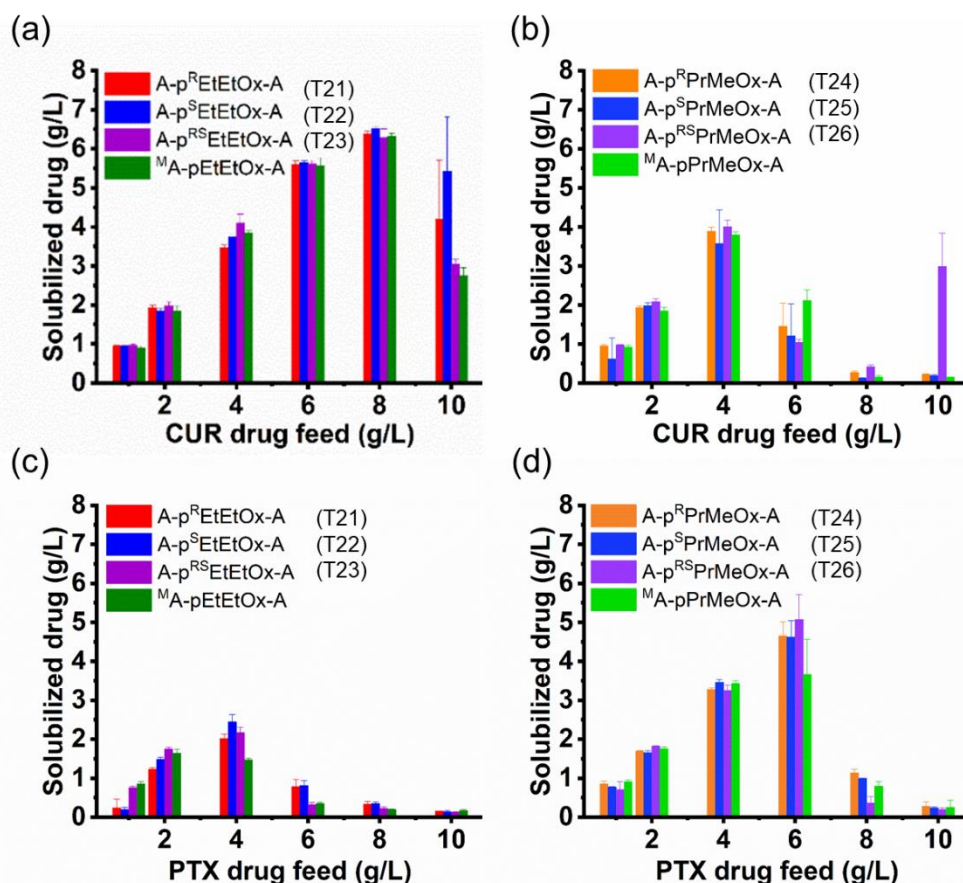


Figure 4.29 The solubilized CUR concentrations of CUR formulated (a) A-pEtEtOx-A and (b) A-pPrMeOx-A series in dependence of the CUR feed concentration. Solubilized PTX concentrations of PTX formulated (c) A-pEtEtOx-A and (d) A-pPrMeOx-A series in dependence of the PTX feed concentration. Polymer feed was 10 g/L. The data is given as means \pm SD (n = 3, with the exception of A-p^{RS}PrMeOx-A/CUR=10/10 g/L which is n = 5).

With respect to the maximum drug loading, there was no significant difference within each polymer series, but the difference between A-pEtEtOx-A series and A-pPrMeOx-A series was obvious (**Fig. 4.30a**). The maximum LC of A-pEtEtOx-A series was CUR 39-40 wt% (6.3-6.5 g/L) and PTX 17-20 wt% (2.0-2.4 g/L). The maximum CUR LC of A-pPrMeOx-A series was 28-29 wt% (3.6-4.0 g/L), while the maximum PTX LC was 32-34 wt% (4.6-5.0 g/L). The A-pEtEtOx-A series polymer solubilize more CUR than PTX, while the A-pPrMeOx-A series polymer tended to load more PTX than CUR. The different positioning of a methylene group between the amide side-chain and the backbone branch led to specific drug loading of A-pEtEtOx-A and A-pPrMeOx-A for CUR and PTX, respectively. A similar specific drug loading between constitutional isomers was also found in the work of Lübtow *et al.*, which showed that a migration of a methylene group from the polymer side-chain to the polymer main chain (comparing A-pBuOx-A and A-pPrOzi-A) led to a specific drug loading for CUR and PTX, respectively.¹⁵² Comparing the maximum CUR and PTX LC of A-pEtEtOx-A and A-pPrMeOx-A with other constitutional isomers in literature, the order for CUR is A-pPrOzi-A (≈ 54 wt%) > A-pEtEtOx-A (≈ 40 wt%) > A-pPrMeOx-A (≈ 29 wt%) \geq A-pBuOx-A (≈ 24 wt%), the order for PTX is A-pBuOx-A (≈ 48 wt%) > A-pPrMeOx-A (≈ 32 wt%) > A-pPrOzi-A (≈ 25 wt%) > A-pEtEtOx-A (≈ 18 wt%).

The A-pEtEtOx-A and A-pPrMeOx-A series triblock copolymers were also used to solubilize R-IBU, S-IBU and RS-IBU comparing the solubilization of a chiral drug in chiral and achiral POx for the first time. Both series of polymers had relatively high IBU LC, and the maximum IBU LC of triblock copolymers is shown in **Fig.4.30b**. In the A-pEtEtOx-A series formulations, the A-p^REtEtOx-A/R-IBU showed the highest LC of 37 wt%, and the A-p^{RS}EtEtOx-A/S-IBU showed the lowest LC of 32 wt%. In the A-pPrMeOx-A series, the highest LC was A-p^{RS}PrMeOx-A/R-IBU (36 wt%) and the lowest LC were A-p^RPrMeOx-A/RS-IBU and ^MA-pPrMeOx-A/S-IBU (31 wt%). The maximum LC values of the rest formulations fell in this range, and no clear regularity was found. No clear specific drug loading was found in the formulations of IBU loaded A-pEtEtOx-A and A-pPrMeOx-A, which was different from the CUR and PTX loaded formulations.

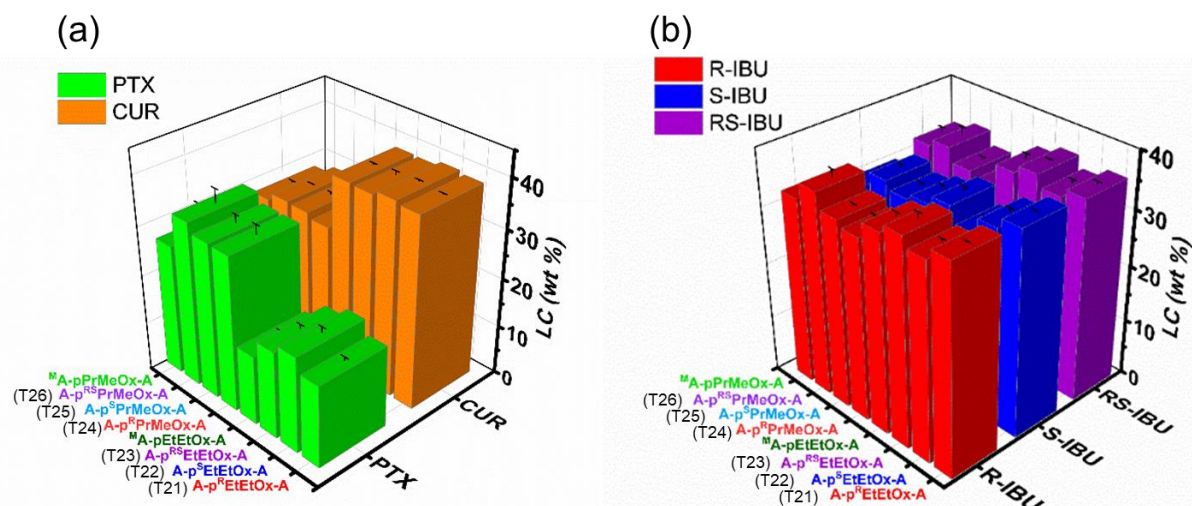


Figure 4.30 The maximum drug loading capacity of triblock copolymers and mixed polymers, for (a) CUR (orange) and PTX (green), and (b) R-IBU (red), S-IBU (blue) and RS-IBU (purple). Polymer feed was 10 g/L.

Before discussing the difference between the polymers, the LC data of R, S and RS-IBU loaded in the same triblock copolymer was arranged in one coordinate system to see the difference of R-, S- and RS-IBU (Fig. 4.31). For the same polymer, R, S and RS-IBU were similarly loaded up to 6 g/L IBU feed. In contrast, when the drug feed was at 8 g/L, the LC values of S-IBU lagged behind R-IBU and RS-IBU in several polymers, especially in A-p^{RS}EtEtOx-A and A-p^{RS}PrMeOx-A. In the meantime, both of A-p^{RS}EtEtOx-A and A-p^{RS}PrMeOx-A (Fig. 4.31c, g) showed the maximum LC of R and RS-IBU at drug feed 8 g/L, while the others had maximum LC at drug feed 6 g/L. The mixture M A-pEtEtOx-A and M A-pPrMeOx-A did not show significant difference between R, S and RS-IBU even up to 8 g/L (Fig. 4.31d, h). Compared to R- and RS-IBU, the relatively low S-IBU loading observed in the synthesized polymers at high drug feed was unexpected and not explained. It is assumed that the stereostructure related self-assembly between the drug and polymer may be responsible. The formulations of 10 g/L drug feed were not stable and observed no systematic difference between the drugs.

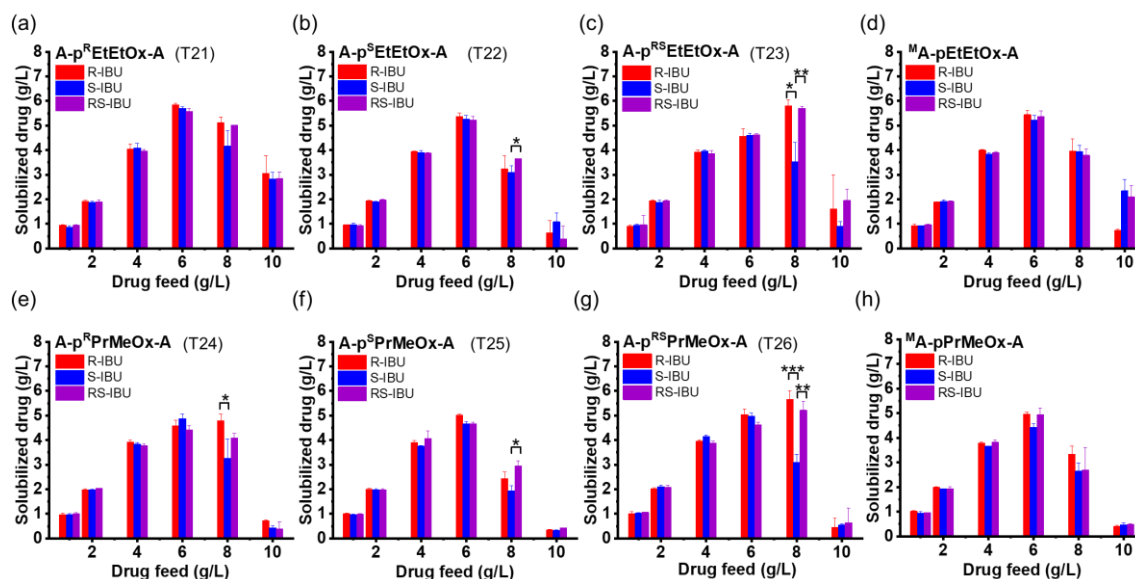


Figure 4.31 Solubilized IBU concentrations of formulation in dependence of the IBU feed concentration (R-IBU, red bar; S-IBU, blue bar; RS-IBU, purple bar). R-IBU, S-IBU and RS-IBU were separately solubilized with (a) A-p^REtEtOx-A (T21), (b) A-p^SEtEtOx-A (T22), (c) A-p^{RS}EtEtOx-A (T23), (d) ^MA-pEtEtOx-A, (e) A-p^RPrMeOx-A (T24), (f) A-p^SPrMeOx-A (T25), (g) A-p^{RS}PrMeOx-A (T26) and (h) ^MA-pPrMeOx-A. Polymer feed was 10 g/L. Data is given as means \pm SD (n = 3). * p<0.05; ** p<0.01; *** p<0.001.

The solubilized IBU concentration of the same IBU formulated A-pEtEtOx-A series polymers are shown in **Fig. 4.32** to see the difference between polymers. No obvious difference of the IBU loading was observed in A-pEtEtOx-A polymers including the mixture until the IBU feed reached 6 g/L. At 6 g/L IBU feed, the A-p^{RS}EtEtOx-A showed the lowest drug loading of R-, S- and RS-IBU and the A-p^REtEtOx-A showed the highest drug loading, while the ^MA-pEtEtOx-A and A-p^SEtEtOx-A had similar and intermediate drug loading. In contrast, the drug loading of A-p^{RS}EtEtOx-A was the highest for R and RS-IBU at 8 g/L feed (**Fig. 4.32a, c**), the A-p^SEtEtOx-A turned to have the lowest drug loading for all three IBU. Different from the A-pEtEtOx-A series, the A-pPrMeOx-A series did not show regular difference in drug loading between each other at 6 g/L IBU feed (**Fig. 4.33**). However, similar to the formulations of A-pEtEtOx-A series at 8 g/L IBU feed, the A-p^{RS}PrMeOx-A showed highest drug loading for R- and RS-IBU, and the A-p^SPrMeOx-A had low drug loading. The chirality distinction of the A-pEtEtOx-A series appeared at lower drug feed (6 g/L) than A-pPrMeOx-A series (8 g/L), to a certain degree, the chirality of pEtEtOx block had more impact on the solubilization of IBU than that of pPrMeOx block. Besides, the triblock copolymers containing p^SEtEtOx or p^SPrMeOx blocks showed low drug loading at high IBU feed (8 g/L). It seems that the S-isomer

“disadvantage” discussed above for S-IBU also appears in A-p^SEtEtOx-A and A-p^SPrMeOx-A, but it can't be explained at the moment.

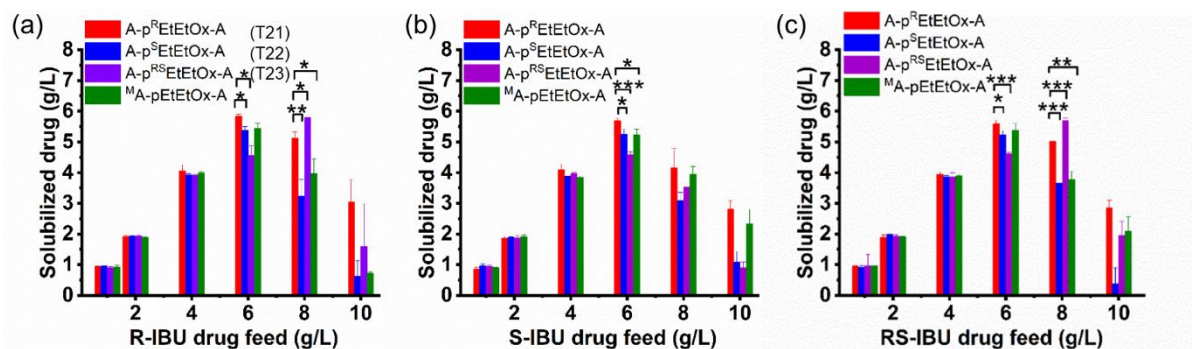


Figure 4.32 Solubilized (a) R-IBU, (b) S-IBU and (c) RS-IBU concentrations of IBU formulated A-p^REtEtOx-A (red), A-p^SEtEtOx-A (blue), A-p^{RS}EtEtOx-A (purple) and ^MA-pEtEtOx-A (green) in dependence of the IBU feed concentration. Polymer feed was 10 g/L. Data is given as means \pm SD (n = 3). * p<0.05; ** p<0.01; *** p<0.001.

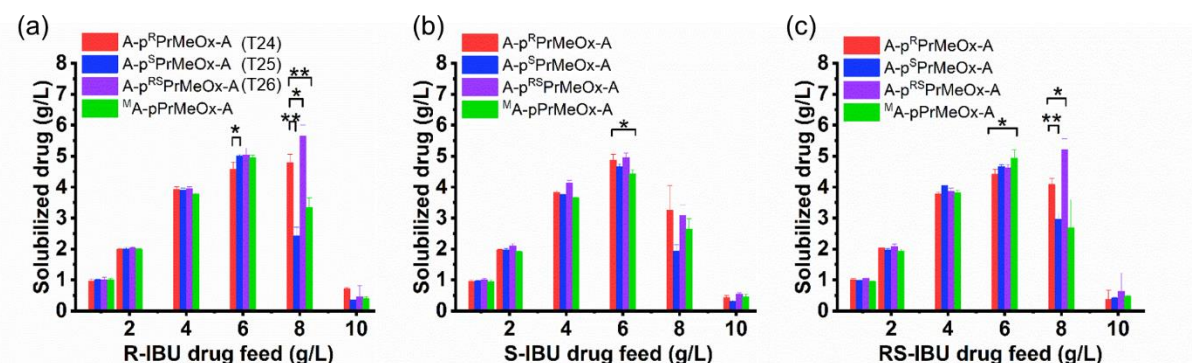


Figure 4.33 Solubilized (a) R-IBU, (b) S-IBU and (c) RS-IBU concentrations of IBU formulated A-p^RPrMeOx-A (light red), A-p^SPrMeOx-A (light blue), A-p^{RS}PrMeOx-A (light purple) and ^MA-pPrMeOx-A (light green) in dependence of the IBU feed concentration. Polymer feed was 10 g/L. Data is given as means \pm SD (n = 3). * p<0.05; ** p<0.01; *** p<0.001.

4.4.3 Dynamic light scattering

The hydrodynamic diameter (D_h) of unloaded, CUR loaded and IBU loaded polymer micelles were analyzed by dynamic light scattering (DLS). For the unloaded samples, the triblock copolymers were dissolved in PBS (polymer concentration 10 g/L), filtered with 0.45 μ m PVDF filter and measured at day 0 and 7 by DLS at 25 $^{\circ}$ C. The DLS profiles of the polymer

solutions were bi- or multimodal with broad size distribution, indicating heterogeneous particle populations (**Fig. 4.34a-b**). Comparing the size distribution by intensity, volume and number, using the DLS profiles of ^MA-pEtEtOx-A and ^MA-pPrMeOx-A at day 0 as examples (**Fig. 4.34e-f**), it becomes clear that mainly small self-assemblies (presumably micelles) of $D_h \approx 5$ nm were present in the ^MA-pEtEtOx-A and ^MA-pPrMeOx-A solution, along with very few but much larger particles (apparent $D_h \leq 250$ nm). It also should be noted that the apparent hydrodynamic sizes are based on the assumption of spherical shape. It can not be ruled out that these self-assemblies do have different morphologies.

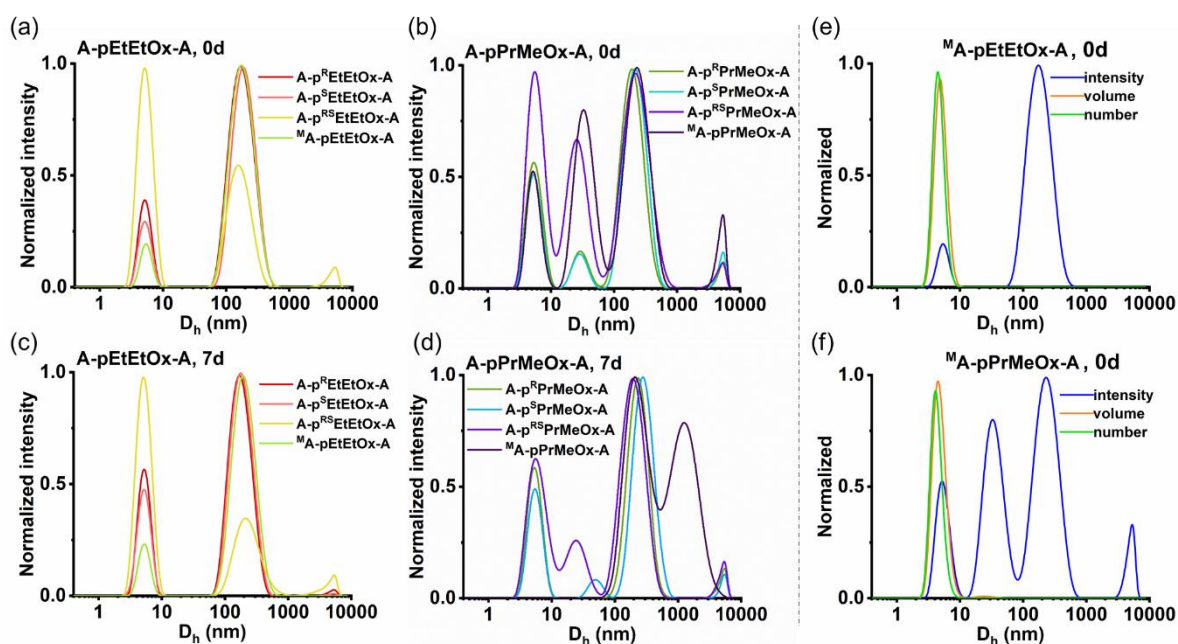


Figure 4.34 Particle size distribution by intensity determined by DLS of A-pEtEtOx-A series at day 0 (a) and day 7 (c), A-pPrMeOx-A series at day 0 (b) and day 7 (d). Particle size distribution of intensity, volume and number determined by DLS of (e) ^MA-pEtEtOx-A and (f) ^MA-pPrMeOx-A at day 0. Polymer concentration: 10 g/L in PBS. The samples were measured at 25 °C after filtration using 0.45 μ m PVDF syringe filter, afterwards no further filtration was applied on the same sample.

However, though the DLS samples were all transparent when freshly prepared, three set of polymer solutions turned turbid after some time: ^MA-pPrMeOx-A solutions (10 g/L) were found turbid at day 7, while A-p^RPrMeOx-A and A-p^SPrMeOx-A solutions (10 g/L) showed only a slight turbidity after one month (**Fig. 4.35**). The noticeable change of ^MA-pPrMeOx-A solutions on the size distribution can also be seen in the DLS profiles at day 7 (**Fig. 4.34c-d**). In the meantime, the A-p^{RS}PrMeOx-A solutions and all A-pEtEtOx-A series remained transparent

and retained the same particle size distribution even after one month. Interestingly, when the polymer concentration was very high (≈ 90 g/L) and stored for one year, A-p^RPrMeOx-A and A-p^SPrMeOx-A solutions showed turbid as expected, but A-p^REtEtOx-A and A-p^SEtEtOx-A solutions exhibited the sediment of transparent substances, only the A-p^{RS}EtEtOx-A and A-p^{RS}PrMeOx-A solution were still homogeneous.

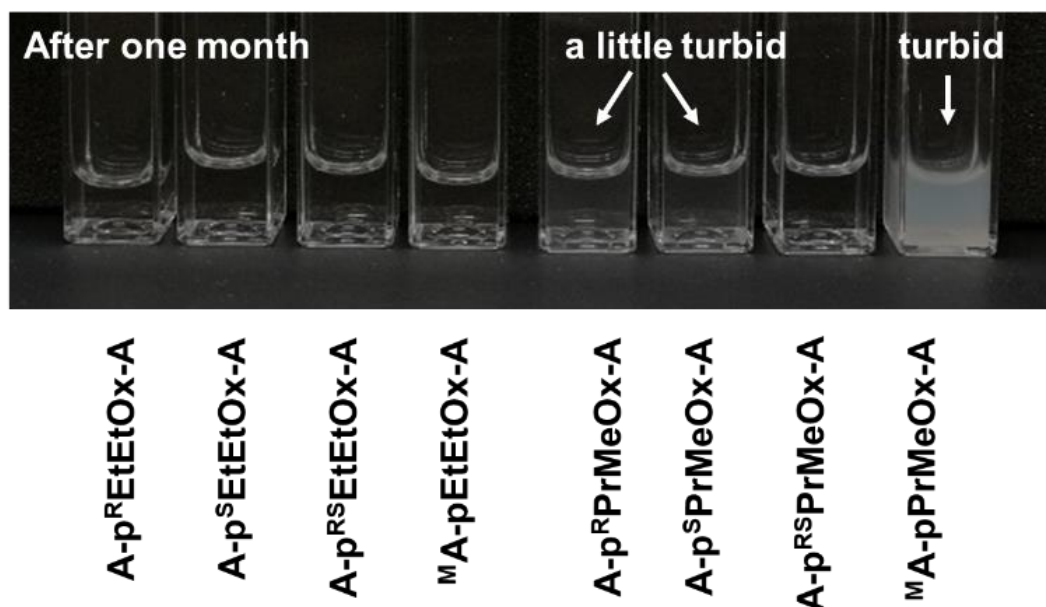


Figure 4.35 Photographs of DLS samples (in PBS) after storage under ambient conditions for one month: 10 g/L polymer solutions of A-p^REtEtOx-A, A-p^SEtEtOx-A, A-p^{RS}EtEtOx-A, ^MA-pEtEtOx-A, A-p^RPrMeOx-A, A-p^SPrMeOx-A, A-p^{RS}PrMeOx-A and ^MA-pPrMeOx-A (from left to right).

To investigate the origin of turbidity, XRD measurements of A-p^RPrMeOx-A, A-p^SPrMeOx-A and ^MA-pPrMeOx-A solutions were performed again after freeze-drying the corresponding polymers from cloudy water (Millipore) suspension as well as other polymer solutions, but signals suggesting crystalline domains were not found either in cloudy or non-cloudy samples (**Fig. 4.36**). Considering that the chiral A-pPrMeOx-A forms secondary structure more easily than chiral A-pEtEtOx-A, it is assumed that an enantioselective aggregation happened easily when two chiral A-pPrMeOx-A solutions were mixed as ^MA-pPrMeOx-A solutions, similar to enantioselective crystallization (but no crystallization occurred in this case).⁵⁷ As for the slight turbidity of A-p^RPrMeOx-A and A-p^SPrMeOx-A solutions observed after one month, further investigation on whether secondary structure of chiral polymers is able to enhance

the fusion of the micelles should be conducted. Besides, the turbid DLS samples were also stored at 4 °C for several days, but did not revert to transparent again, which indicates that the turbidity is caused by self-assembly, and the thermoresponsive behavior of the hydrophobic block appears not to be sufficient to revert the self-assembly.

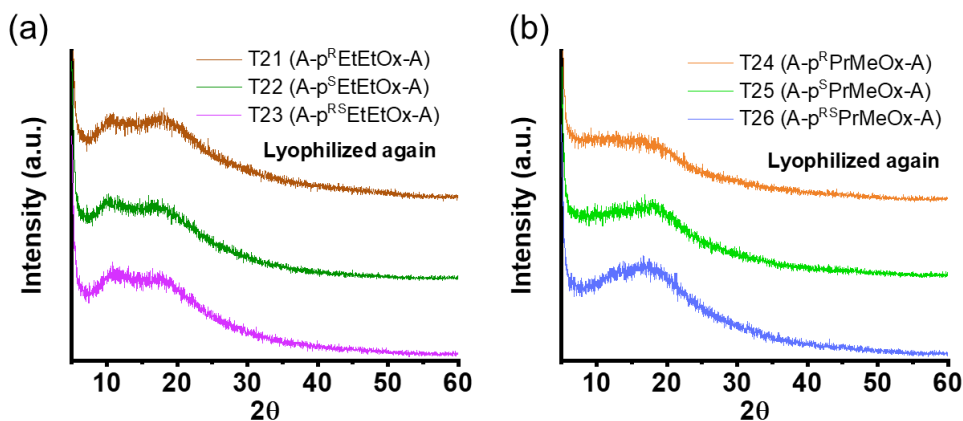


Figure 4.36 XRD patterns of lyophilized turbid triblock copolymer/water solution, polymer is (a) A-p^REtEtOx-A, A-p^SEtEtOx-A, A-p^{RS}EtEtOx-A and (b) A-p^RPrMeOx-A, A-p^SPrMeOx-A, A-p^{RS}PrMeOx-A.

For the CUR loaded samples, the formulations were prepared via thin-film hydration method in PBS with a ratio of polymer/CUR = 10/2 g/L, filtered with 0.45 μm PVDF filter and measured at day 0 and 7 by DLS at 25 °C. The size of CUR loaded micelles was essentially monomodal with a narrow size distribution ($D_h \approx 25$ nm, PDI < 0.11, **Fig. 4.37a-b**), which was more uniform than the blank micelles. The size and distribution did not change after diluting the samples with H₂O 1/2 and 1/10 (v/v) (to polymer concentration 5 and 1 g/L) (data not shown). Simultaneously, the CUR loaded formulations were quite stable, size and size distribution showed no obvious change at day 7, except for ^MA-pPrMeOx-A/CUR (**Fig. 4.37c-d**). Although the scattering intensity of ^MA-pPrMeOx-A/CUR showed a narrow distribution of larger particles ($D_h \approx 200$ nm) after 7 days' storage, the size distribution by volume and number was dominated by small particles ($D_h \approx 25$ nm) (**Fig. 4.37e**). After one month, all the formulations were still optically clear, including ^MA-pPrMeOx-A/CUR (**Fig. 37f**)

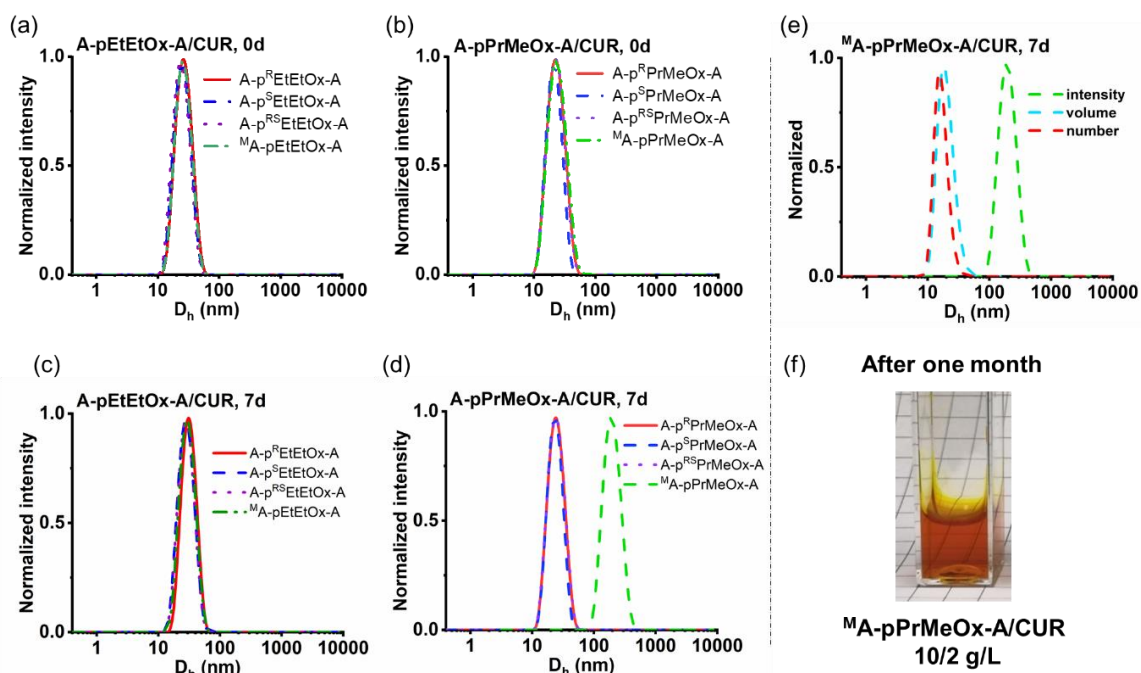


Figure 4.37 The size distribution by intensity of (a) formulation A-pEtEtOx-A/CUR (10/2 g/L) at day 0 (a) and day 7 (c), formulation A-pPrMeOx-A/CUR (10/2 g/L) at day 0 (b) and day 7 (d). (e) The size distribution by intensity, volume and number of M A-pPrMeOx-A/CUR formulation (10/2 g/L) at day 7. The samples were measured at 25 °C in PBS after filtration using 0.45 μ m PVDF syringe filter at day 0, then the samples were kept under ambient conditions for 7 days after the first measurement. (f) Photographs of DLS samples of M A-pPrMeOx-A/CUR (10/2 g/L) formulation after storage under ambient conditions for one month.

The S-IBU loaded formulations for DLS were prepared in the same way as the sample of CUR loaded formulation. The size of both series of formulations fell between 10 and 20 nm (all PDI < 0.23, **Fig. 4.38a-b**) with A-p^REtEtOx-A, M A-pEtEtOx-A and M A-pPrMeOx-A showing somewhat broader distributions, which primarily due to a minor population at larger sizes, especially in the case of A-p^REtEtOx-A. S-IBU loaded formulations appeared less uniform compared to the CUR loaded formulations, but also did not show clear trend between the polymers with different chiralities at day 0. Most of the formulations were still transparent and their size and size distribution were even more uniform at day 7 (**Fig. 4.38c-d**), except M A-pPrMeOx-A/S-IBU. The formulation of M A-pPrMeOx-A/S-IBU (day 7) was different from the M A-pPrMeOx-A/CUR formulation that the size distribution by volume and number was dominated by large particles (**Fig. 4.38e**). It was turbid similar to the unloaded M A-pPrMeOx-A solution (**Fig. 4.38f**). Besides, the rest S-IBU loaded formulations remained transparent after one month. The S-IBU powder and some lyophilized S-IBU loaded formulations were also

measured by XRD. The XRD pattern of the S-IBU showed the crystalline nature of the model drug (**Fig. 4.39a**). In contrast, crystallinity was not observed in the lyophilized formulations even after 2 months' storage at ambient conditions (**Fig. 4.39b-c**).

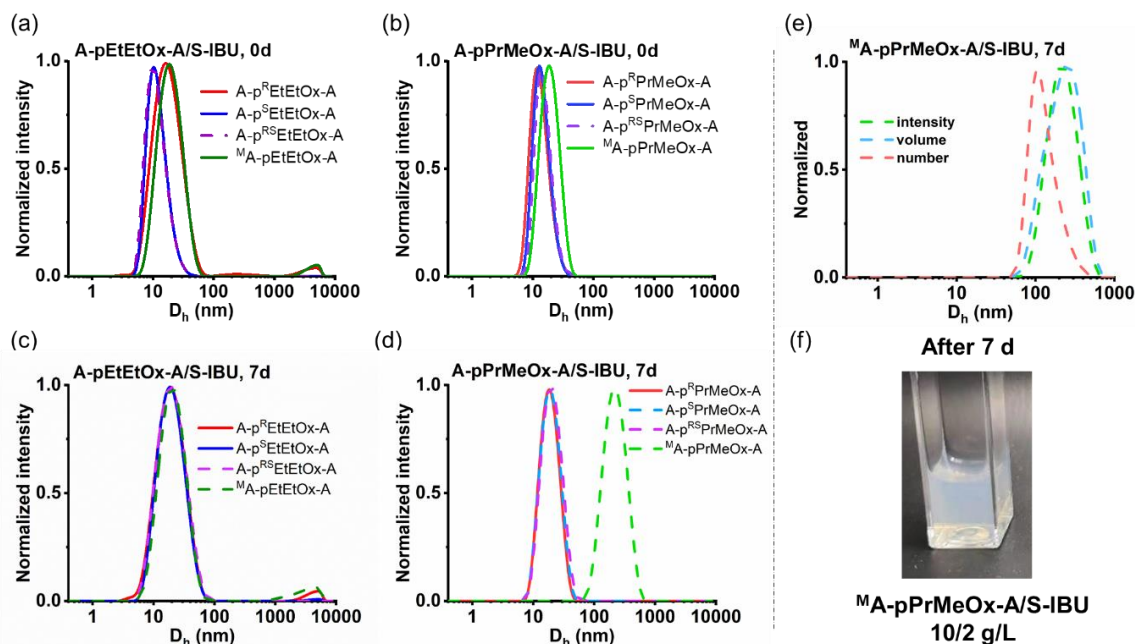


Figure 4.38 The size distribution by intensity of (a) formulation A-pEtEtOx-A/S-IBU (10/2 g/L) at day 0 (a) and day 7 (c), formulation A-pPrMeOx-A/S-IBU (10/2 g/L) at day 0 (b) and day 7 (d). (e) The size distribution by intensity, volume and number of M A-pPrMeOx-A/S-IBU formulation (10/2 g/L) at day 7. The samples were measured at 25 °C in PBS after filtration using 0.45 μ m PVDF syringe filter at day 0, then the samples were kept under ambient conditions for 7 days after the first measurement. (f) Photographs of DLS samples of M A-pPrMeOx-A/S-IBU (10/2 g/L) formulation after storage under ambient conditions for 7 days.

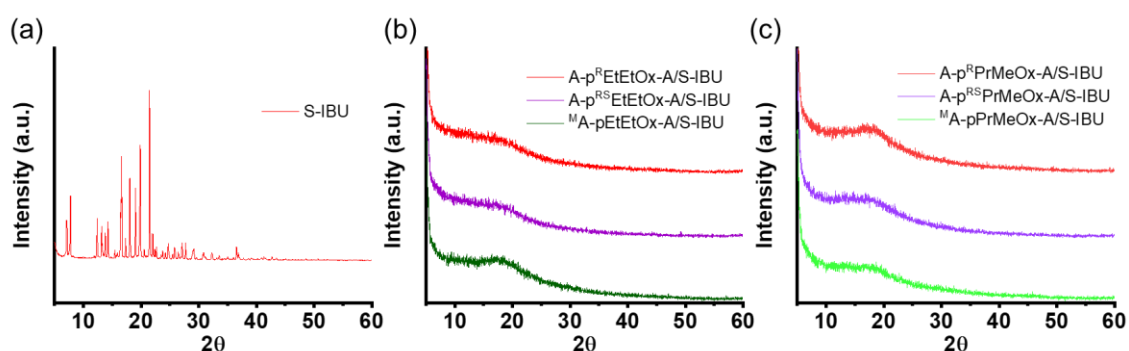


Figure 4.39 XRD patterns of (a) S-IBU powder, (b) lyophilized A-pEtEtOx-A/S-IBU formulation and (c) lyophilized A-pPrMeOx-A/S-IBU formulation.

4.4.4 Long-term stability studies

The long-term stability study was performed to investigate the potential shelf-life of the formulations. The formulations of A-pEtEtOx-A and A-pPrMeOx-A series were prepared with model drugs (CUR, PTX and IBU) via thin-film hydration, then stored at ambient conditions containing the initial precipitate (if any). The samples for drug concentration analysis were collected at day 0, 1, 8, 20, 30 and 60 after centrifugation which settled the precipitate (if any). The soluble drug concentration in the supernatant was then quantified. As the stability of most formulations formulated with CUR and PTX follows the certain pattern, the CUR and PTX loaded ^MA-pEtEtOx-A and ^MA-pPrMeOx-A formulations are shown as examples, as well as the exception case of 10 g/L CUR feed A-p^{RS}PrMeOx-A formulation.

Overall, both of CUR loaded ^MA-pEtEtOx-A and ^MA-pPrMeOx-A formulations were relatively stable. Up to 4 g/L CUR feed, the CUR loaded ^MA-pEtEtOx-A formulations were stable even for 60 days (**Fig. 4.40a**). In contrast, at 6 g/L CUR feed and above, a gradual but moderate decrease in drug loading was observed (**Fig. 4.40a, d-f**). Interestingly, the A-pPrMeOx-A formulation series behaved differently compared to A-pEtEtOx-A series. Except the CUR loaded A-p^{RS}PrMeOx-A (**Fig. 4.40c, i**), the rest of the A-pPrMeOx-A formulations were similar to ^MA-pPrMeOx-A formulation (**Fig. 4.40b, g-h**). Up to a CUR feed of 6 g/L, the drug loading of ^MA-pPrMeOx-A formulations did not reduce after 60 days. However, at CUR feed of 8 and 10 g/L, the CUR concentration detected in the supernatant increased gradually and quite significantly. For example, the drug loading of 8 g/L CUR feed ^MA-pPrMeOx-A formulation increased by 10-fold during the storage, from 0.16 ± 0.04 g/L (day 0) to 1.66 ± 0.45 g/L (day 60). Similar phenomenon was also observed in some POx/POzi micelles with moderately hydrophobic block, such as in the CUR loaded A-pBuOx-A formulation (CUR feed ≥ 5 g/L)¹⁷³ and CUR loaded A-EtHepOx-A formulation (CUR feed 2-10 g/L)¹⁶³. It is surmised that a drug/polymer coacervate forms at the beginning and redissolves over time, probably via an internal reorganization in the polymer drug self-assembly.^{163, 191} Such time-depented change in the self-assembly of nanoformulations and its effect on the biodistribution and pharmacological performance has been recently reported by Kabanov.¹⁹¹

The exception in the A-pPrMeOx-A series formulation was the 10 g/L CUR feed A-p^{RS}PrMeOx-A formulation which showed unexpectedly high drug loading (LC = 23 wt% at day 0) (**Fig. 4.29b**). The CUR drug loading slightly decreased at first, followed by a stronger

increase leading to a higher drug concentration (LC = 32 wt% at day 60) (**Fig. 4.40c**). A satisfactory explanation can not be provided at present.

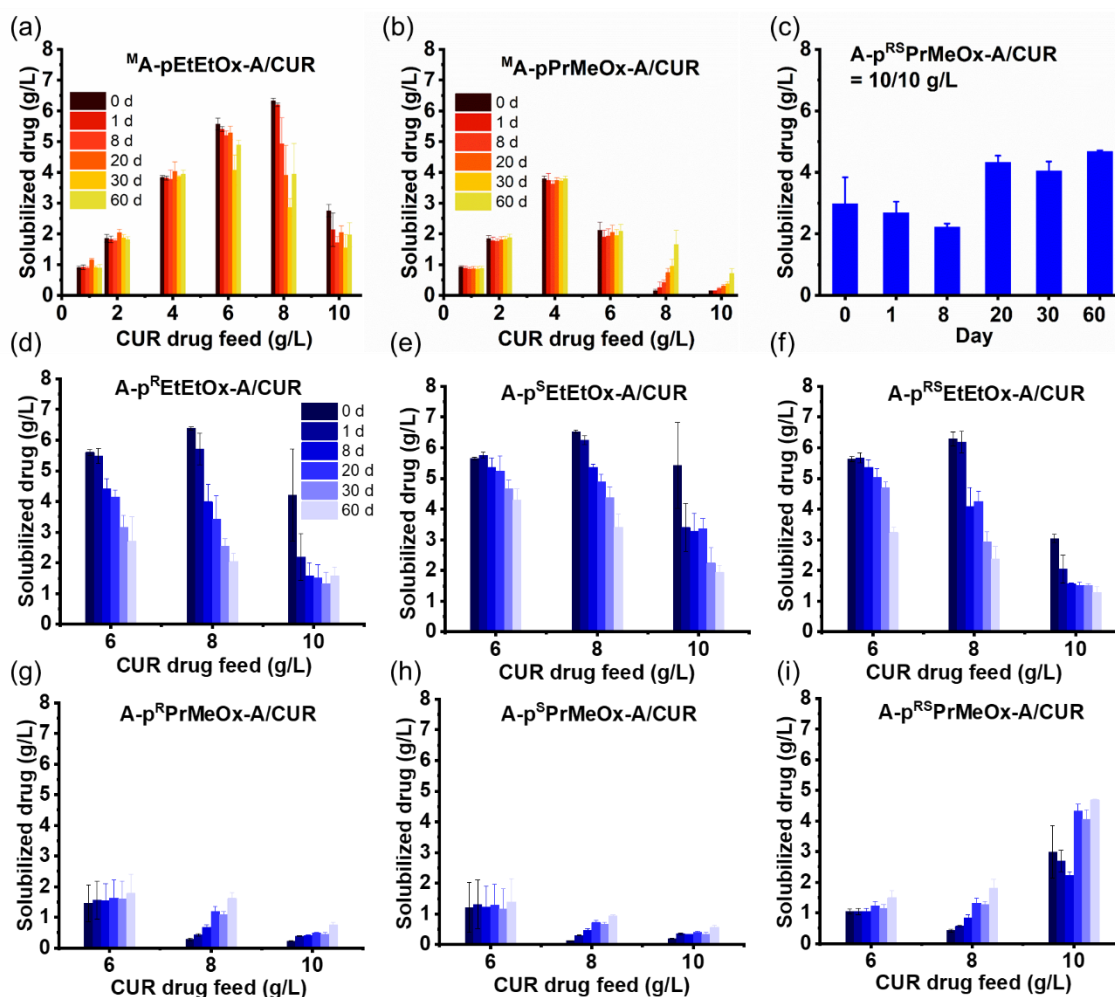


Figure 4.40 Long term stability of CUR-loaded (a) M A-pEtEtOx-A and (b) M A-pPrMeOx-A formulation in dependence of CUR feed concentration (polymer feed is 10 g/L, CUR feed is 1-10 g/L, 0-60 d). (c) Long term stability of CUR-loaded A-p^{RS}PrMeOx-A formulation (polymer/CUR= 10/10 g/L, 0-60 d). Long term stability of CUR-loaded (d) A-p^REtEtOx-A, (e) A-p^SEtEtOx-A, (f) A-p^{RS}EtEtOx-A, (g) A-p^RPrMeOx-A, (h) A-p^SPrMeOx-A, (i) A-p^{RS}PrMeOx-A formulation in dependence of CUR feed concentration (polymer feed is 10 g/L, CUR feed is 6-10 g/L, 0-60 d). Data is given as means \pm SD (n = 3).

The long-term stability of PTX-loaded M A-pEtEtOx-A and M A-pPrMeOx-A formulations was studied to reveal the stability of A-pEtEtOx-A and A-pPrMeOx-A series formulation, respectively. The 2 g/L PTX feed M A-pEtEtOx-A formulation was quite stable for 24 h, while the drug loading dropped rapidly afterwards (LC from 14 wt% at day 1 to 6 wt% at day 8) (**Fig. 4.41a**). In the supernatant of all M A-pEtEtOx-A/PTX formulations, the PTX LC was

less than 3 wt% at day 20. In comparison, up to 4 g/L PTX feed, the $^M\text{A-pPrMeOx-A}$ formulations were stable within 24 h, as no LC reduction was observed (**Fig. 4.41b**). The maximum PTX loaded $^M\text{A-pPrMeOx-A}$ formulations (6 g/L PTX feed) showed a reduction of 3 wt% LC at 24 h. However, similar to the $^M\text{A-pEtEtOx-A/PTX}$ formulations, the PTX loaded $^M\text{A-pPrMeOx-A}$ formulations remained less than 3 wt% LC at day 20.

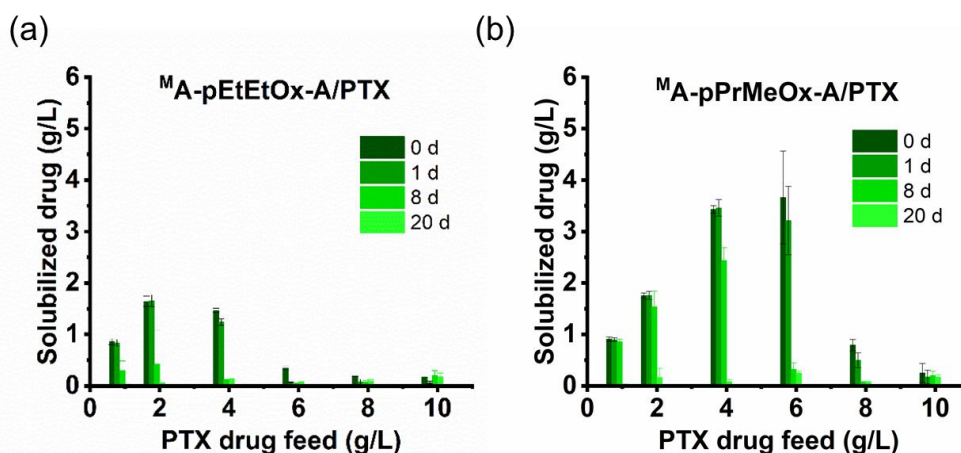


Figure 4.41 Long term stability of PTX-loaded (a) physical mixture $^M\text{A-pEtEtOx-A}$ and (b) $^M\text{A-pPrMeOx-A}$ formulation in dependence of PTX feed concentration (polymer feed is 10 g/L, PTX feed is 1-10 g/L, 0-20 d). Data is given as means \pm SD ($n = 3$).

As mentioned in the drug loading part, most of the formulations had the maximum LC at 6 g/L IBU feed (also see **Fig. 4.42** and **4.43**). The long-term stability of $^M\text{A-pEtEtOx-A/RS-IBU}$ and $^M\text{A-pPrMeOx-A/RS-IBU}$ formulations is used as examples of general behavior of A-pEtEtOx-A and A-pPrMeOx-A series formulation (**Fig. 4.42I** and **4.43I**). The IBU loaded formulations were not as stable as CUR loaded formulations, and the LC of $^M\text{A-pEtEtOx-A/RS-IBU}$ decreased very slowly in 30 days up to 6 g/L RS-IBU feed (**Fig. 4.42I**). However, when the drug feed was 8 and 10 g/L, the LC dropped significantly around day 20, and remained 5 wt% and 4 wt% at day 60, respectively. Comparing with the IBU loaded A-pEtEtOx-A formulations, the A-pPrMeOx-A series formulations were relatively more stable. At all RS-IBU feed, the drug loading of $^M\text{A-pPrMeOx-A/RS-IBU}$ reduced evenly and slowly over 60 days (**Fig. 4.43I**). Eventually, only 7 wt% LC loss was observed at 6 g/L RS-IBU feed $^M\text{A-pPrMeOx-A}$ formulation at day 60. When the drug feed was 8 and 10 g/L, the LC remained 8 wt% and 3 wt% at day 60, respectively.

Because the R- and RS-IBU loaded A-p^{RS}EtEtOx-A and A-p^{RS}PrMeOx-A showed the maximum LC at drug feed of 8 g/L, the A-p^{RS}EtEtOx-A/RS-IBU and A-p^{RS}PrMeOx-A/RS-IBU

formulations are used to discuss the special cases (Fig. 4.42k and 4.43k). Similar to the general A-pEtEtOx-A/IBU formulations, the drug loading of A-p^{RS}EtEtOx-A/RS-IBU (up to 6 g/L RS-IBU feed) declined gradually over 30 days (Fig. 4.42k). However, they were not very stable at 8 g/L RS-IBU feed, as the LC had a 6 wt% loss within 24 hours and finally dropped to the same level of ^MA-pEtEtOx-A/RS-IBU after 60 days. Likewise, the A-p^{RS}PrMeOx-A/RS-IBU formulations were relatively stable for 60 days at 6 g/L RS-IBU feed, but also had unsatisfactory stability at 8 g/L RS-IBU feed (Fig. 4.43k). At day 60, the LC of IBU loaded formulation does not appear to be significantly influenced by the chirality of copolymers.

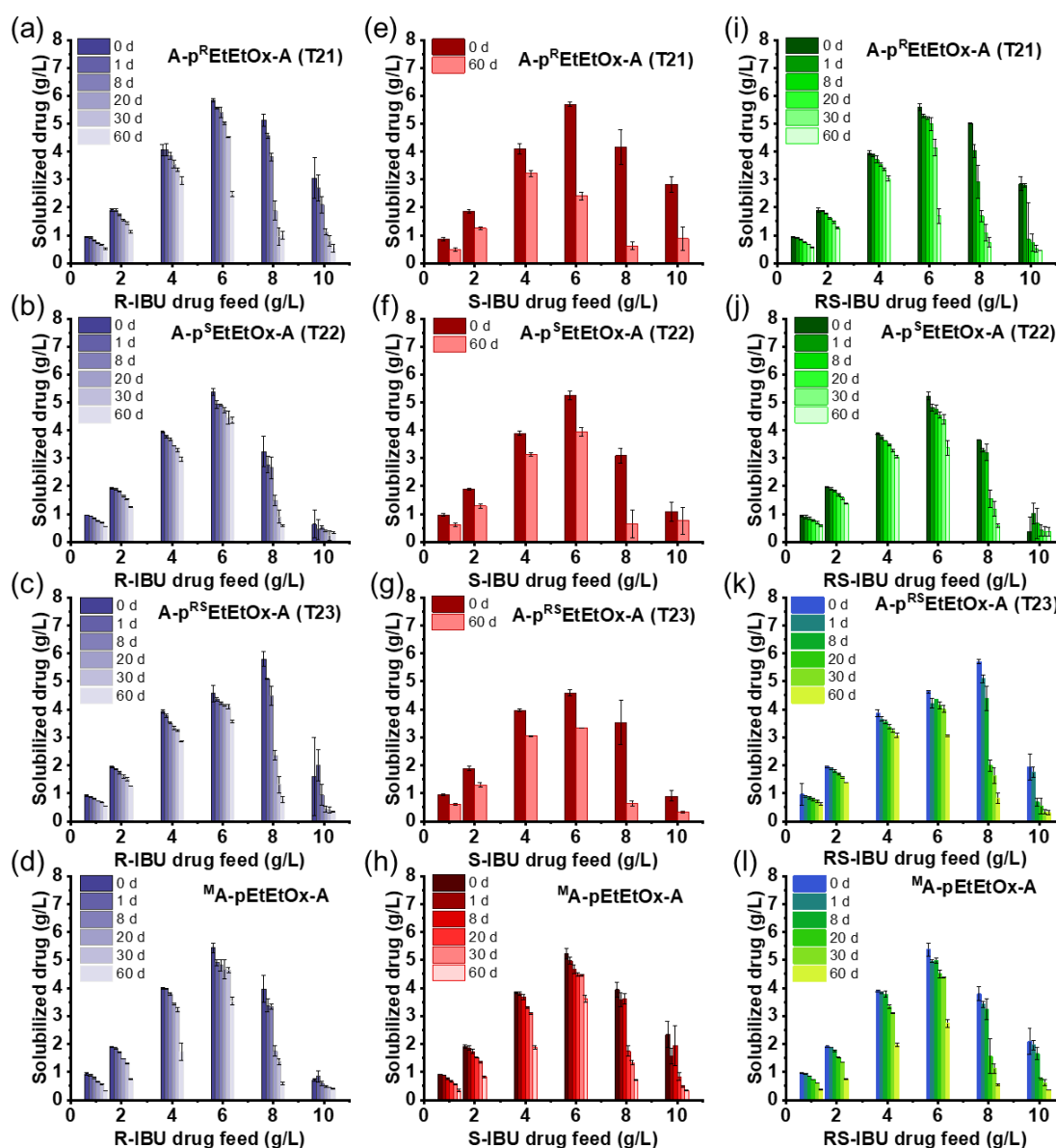


Figure 4.42 Long term stability of (a-d) the R-IBU, (e-h) S-IBU and (i-l) RS-IBU loaded A-pEtEtOx-A formulation in dependence of IBU feed concentration (polymer feed is 10 g/L, IBU feed is 1-10 g/L). Data is given as means \pm SD ($n = 3$).

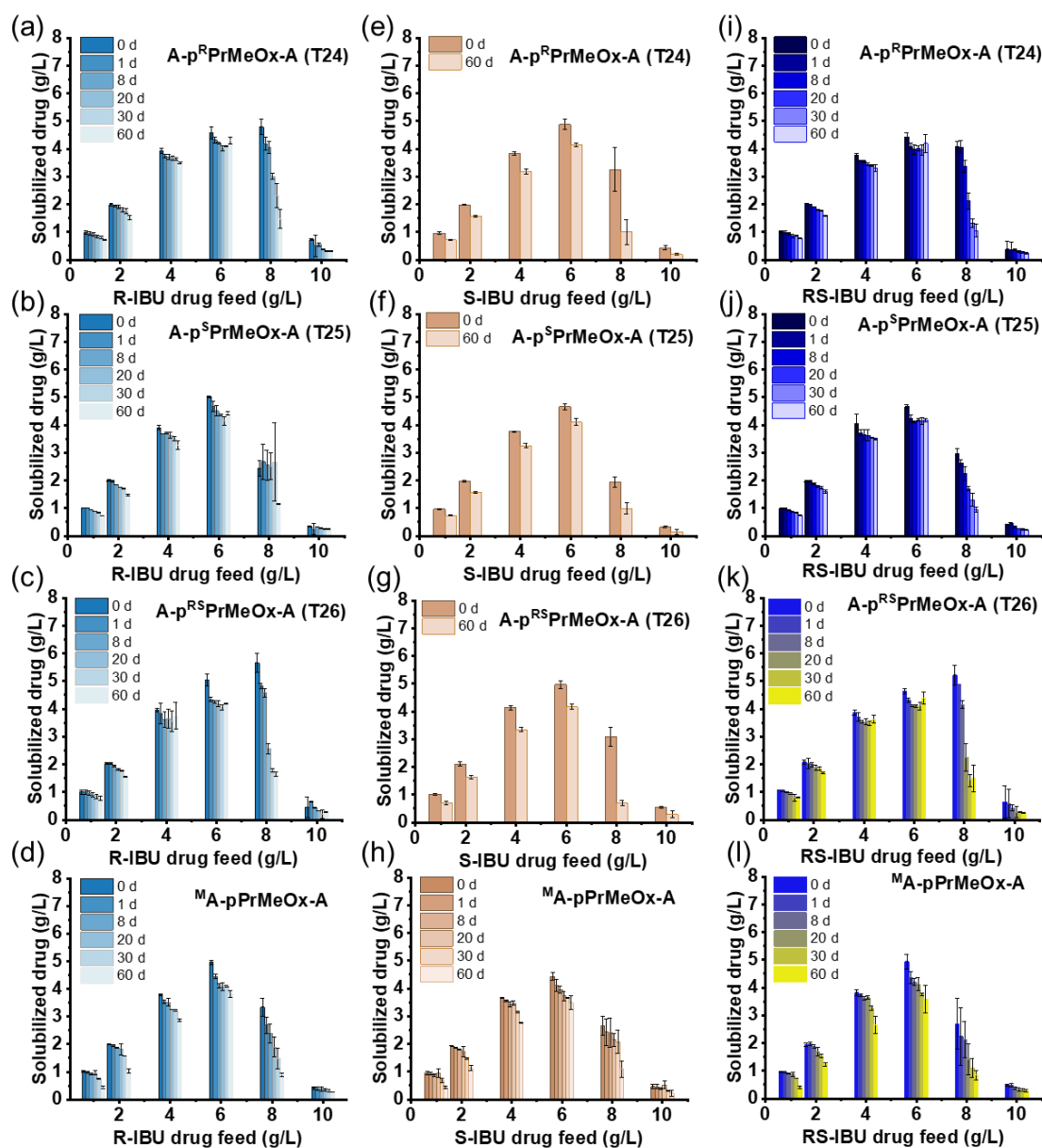


Figure 4.43 Long term stability of (a-d) the R-IBU, (e-h) S-IBU and (i-l) RS-IBU loaded A-pPrMeOx-A formulation in dependence of IBU feed concentration (polymer feed is 10 g/L, IBU feed is 1-10 g/L). Data is given as means \pm SD (n = 3).

4.4.5 Conclusion

CUR, PTX and IBU loaded formulations were prepared through thin film hydration method to investigate the influence of triblock copolymers on the solubilization of different drugs. To conclude, polymers T1-T10 demonstrated suboptimal performance in terms of in loading CUR and even worse in loading PTX, while polymer T21-26 deserved further study with relatively good loading capacity of CUR, PTX and IBU. The maximum CUR LC was ≈ 40 wt% in A-pEtEtOx-A, ≈ 29 wt% in A-pPrMeOx-A formulations, the maximum PTX LC was ≈ 18 wt% in A-pEtEtOx-A, ≈ 32 wt% in A-pPrMeOx-A, the maximum IBU LC was ≈ 34 wt% in A-pEtEtOx-A and A-pPrMeOx-A. For both A-pEtEtOx-A and A-pPrMeOx-A series, the chiral, racemic triblock copolymers and the 1/1 (w/w) mixtures of two corresponding chiral copolymers had similar LC for CUR or PTX in most cases, except the special case of A-p^{RS}PrMeOx-A/CUR=10/10 (g/L). Comparing the A-pPrMeOx-A with A-pEtEtOx-A, a methylene group shifted from the *N*-substituting side chain to the backbone branch can also lead to specific drug loading of CUR and PTX, which is similar to the isomeric pair of A-pBuOx-A and A-pPrOzi-A. However, the specific drug loading was not evident in IBU loaded formulations. In the IBU loaded formulations, the chirality of triblock copolymers hardly affected the drug loading of all IBU at low drug feed, while showed influence at high drug feed. The LC of A-p^SEtEtOx-A and A-p^SPrMeOx-A are noticeably lower than their R- and RS- isomers at 8 g/L IBU feed. In the meantime, the chirality of IBU showed influence in the LC of several polymers, where the LC values of S-IBU were lower than those of R- and RS-IBU in same polymer at high drug feed. Long term stability study showed that most of the CUR and IBU loaded formulations were relatively stable, but the LC of PTX loaded formulations dropped significantly in 8 days.

5 Summary

Motivated by the perceived great potential of chiral polymers, the presented work aimed at the investigation of synthesis, solubility and optical activity of chiral poly(2,4-disubstituted-2-oxazoline)s. A novel polymeric carrier based on ABA-type triblock copolymers poly(2-oxazoline)s with chiral and racemic hydrophobic blocks was developed for the formulation of chiral and achiral drugs (**Fig. 5.1**). Poly(2-methyl-2-oxazoline) (pMeOx) was used as hydrophilic A block, and poly(2-ethyl-4-ethyl-2-oxazoline) (pEtEtOx) and poly(2-propyl-4-methyl-2-oxazoline) (pPrMeOx) were used as hydrophobic B blocks. Curcumin (CUR), paclitaxel (PTX) and chiral/racemic ibuprofen (R/S/RS-IBU) were applied as model drugs. Nanoformulations were prepared consisting of these triblock copolymers and model drugs.

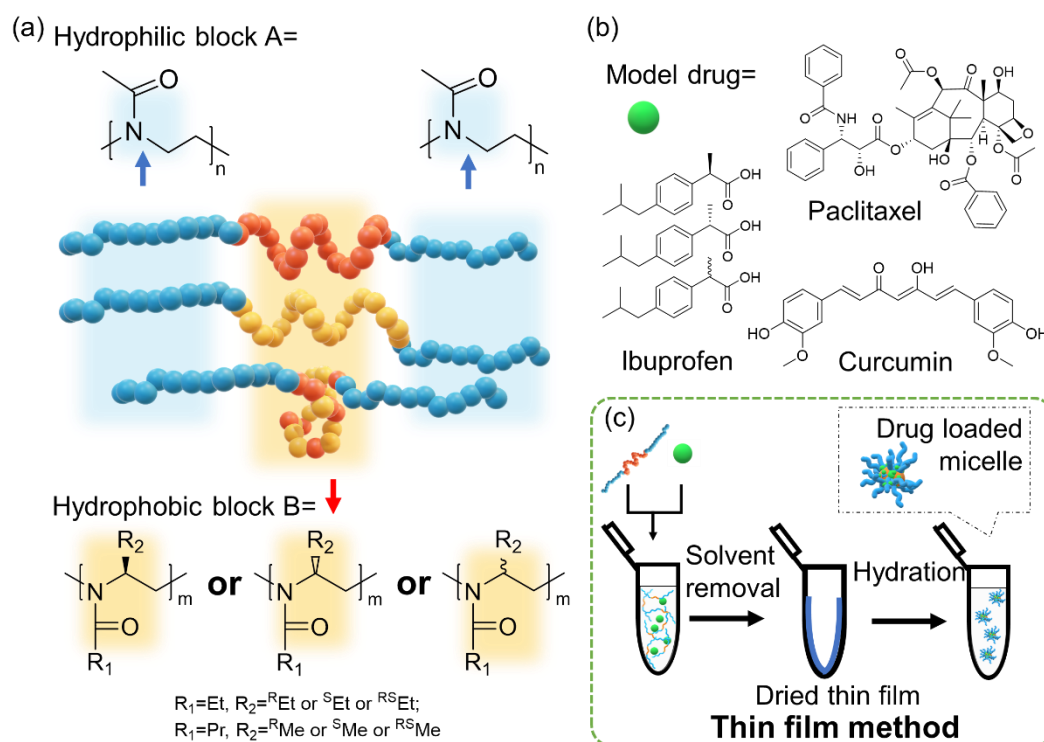


Figure 5.1 (a) Chemical structures of the ABA triblock copolymers used in this study, where hydrophilic A block is poly(2-methyl-2-oxazoline) (pMeOx) and the hydrophobic B block is poly(2-ethyl-4-ethyl-2-oxazoline) ($p^R\text{EtEtOx}$, $p^S\text{EtEtOx}$, $p^{RS}\text{EtEtOx}$) or poly(2-propyl-4-methyl-2-oxazoline) ($p^R\text{PrMeOx}$, $p^S\text{PrMeOx}$, $p^{RS}\text{PrMeOx}$). (b) Chemical structure of the model drugs used in this study, paclitaxel, curcumin and ibuprofen. (c) Schematic representation of the formulation procedure (thin film hydration method).

Synthesis

The synthesis of ^REtEtOx has been reported by Bloksma *et al.* previously ²⁰, and the PrMeOx was synthesized for the first time in this work. The monomer EtEtOx and PrMeOx with different chirality were successfully synthesized from nitrile and alkanolamine (enantiomeric or racemic) in this work. The corresponding homopolymers were polymerized via living cationic ring-opening polymerization (LCROP), as well as the triblock copolymers comprising pMeOx as hydrophilic A blocks and pEtEtOx (or pPrMeOx) as hydrophobic B blocks. The polymers were analysed with ¹H-NMR spectroscopy and size-exclusion chromatography (SEC). The polymerization was well controlled with the result of low dispersity ($\mathcal{D} < 1.2$) and the degree of polymerization (DP) was reasonably close to the initial monomer to initiator ratio $[M]_0:[I]_0$.

Physicochemical properties of homopolymers and triblock copolymers

Homopolymer p^REtEtOx has been reported by Bloksma *et al.* previously ²⁰, and pPrMeOx was obtained for the first time in this work. For both of the pEtEtOx and pPrMeOx, thermoresponsive behavior were observed. Both polymers had low water solubility at RT (<0.5 g/L) but relatively high solubility at 4 °C (8-10 g/L). This is the first time that C4 substituted POx have been found to be thermoresponsive. As for the triblock copolymers, the chain length, ratio of hydrophobic and hydrophilic chain length, and chirality affected solubility. The triblock copolymers T1-T3 and T6-T8 (10-30 DP A block and ≈10 DP B block) were poorly soluble in water and ethanol (< 20 g/L), when the A block got longer (T4-T5 and T9-T10), the solubility was improved in both water and ethanol (≥20 g/L). The triblock copolymers with ≈35 DP A block and ≈20 DP B block (T21-T26) were excellently soluble in water and ethanol (≥200 g/L). In the meantime, the self-assembly resulting from the stereostructure was also related to the turbidity of some samples (A-p^RPrMeOx-A, A-p^SPrMeOx-A and ^MA-pPrMeOx-A) in aqueous solution after some time storage. However, the exact reason for this turbidity requires more investigation.

The homopolymers and triblock copolymers were further characterized by thermogravimetric analysis (TGA) and differential scanning calorimetry (DSC) to understand the thermal properties. The thermal stability of pEtEtOx and pPrMeOx series homopolymers were similar that the onset temperature of major mass loss T_d was around 350 °C and not much influenced by the chain length and chirality. The triblock copolymers were slightly more stable

than the homopolymers with a T_d of major mass loss at ≈ 370 °C, and not significantly influenced by the chirality and ratio of A and B block. Though the glass transition temperature (T_g) value of homopolymers and triblock copolymers was also not influenced by the chirality, it increased with the chain length when the chain was short (DP=10-20). When the DP ranged between 30-40, the T_g value of homopolymers increased slowly and eventually plateaued at ≈ 87 °C for pEtEtOx and ≈ 60 °C for pPrMeOx. Clearly, the polymer chain of pPrMeOx was more flexible than pEtEtOx since the T_g of pPrMeOx was much lower than the pEtEtOx. The chain length of most triblock copolymers was above DP 50, continuing to lengthen the hydrophilic or hydrophobic block did not significantly change the T_g , which was around 76 °C for the A-pEtEtOx-A and around 71 °C for the A-pPrMeOx-A. Besides, no T_m was detected by DSC, either in homopolymers or triblock copolymers. It indicated that the synthesized polymers in this work were all amorphous regardless of their chirality and DP, which was also confirmed by the X-ray diffraction (XRD) analysis.

The polymers were studied by circular dichroism (CD) spectroscopy in solution. The homopolymers and triblock copolymers synthesized from chiral monomers retained the chirality of the monomers and were able to form the secondary structure in methanol, as well as in water for the triblock copolymers. In contrast, the polymers synthesized from racemic monomers and the 1/1 (w/w) mixture of two corresponding chiral polymers did not show the Cotton effect (CE) in solution. That is, either they did not form secondary structure or formed secondary structure but with 50/50 mixture negate effect.

Chiral/racemic triblock copolymer based micelles as a drug delivery system

With increasing interest, POx have been investigated in a wide range of applications, especially in the biomedical field, *e.g.*, the delivery of drugs, proteins and genes. Considering chirality is an essential property for many biologically relevant molecules, including a lot of drugs, it is interesting to develop chiral drug delivery systems based on POx. Though some research on chiral POx has been published, a drug formulation based on main chain chiral POx triblock copolymer has not been studied before. In order to understand the stereoregular polymers as drug carriers, A-pEtEtOx-A and A-pPrMeOx-A series amphiphilic triblock copolymers were formulated with CUR, PTX and chiral/racemic IBU. The drug loaded micelles were prepared through the thin film hydration method, followed by the characterization of loading capability. When the hydrophobic B blocks of A-pEtEtOx-A and A-pPrMeOx-A was

short ($DP \approx 10$) and the hydrophilic A block varied from DP 10 to 50, the synthesized triblock copolymer T1-T10 had low drug loading for CUR and PTX. It is related to the water solubility of the polymers and also the ratio of hydrophilic and hydrophobic segments. Compared with the T1-T10, the triblock copolymer T21-T26 composed of $DP \approx 35$ hydrophilic A block and $DP \approx 20$ hydrophobic B block had higher drug loading for both CUR and PTX. Therefore, the T21-T26 were further applied to formulate with IBU and characterize the hydrodynamic diameter (D_h), drug loading capability (LC) and long-term stability in the form of the formulation. The polymer T21-T26 were abbreviated as A-p^REtEtOx-A, A-p^SEtEtOx-A, A-p^{RS}EtEtOx-A, A-p^RPrMeOx-A, A-p^SPrMeOx-A, A-p^{RS}PrMeOx-A to facilitate the understanding of the stereostructure of polymers. The ^MA-pEtEtOx-A and ^MA-pPrMeOx-A represented the 1/1 (w/w) mixtures of two corresponding chiral triblock copolymers.

Both A-pEtEtOx-A and A-pPrMeOx-A series triblock copolymers were homogeneous in aqueous solution (polymer 10 g/L) when freshly prepared. However, A-p^RPrMeOx-A, A-p^SPrMeOx-A and ^MA-pPrMeOx-A solutions turned turbid after some time. The drug (CUR and IBU) was found to have a beneficial effect in facilitating the formation of more uniformly-sized micelles. The hydrodynamic size of the fresh drug loaded micelle (polymer/drug=10/2 g/L) was essentially monomodal with a narrow size distribution (CUR loaded micelle $D_h \approx 25$ nm, PDI < 0.11; S-IBU loaded micelle D_h 10-20 nm, PDI < 0.23). Most of the formulations remained transparent for one month, however, even though the drug helped to stabilize the micelles, the formulation ^MA-pPrMeOx-A/S-IBU was turbid after several days, similar to the unloaded ^MA-pPrMeOx-A solution. The turbidity of either polymer solutions or formulations resulted from the self-assembly, not crystallization of polymer or drugs, as was confirmed by XRD analysis.

T21-26 exhibited good performance in loading CUR and PTX. At the same CUR or PTX drug feed of A-pEtEtOx-A (or A-pPrMeOx-A) formulation, the chiral, racemic polymer and the 1/1 (w/w) mixtures had similar LC in most cases, except the unexpectedly high drug loading of A-p^{RS}PrMeOx-A/CUR at 10/10 g/L feed. However, their maximum LC depended significantly on the type of the hydrophobic block rather than the chirality. The maximum CUR LC achieved ≈ 40 wt% in A-pEtEtOx-A and ≈ 29 wt% in A-pPrMeOx-A formulations. The maximum PTX LC was ≈ 18 wt% in A-pEtEtOx-A and ≈ 32 wt% in A-pPrMeOx-A. Comparing the hydrophobic blocks of two series, a methylene group located on the *N*-substituting side chain (A-pPrMeOx-A) or backbone branch (A-pEtEtOx-A) leads to specific drug loading of CUR and PTX, which is similar to the isomeric pair of A-pBuOx-A and A-pPrOzi-A. In contrast, when the A-pEtEtOx-

A and A-pPrMeOx-A series polymers were formulated with chiral and racemic IBU, the two series did not show specific difference in drug loading. In general, the maximum IBU LC was 32-37 wt% in A-pEtEtOx-A formulations and 31-36 wt% in A-pPrMeOx-A formulations, and notable regularity between the stereoisomers was not found. Considering the solubilized drug concentration at the same IBU feed, the chirality of the triblock copolymers had an influence at high drug feed (IBU 8 g/L and above, polymer 10 g/L), while there was no apparent effect at 1-6 g/L drug feed. Interestingly, along with the influence of the IBU chirality at high drug feed, the polymers A-p^SEtEtOx-A and A-p^SPrMeOx-A showed lower drug loading than their R- and RS-isomers at high S-IBU feed, especially at 8 g/L. It can not be explained in detail at the moment, but it probably is related to the stereostructure related self-assembly between the drug and polymer.

In summary, chiral/racemic pEtEtOx and pPrMeOx can be synthesized from the corresponding chiral/racemic oxazoline monomers via LCROP. The synthesized homopolymers are poorly water soluble but show thermoresponsive behavior in water solution. The chiral homopolymers and triblock copolymers containing chiral pEtEtOx or pPrMeOx block are able to form the secondary structure in solution, while the racemic isomers and 1/1 (w/w) mixtures either did not form secondary structure or formed secondary structure but with 50/50 mixture negate effect. Both A-pEtEtOx-A and A-pPrMeOx-A series polymers have good drug loading capability for CUR, PTX and IBU, and there is also possibility of applying them for the loading of other hydrophobic drugs. It is worth noting that the chirality of the polymers may affect the stability of micelles, micelle size, size distribution, drug loading, *etc.*, but this requires verification for particular systems. Apart from the stereostructure of the polymers, the chirality of the drugs might also influence drug loading to some degree. The difference between POx with different chirality requires further investigations, especially the interactions between chiral/racemic POx and biological systems should be a matter for future investigations.

6 Zusammenfassung

Motiviert durch das wahrgenommene große Potential chiraler Polymere zielte die vorliegende Arbeit auf die Untersuchung der Synthese, Löslichkeit und optischen Aktivität von chiralen Poly(2,4-disubstituierten-2-oxazolin)en ab. Für die Formulierung von chiralen und achiralen Arzneimitteln wurde ein neuartiger polymerer Träger auf der Basis von ABA-Typ Triblock-Copolymeren aus Poly(2-oxazolin)en mit chiralen und racemischen hydrophoben Blocken entwickelt (**Abbildung 5.1**). Poly(2-methyl-2-oxazolin) (pMeOx) wurde als hydrophiler A Block und Poly(2-ethyl-4-ethyl-2-oxazolin) (pEtEtOx) und Poly(2-propyl-4-methyl-2-oxazolin) (pPrMeOx) als hydrophober B Block verwendet. Als Modellarzneimittel wurden Curcumin (CUR), Paclitaxel (PTX) und chirales/racemisches Ibuprofen (R/S/RS-IBU) eingesetzt. Es wurden Nanoformulierungen hergestellt, die aus diesen Triblock-Copolymeren und Modellarzneimitteln bestehen.

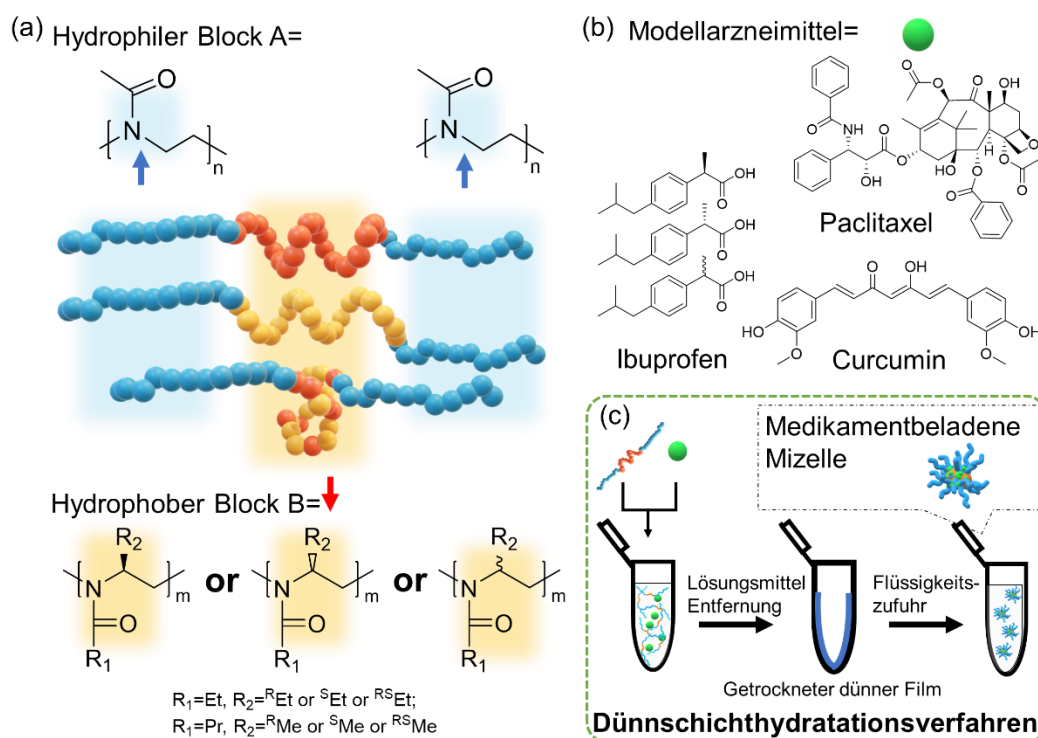


Abbildung 5.1 (a) Chemische Strukturen der in dieser Studie verwendeten ABA Triblock-Copolymere, wobei der hydrophile A Block stets Poly(2-methyl-2-oxazolin) (pMeOx) war und der hydrophobe B Block zwischen Poly(2-ethyl-4-ethyl-2-oxazolin) (p^REtEtOx, p^SEtEtOx,

p^{RS}EtEtOx) oder Poly(2-propyl-4-methyl-2-oxazolin) (p^RPrMeOx, p^SPrMeOx, p^{RS}PrMeOx) variiert wurde. (b) Chemische Struktur der in dieser Studie verwendeten Modellarzneimittel Paclitaxel, Curcumin und Ibuprofen. (c) Schematische Darstellung des Formulierungsverfahrens (Dünnschichthydratationsverfahren).

Synthese

Über die Synthese von ^REtEtOx wurde bereits von Bloksma *et al.* berichtet ²⁰, und PrMeOx wurde in dieser Arbeit zum ersten Mal synthetisiert. Die Monomere EtEtOx und PrMeOx mit unterschiedlicher Chiralität wurden in dieser Arbeit erfolgreich aus Nitril und dem entsprechenden Alkanolamin (enantiomer oder racemisch) synthetisiert. Die entsprechenden Homopolymere wurden durch lebende kationische Ringöffnungspolymerisation (LCROP) polymerisiert, ebenso wie die Triblock-Copolymere, die pMeOx als hydrophilen A Block und pEtEtOx (oder pPrMeOx) als hydrophoben B Block enthalten. Die Polymere wurden mit ¹H-NMR -Spektroskopie und Größenausschlusschromatographie (SEC) analysiert. Die Polymerisation verlief gut kontrolliert, mit dem Ergebnis einer geringen Dispersität ($\bar{M}_w/\bar{M}_n < 1,2$), und der Polymerisationsgrad (DP) lag recht nahe am anfänglichen Monomer/Initiator-Verhältnis $[M]_0/[I]_0$.

Physikochemischen Eigenschaften von Homopolymeren und Triblock-Copolymeren

Das Homopolymer pEtEtOx wurde bereits von Bloksma *et al.* beschrieben ²⁰, und pPrMeOx wurde in dieser Arbeit zum ersten Mal erhalten. Sowohl beim pEtEtOx als auch bei pPrMeOx wurde ein thermoresponsives Verhalten beobachtet, das eine geringe Wasserlöslichkeit bei RT (<0,5 g/L), aber eine relativ hohe Löslichkeit bei 4 °C (8-10 g/L) aufwies. Dies ist das erste Mal, dass sich C4-substituiertes POx als thermoresponsiv erwiesen hat. Was die Triblock-Copolymere betrifft, die Kettenlänge, das Verhältnis von hydrophober und hydrophiler Kettenlänge und die Chiralität beeinflussen die Löslichkeit. Die Triblock-Copolymere T1-T3 und T6-T8 (10-30 DP A Block und ≈ 10 DP B Block) waren in Wasser und Ethanol schlecht löslich (< 20 g/L), während der längere A Block (T4-T5 und T9-T10) die Löslichkeit in Wasser und Ethanol verbesserte (≥ 20 g/L). Die Triblock-Copolymere mit ≈ 35 DP A Block und ≈ 20 DP B Block (T21-T26) waren hervorragend in Wasser und Ethanol (≥ 200 g/L) löslich. Die aus der Stereostruktur resultierende Selbstorganisation stand auch im

Zusammenhang mit der Trübung einiger Proben (A-p^RPrMeOx-A, A-p^SPrMeOx-A and ^MA-pPrMeOx-A) in wässriger Lösung nach einiger Zeit der Lagerung. Der genaue Grund für diese Trübung muss jedoch noch genauer untersucht werden.

Die Homopolymere und Triblock-Copolymere wurden durch thermogravimetrische Analyse (TGA) und dynamische Differenzkalorimetrie (DSC) weiter charakterisiert, um die thermischen Eigenschaften zu verstehen. Die thermische Stabilität der Homopolymere der pEtEtOx- und pPrMeOx-Reihe war ähnlich, die Anfangstemperatur des größten Massenverlustes T_d lag bei etwa 350 °C und wurde durch die Kettenlänge und Chiralität nicht wesentlich beeinflusst. Die Triblock-Copolymere waren etwas stabiler als die Homopolymere mit einer T_d des größten Massenverlustes bei ≈ 370 °C und wurden von der Chiralität und dem Verhältnis von A und B Block nicht wesentlich beeinflusst. Obwohl die Glasübergangstemperatur (T_g) von Homopolymeren und Triblock-Copolymeren auch nicht von der Chiralität beeinflusst wurde, stieg sie für kurze Ketten mit der Kettenlänge an ($DP=10-20$). Wenn der DP zwischen 30 und 40 lag, stieg der T_g -Wert der Homopolymere langsam an und erreichte schließlich ein Plateau bei ≈ 87 °C für pEtEtOx und ≈ 60 °C für pPrMeOx. Offensichtlich war die Polymerkette von pPrMeOx flexibler als die von pEtEtOx, da die T_g von pPrMeOx deutlich niedriger war als die von pEtEtOx. Die Kettenlänge der meisten Triblock-Copolymere lag über DP 50, eine weitere Verlängerung des hydrophilen oder hydrophoben Blocks änderte die T_g nicht wesentlich, die bei A-pEtEtOx-A bei etwa 76 °C und bei A-pPrMeOx-A bei etwa 71 °C lag. Außerdem wurde bei der DSC keine T_m festgestellt, weder bei den Homopolymeren noch bei den Triblock-Copolymeren. Dies deutet darauf hin, dass die in dieser Arbeit synthetisierten Polymere unabhängig von ihrer Chiralität und ihrem DP alle amorph sind, was auch durch die Röntgenbeugungsanalyse (XRD) bestätigt wurde.

Die Polymere wurden mittels Circular dichroismus (CD)-Spektroskopie in Lösung untersucht. Die aus chiralen Monomeren synthetisierten Homopolymere und Triblock-Copolymere behielten die Chiralität der Monomere bei und waren in der Lage, die Sekundärstruktur in Methanol und bei den Triblock-Copolymeren auch in Wasser zu bilden. Im Gegensatz dazu zeigten die aus racemischen Monomeren synthetisierten Polymere und die 1/1 (w/w) Mischung der beiden entsprechenden chiralen Polymere in Lösung nicht den Cotton-Effekt (CE). Das heißt, entweder bildeten sie keine Sekundärstruktur oder sie bildeten eine Sekundärstruktur, aber bei einer 50/50-Mischung wurde der Effekt negiert.

Mizellen auf der Basis von chiralen/racemischen Triblock-Copolymeren als Arzneimittelabgabesystem

Mit wachsendem Interesse wurden POx in einem breiten Spektrum von Anwendungen untersucht, insbesondere im biomedizinischen Bereich, z. B. bei der Verabreichung von Arzneimitteln, Proteinen und Genen. Da Chiralität eine wesentliche Eigenschaft vieler biologisch relevanter Moleküle ist, darunter auch vieler Arzneimittel, ist es interessant, chirale Arzneimittelabgabesysteme auf der Grundlage von POx zu entwickeln. Obwohl bereits einige Forschungsarbeiten über chirale POx veröffentlicht wurden, ist eine Arzneimittelformulierung auf der Grundlage eines chiralen (Hauptkette) POx Triblock-Copolymer noch nicht untersucht worden. Um die stereoregulären Polymere als Arzneimittelträger zu verstehen, wurden amphiphile Triblock-Copolymere der Reihen A-pEtEtOx-A und A-pPrMeOx-A mit CUR, PTX und chiralem/racemischem IBU formuliert. Die arzneimittelbeladenen Mizellen wurden mit Hilfe der Dünnschichthydratationsverfahren hergestellt und anschließend die Beladungsfähigkeit charakterisiert. Wenn der hydrophobe A Block von A-pEtEtOx-A und A-pPrMeOx-A kurz war ($DP \approx 10$) und der hydrophile B Block von DP 10 bis 50 variierte, hatte das synthetisierte Triblock-Copolymer T1-T10 eine niedrige Wirkstoffbeladung für CUR und PTX. Sie hängt mit der Wasserlöslichkeit der Polymere und dem Verhältnis von hydrophilen und hydrophoben Segmenten zusammen. Im Vergleich zu T1-T10 wies das Triblock-Copolymer T21-T26, das aus dem hydrophilen A Block mit $DP \approx 35$ und dem hydrophoben B Block mit $DP \approx 20$ zusammengesetzt war, sowohl für CUR als auch für PTX eine höhere Wirkstoffbeladung auf. Daher wurden die T21-T26 zur Formulierung mit IBU verwendet, um den hydrodynamischen Durchmesser (D_h), die Fähigkeit zur Wirkstoffbeladung (LC) und die Langzeitstabilität in Form der Formulierung zu bestimmen. Die Polymere T21-T26 wurden als A-p^REtEtOx-A, A-p^SEtEtOx-A, A-p^{RS}EtEtOx-A, A-p^RPrMeOx-A, A-p^SPrMeOx-A, A-p^{RS}PrMeOx-A abgekürzt, um das Verständnis der Stereostruktur der Polymere zu erleichtern. Die ^MA-pEtEtOx-A und ^MA-pPrMeOx-A stellten die 1/1 (w/w) Mischungen von zwei entsprechenden chiralen Triblock-Copolymeren dar.

Sowohl die Triblock-Copolymere der A-pEtEtOx-A- als auch der A-pPrMeOx-A-Reihe waren in wässriger Lösung (Polymer 10 g/L) homogen, wenn sie frisch hergestellt wurden. Die Lösungen von A-p^RPrMeOx-A, A-p^SPrMeOx-A und ^MA-pPrMeOx-A wurden jedoch nach einiger Zeit trüb. Der Wirkstoff (CUR und IBU) war vorteilhaft für die Bildung einheitlicherer Mizellen. Die hydrodynamische Größe der frischen, mit dem Wirkstoff beladenen Mizelle

(Polymer/Arzneimittel=10/2 g/L) war im Wesentlichen monomodal mit einer engen Größenverteilung (mit CUR beladene Mizelle $D_h \approx 25$ nm, $PDI < 0,11$; mit S-IBU beladene Mizelle D_h 10-20 nm, $PDI < 0,23$). Die meisten Formulierungen blieben einen Monat lang transparent, doch obwohl das Arzneimittel zur Stabilisierung der Mizellen beitrug, war die Formulierung $^M A$ -pPrMeOx-A/S-IBU nach einigen Tagen trüb, ähnlich wie die unbeladene $^M A$ -pPrMeOx-A-Lösung. Die Trübung der Polymerlösungen oder der Formulierungen resultierte aus der Selbstorganisation und nicht aus der Kristallisation des Polymers oder der Arzneimittel, was durch eine XRD-Analyse bestätigt wurde.

T21-26 zeigte eine gute Leistung beim Laden von CUR und PTX. Bei gleicher CUR- oder PTX-Beladung der A-pEtEtOx-A (oder A-pPrMeOx-A) Formulierung wiesen das chirale, racemische Polymer und die 1/1 (w/w) Mischungen in den meisten Fällen eine ähnliche LC auf, mit Ausnahme der unerwartet hohen Medikamentenbeladung von A-p^{RS}PrMeOx-A/CUR bei 10/10 g/L Beladung. Die maximale LC hing jedoch wesentlich von der Art des hydrophoben Blocks und nicht von der Chiralität ab. Die maximale LC von CUR betrug ≈ 40 wt% in A-pEtEtOx-A und ≈ 29 wt% in A-pPrMeOx-A-Formulierungen. Die maximale PTX-LC betrug ≈ 18 wt% in A-pEtEtOx-A und ≈ 32 wt% in A-pPrMeOx-A. Vergleicht man die hydrophoben Blöcke der beiden Serien, so führt eine Methylengruppe an der N-substituierten Seitenkette (A-pPrMeOx-A) oder am Rückgrat (A-pEtEtOx-A) zu einer spezifischen Wirkstoffbeladung von CUR und PTX, die dem isomeren Paar von A-pBuOx-A und A-pPrOzi-A ähnlich ist. Wurden die Polymere der Serien A-pEtEtOx-A und A-pPrMeOx-A dagegen mit chiraalem und racemischem IBU formuliert, zeigten die beiden Serien keine spezifischen Unterschiede in der Wirkstoffbeladung. Im Allgemeinen betrug die maximale IBU LC 32-37 wt% in A-pEtEtOx-A-Formulierungen und 31-36 wt% in A-pPrMeOx-A-Formulierungen, wobei keine nennenswerte Regelmäßigkeit festgestellt wurde. Betrachtet man die Konzentration des gelösten Wirkstoffs bei gleicher IBU-Zufuhr, so hatte die Chiralität der Triblock-Copolymere einen Einfluss bei hoher Wirkstoffzufuhr (IBU 8 g/L und mehr; Polymer 10 g/L), während sie bei 1-6 g/L Wirkstoffzufuhr keinen eindeutigen Einfluss hatte. Interessanterweise zeigten die Polymere A-p^SEtEtOx-A und A-p^SPrMeOx-A zusammen mit dem Einfluss der IBU-Chiralität bei hoher Wirkstoffzufuhr eine geringere Wirkstoffbeladung als ihre R- und RS-Isomere bei hoher S-IBU-Zufuhr, insbesondere bei 8 g/L. Dies kann im Moment nicht im Detail erklärt werden, hängt aber wahrscheinlich mit der stereostrukturbedingten Selbstanordnung zwischen dem Arzneimittel und dem Polymer zusammen.

Zusammenfassend lässt sich sagen, dass chirale/racemische pEtEtOx und pPrMeOx aus den entsprechenden chiralen/racemischen Oxazolin-monomeren mittels LCROP synthetisiert werden können. Die synthetisierten Homopolymere sind schlecht wasserlöslich, zeigen aber ein thermoresponsives Verhalten in wässriger Lösung. Die chiralen Homopolymere und Triblock-Copolymere, die einen chiralen pEtEtOx- oder pPrMeOx-Block enthalten, sind in der Lage, die Sekundärstruktur in Lösung zu bilden, während die racemischen Isomere und 1/1 (w/w)-Mischungen entweder keine Sekundärstruktur bildeten oder die Sekundärstruktur bildeten, aber bei einer 50/50-Mischung den Effekt negierten. Sowohl die Polymere der A-pEtEtOx-A- als auch der A-pPrMeOx-A-Reihe können CUR, PTX und IBU gut aufnehmen, und es besteht auch die Möglichkeit, sie für die Beladung mit anderen hydrophoben Wirkstoffen einzusetzen. Es ist erwähnenswert, dass die Chiralität der Polymere die Stabilität der Mizellen, die Mizellengröße, die Größenverteilung, die Wirkstoffbeladung usw. beeinflussen kann, aber dies muss für bestimmte Systeme überprüft werden. Abgesehen von der Stereostruktur der Polymere könnte auch die Chiralität der Wirkstoffe die Wirkstoffbeladung bis zu einem gewissen Grad beeinflussen. Der Unterschied zwischen POx mit unterschiedlicher Chiralität erfordert weitere Untersuchungen, insbesondere die Wechselwirkungen zwischen chiralen/racemischen POx und biologischen Systemen sind Gegenstand künftiger Untersuchungen. (This German summary was written based on the English summary, with the help of open and free translation tools from Deepl and Google translate.)

7 Experimental

7.1 Reagents and solvents

All chemicals and solvents used in this work were purchased from Sigma-Aldrich (Steinheim, Germany), Acros (Geel, Belgium), abcr (Karlsruhe, Germany) and TCI (Eschborn, Germany), and used as received unless otherwise stated. Curcumin (CUR) powder from *Curcuma longa* (Turmeric) was purchased from Sigma-Aldrich (curcumin = 79%; demethoxycurcumin = 17%, bisdemethoxycurcumin = 4%; determined by HPLC analysis). Paclitaxel (PTX) was purchased from LC Laboratories (Woburn, MA, USA). (R)-(-)-ibuprofen (R-IBU) (98.5%) was purchased from MedChemExpress (distributor Hycultec, Beutelsbach, Germany). (S)-(+)-ibuprofen (S-IBU) (99%) and racemic ibuprofen (RS-IBU) (pharmaceutical secondary standard; certified reference material) was purchased from Sigma-Aldrich. (R)-(-)-2-Amino-1-propanol (purity 98%), (S)-(+)-2-Amino-1-propanol (purity 98%), (R)-(-)-2-Amino-1-butanol (purity 98%), (S)-(+)-2-Amino-1-butanol (purity 98%) were purchased from abcr. DL-2-Amino-1-propanol (purity 98%) and DL-2-Amino-1-butanol (purity 98%) were purchased from TCI. Deuterated solvents for NMR analysis were obtained from Deutero GmbH (Kastellaun, Germany).

Monomers (R)-2-ethyl-4-ethyl-2-oxazoline (^REtEtOx), (S)-2-ethyl-4-ethyl-2-oxazoline (^SEtEtOx), (RS)-2-ethyl-4-ethyl-2-oxazoline (^{RS}EtEtOx), (R)-2-propyl-4-methyl-2-oxazoline (^RPrMeOx), (S)-2-propyl-4-methyl-2-oxazoline (^SPrMeOx) and (RS)-2-propyl-4-methyl-2-oxazoline (^{RS}PrMeOx) were synthesized in the group (see below). The substances used for polymerization, such as methyl trifluoromethylsulfonate (MeOTf), monomers and sulfolane were refluxed over CaH₂, distilled and stored under argon in glovebox.

7.2 Equipment & methods of measurement

7.2.1 Equipment

Glovebox

A LabMaster 130 (MBraun, Garching, Germany) comprising nitrogen atmosphere (5.0, Linde AG, Germany) was used to store chemicals and to weigh moisture or oxygen sensitive substances under inert conditions.

Nuclear Magnetic Resonance (NMR) Spectroscopy

NMR spectra were measured with a Fourier 300 (^1H , 300.12 MHz; ^{13}C , 75.48 MHz), Bruker Biospin (Rheinstetten, Germany) at a temperature of 298 K and evaluated using MestReNova V.6.0.2-5475 software (Mestrelab Research, Santiago de Compostela, Spain). All chemical shifts of signals were given in ppm. The spectra were calibrated to the signals of residual protonated solvent signals (CDCl_3 7.26 ppm).

Size exclusion chromatography (SEC)

Depending on the solvent and column, SEC measurement was performed on one of the three systems described below.

HFIP SEC with PSS PFG linear M column (SEC #): SEC was conducted on an Agilent 1260 Infinity System, Polymer Standard Service (Mainz, Germany) with hexafluoroisopropanol (HFIP) containing 3 g/L potassium trifluoroacetate; precolumn: 50 mm \times 8 mm PSS PFG linear M (particle size 7 μm); main column: 2 columns 300 \times 8 mm PSS PFG linear M (particle size 7 μm ; pore size 0.1-1000 kDa). The columns were kept at 40 $^\circ\text{C}$ and flow rate was 0.7 mL/min. Prior to each measurement, samples were dissolved in HFIP/potassium trifluoroacetate and filtered through 0.2 μm PTFE filters, Roth (Karlsruhe, Germany). Conventional calibration was performed with PEG standards (0.1-1000 kg/mol) and data was processed with Win-GPC software.

HFIP SEC with AppliChrom ABOA HFIP-P350 column (SEC ##): SEC was performed on the same Agilent 1260 Infinity System, Polymer Standard Service (Mainz, Germany) with hexafluoroisopropanol (HFIP) containing 3 g/L potassium trifluoroacetate; precolumn: 50 mm \times 8 mm PSS PFG linear M (particle size 7 μm); main column: 8 \times 300 mm AppliChrom ABOA HFIP-P350 (pore size 0.1-1000 kDa). The columns were kept at 40 $^\circ\text{C}$ and flow rate was 0.3

mL/min. Prior to each measurement, samples were dissolved in HFIP/potassium trifluoroacetate and filtered through 0.2 μm PTFE filters, Roth (Karlsruhe, Germany). Conventional calibration was performed with PEG standards (0.1-1000 kg/mol) and data was processed with Win-GPC software.

Chloroform SEC with Malvern LC4000L column (SEC^{###}): SEC of pPrMeOx homopolymers was also performed on an alternative GPC system, Malvern GPCMax system (Malvern, UK) with a VE 3580 RI detector, PSS Polymer Standard Service (Mainz, Germany); two Malvern LC4000L column: 300 \times 8 mm (exclusion limit: 400 kDa). Chloroform was used as the eluent with a 100 μL sample volume injection. The columns were kept at 35 $^{\circ}\text{C}$ and flow rate was 1 mL/min. Prior to each measurement, samples were dissolved in chloroform and filtered through 0.2 μm PTFE filters, Roth (Karlsruhe, Germany). Conventional calibration was performed with polystyrene standards (1.2-40 kDa) and data was processed with OmniSEC software.

Thermogravimetric Analysis (TGA)

A TG 209 F1 IRIS (NETZSCH, Selb, Germany) was used for thermogravimetric analysis. The samples (5-10 mg) were added into aluminium oxide crucibles (NETZSCH, Selb, Germany) and heated under synthetic air from 30 $^{\circ}\text{C}$ to 900 $^{\circ}\text{C}$ (10 $^{\circ}\text{C}/\text{min}$) while detecting the mass loss. The corresponding NETZSCH Proteus-Thermal Analysis-V.5.2.1 software was used to evaluate the obtained data.

Differential Scanning Calorimetry (DSC)

DSC was performed on a DSC 204 F1 Phoenix (NETZSCH, Selb, Germany) under N_2 -atmosphere (20.0 mL/min). The samples were placed in aluminium pans with pierced crimped-on lids and heated from 30 $^{\circ}\text{C}$ to 190 $^{\circ}\text{C}$ and subsequently cooled to -50 $^{\circ}\text{C}$ (10 $^{\circ}\text{C}/\text{min}$). The heating/cooling cycle was repeated two additional times from -50 $^{\circ}\text{C}$ to 190 $^{\circ}\text{C}$ (10 $^{\circ}\text{C}/\text{min}$). Sample evaluation was performed as described for the TGA.

X-ray diffraction (XRD)

XRD was performed on a D8 Advance diffractometer with DaVinci design (Bruker AXS, Karlsruhe, Germany). The following measurement parameters were applied: a 2θ range of 5-60 $^{\circ}$, a step size of 0.02 $^{\circ}2\theta$, an integration time of 2 s, copper $\text{K}\alpha$ radiation, generator settings of 20 kV and 5 mA and a 0.344 $^{\circ}$ divergence slit. The data was exported by software DIFFRAC.EVA (Bruker AXS, Karlsruhe, Germany).

Fluorescence Spectroscopy

Fluorescence spectra were taken in a FP-8300 spectrofluorometer (JASCO, Gross-Umstadt, Germany) with a Peltier element for temperature regulation. The obtained spectra were evaluated in the corresponding JASCO spectra manager V.2.07.00 software.

Water Determination according to Karl Fischer

Water content of the applied solvents was determined by coulometric titration using a TitroLine 7500 KF trace (SI analytics, Mainz, Germany) with HYDRANAL[®] - Coulomat E as reagent.

Circular dichroism (CD) Spectroscopy

CD spectra were measured with a JASCO J-810 circular dichroism spectrometer (JASCO International Co., Ltd., Tokyo, Japan). The following scanning conditions were used: 200 nm/min scanning rate; 1 nm bandwidth; 0.5 nm data pitch; 1 s response time; and 3 accumulations. Samples were dissolved in methanol or water (0.1 g/L polymer concentration) and measured in a 1 mm path length quartz cuvette (110-QS, Hellma Analytics).

Ultraviolet-visible (UV-Vis) spectroscopy

CUR quantification was performed by UV-Vis absorption on a BioTek Eon Microplate Spectrophotometer, Thermo Fisher Scientific (Waltham, MA). A standard curve was obtained with known amounts of CUR, dissolved in ethanol. Samples were prepared in Rotilabo F-Type 96 well plates, Carl Roth GmbH & Co. KG (Karlsruhe, Germany) at a constant volume of 200 μ L. Spectra were recorded from 300 to 700 nm at 25 °C. Curcumin absorption was detected at 430 nm. Prior to UV-Vis absorption measurements, the aqueous formulations were appropriately diluted with ethanol to give a final absorbance between 0.3 and 2.5 (diluted at least 1/20 (v/v)).

High Performance Liquid Chromatography (HPLC)

HPLC analysis was carried out using a prominence LC-20A modular HPLC system (Shimadzu, Duisburg, Germany) equipped with a system controller CBM-20A, a solvent delivery unit LC-20 AT (double plunger), an on-line degassing unit DGU-20A, an auto-sampler SIL-20AC, a photo-diode array detector SPD-M20A, a column oven CTO-20AC, and a refractive index detector RID-20A. As stationary phase, a ZORBAX Eclipse Plus, Agilent (Santa Clara, CA, USA) C18 column (4.6 x 100 mm; 3.5 μ m) was used. The volume of samples injected was 20 μ L and elution was performed using a mobile phase of H₂O and acetonitrile (ACN)

containing 0.05% trifluoroacetic acid (TFA) at 40 °C and a flow rate of 1 mL/min. Detection of paclitaxel (PTX) and ibuprofen (IBU) was performed at 220 nm.¹⁹²⁻¹⁹⁴

Quantification of PTX and IBU was performed with a stepwise gradient. For PTX, within the first 10 min, the proportion of ACN was increased from 40% to 60%. Solvent proportion was kept constant for 5 min prior to decrease it to initial proportion of 40% ACN within 0.5 min. The retention time was 8.2 min.

For IBU, the proportion of ACN was increased from 40% to 60% ACN within the first 10 min, afterwards was increased to 80% ACN in 0.1 min and kept constant for 1.9 min, and finally was decreased to initial proportion of 40% ACN in 0.1 min. The retention time was 9.5 min.

Prior to each measurement, samples were centrifuged (9000 rpm; 7788g) with a MIKRO 185 (Hettich, Tuttlingen, Germany) and filtered through 0.4 µm PTFE filter (Rotilabo, Karlsruhe, Germany).

Dynamic Light Scattering (DLS)

Polymer/formulation aqueous solutions were prepared with PBS 10× (pH 7.4) and measured on Zetasizer Nano ZSP from Malvern, (Malvern Instruments, Worcestershire, UK) in disposable cuvettes (UV cuvettes semi micro, BRAND GmbH, Wertheim, Germany) at ambient temperatures (≈ 25 °C). Data was analysed by using Zetasizer software 7.11. All the samples were measured after filtration using 0.45 µm PVDF syringe filter (Rotilabo, Karlsruhe). The filtered samples were further diluted with PBS and measured again to exclude variation due to dilution effect. The data obtained are the average of three measurements of the same solution.

7.2.2 Methods of measurement

Fluorescence Spectroscopy-Critical Micelle Concentration (CMC)

CMC of triblock copolymers was determined using the fluorescence probe pyrene. Pyrene solutions (24 µM, 5.0 mg/L in acetone) were added to glass vials and followed by acetone removal by a gentle stream of argon. Afterwards, various amounts of aqueous polymer stock solutions were added, and the solutions were diluted with water (Millipore) to yield a final pyrene concentration of 5×10^{-7} M. The samples were shaken gently for 30 min and stored overnight at ambient temperature (≈ 20 °C) under the exclusion of light. Fluorescence measurements were

performed in a FP-8300, Jasco from 360 nm to 400 nm ($\lambda_{\text{ex}} = 333 \text{ nm}$) at 25 °C with 10×10 mm fluorescence cuvettes.

The fluorescence spectrum of pyrene shows five characteristic vibronic bands around 360-400 nm.¹⁹⁵ The ratio of the fluorescence intensities of the first and third vibronic bands of pyrene ($I_1:I_3$ ratio) increases characteristically with increasing polarity of the probe environment⁴². The CMC was determined as the concentration at which the fitted $I_1:I_3$ ratio decreased to 90% of its initial value.¹⁷³

Drug Formulation

Drug-loaded polymer micelles were prepared using the thin film hydration method.¹⁵² Ethanolic polymer (20 g/L), curcumin (5 g/L), paclitaxel (5 g/L), R-IBU (5 g/L), S-IBU (5 g/L) or RS-IBU (5 g/L) stock solutions were mixed in desired ratio. After complete removal of the solvent at 50 °C under a mild stream of argon, the films were further dried in vacuum ($\leq 0.2 \text{ mbar}$) for at least 30 min. Subsequently, preheated (37 °C) H₂O (Millipore) was added to obtain final polymer (10 g/L) and desired drug concentrations. To ensure complete solubilization, the solutions were shaken at 55 °C for 15 min, at 1250 rpm with a Thermomixer comfort (Eppendorf AG, Hamburg, Germany). Non-solubilized drug was removed by centrifugation for 5 min at 9000 rpm (relative centrifugal force (rcf) 7788g) by a MIKRO 185 (Hettich, Tuttlingen, Germany). The solubilization experiments were performed with three individually prepared samples and results are presented as means \pm standard deviation (SD).

The loading capacity (LC) and loading efficiency (LE) were calculated using the following equations:

$$\text{LC} = \frac{m_{\text{drug}}}{m_{\text{drug}} + m_{\text{polymer}}} \times 100\%$$

$$\text{LE} = \frac{m_{\text{drug}}}{m_{\text{drug,added}}} \times 100\%$$

Where m_{drug} and m_{polymer} are the weight amounts of the solubilized drug and polymer excipient in solution and $m_{\text{drug,added}}$ is the weight amount of the drug initially added to the dispersion. No loss of polymer during micelles preparation was assumed.

Long-term stability studies

For long-term stability studies, formulation was stored at ambient conditions ($\approx 25\text{ }^{\circ}\text{C}$). The samples were collected at day 0, 1, 8, 20, 30 and 60. Before the determination of the drug loading by HPLC, all samples were centrifuged for 5 min at 9000 rpm with a MIKRO 185 (Hettich, Tuttlingen, Germany). Long-term stabilization experiments were performed with three individually prepared samples and results are presented as means \pm SD, quantification was carried out as described previously.

Statistical analysis.

Statistical significance was calculated by Student's t-test. Differences with a value of $p < 0.05$ were considered statistically significant.

7.3 Methods

7.3.1 Monomer synthesis, general synthetic procedure, GSP 1

The monomers were prepared following the procedure by Witte and Seeliger *et al.*¹⁰⁻¹¹ 1.2 eq of the respective nitrile, 1 eq of alkanolamine and 0.025 eq of zinc acetate dihydrate were added to an argon flushed flask and heated to 130°C under reflux for 2-6 d. The reaction continued until the reaction mixture turned dark brown. Reaction progress was controlled by $^1\text{H-NMR}$ -spectroscopy. Subsequently, the raw product was dissolved in dichloromethane and washed with H_2O for 3-5 times. The organic phase was dried with anhydrous MgSO_4 , filtered and concentrated with rotary evaporator. The residue was mixed with CaH_2 overnight and distilled via vacuum distillation. If necessary, distillation was repeated, and the product was stored under argon atmosphere.

(R)-2-ethyl-4-ethyl-2-oxazoline ($^{\text{R}}\text{EtEtOx}$), No. YNM034 (according to GSP1)

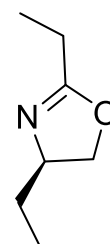
Propionitrile: 18.5 g (0.336 mol, 1.2 eq)

R-(-)-2-Amino-1-butanol: 25 g (0.28 mol, 1 eq)

$\text{ZnAc}_2 \cdot (\text{H}_2\text{O})_2$: 1.5 g (0.0070 mol, 0.025 eq)

Bp: 37°C (10 mbar)

Yield: 15.5 g (0.122 mol, 43.4%) of a colorless liquid



$^1\text{H-NMR}$: $^1\text{H NMR}$ (300 MHz, Chloroform-*d*, 298K): δ = 4.20 (dd, $^3J_{1,2}$ =8.1 Hz, $^2J_{1,3}$ =9.3 Hz, 1H, H¹), 3.99-3.89 (m, 1H, H²), 3.77 (dd, $^3J_{3,2}$ = $^2J_{3,1}$ =7.8 Hz, 1H, H³), 2.21 (qd, $^2J_{4,4'}$ =1.2 Hz, $^3J_{4,6}$ =7.8 Hz, 2H, H⁴), 1.65-1.36 (m, 2H, H⁵), 1.11 (t, $^3J_{6,4}$ =7.8 Hz, 3H, H⁶), 0.86 (t, $^3J_{7,5}$ =7.2 Hz, 3H, H⁷).

(S)-2-ethyl-4-ethyl-2-oxazoline (^SEtEtOx), No. YNM037 (according to GSP1)

Propionitrile: 18.5 g (0.336 mol, 1.2 eq)

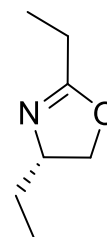
(S)-(+)-2-Amino-1-propanol: 25 g (0.28 mol, 1 eq)

ZnAc₂·(H₂O)₂: 1.5 g (0.0070 mol, 0.025 eq)

Bp: 37°C (9.4 mbar)

Yield: 14.3 g (0.112 mol, 40.0%) of a colorless liquid

$^1\text{H-NMR}$: $^1\text{H NMR}$ (300 MHz, Chloroform-*d*, 298K): δ = 4.20 (dd, $^3J_{1,2}$ =8.1 Hz, $^2J_{1,3}$ =9.3 Hz, 1H, H¹), 3.99-3.89 (m, 1H, H²), 3.77 (dd, $^3J_{3,2}$ = $^2J_{3,1}$ =7.8 Hz, 1H, H³), 2.20 (qd, $^2J_{4,4'}$ =1.2 Hz, $^3J_{4,6}$ =7.5 Hz, 2H, H⁴), 1.65-1.36 (m, 2H, H⁵), 1.11 (t, $^3J_{6,4}$ =7.5 Hz, 3H, H⁶), 0.86 (t, $^3J_{7,5}$ =7.2 Hz, 3H, H⁷).



(RS)-2-ethyl-4-ethyl-2-oxazoline, (^{RS}EtEtOx), No. YNM051 (according to GSP1)

Propionitrile: 18.5 g (0.336 mol, 1.2 eq)

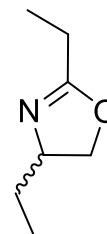
DL-2-Amino-1-butanol: 25 g (0.28 mol, 1 eq)

ZnAc₂·(H₂O)₂: 1.5 g (0.0070 mol, 0.025 eq)

Bp: 39°C (10.9 mbar)

Yield: 17.3 g (0.136 mol, 48.4%) of a colorless liquid

$^1\text{H-NMR}$: $^1\text{H NMR}$ (300 MHz, Chloroform-*d*, 298K): δ = 4.20 (dd, $^3J_{1,2}$ = $^2J_{1,3}$ =8.7 Hz, 1H, H¹), 3.98-3.89 (m, 1H, H²), 3.77 (dd, $^3J_{3,2}$ = $^2J_{3,1}$ =7.8 Hz, 1H, H³), 2.20 (q, $^3J_{4,6}$ =7.5 Hz, 2H, H⁴), 1.65-1.36 (m, 2H, H⁵), 1.11 (t, $^3J_{6,4}$ =7.5, 3H, H⁶), 0.86 (t, $^3J_{7,5}$ =7.5 Hz, 3H, H⁷).



(R)-2-propyl-4-methyl-2-oxazoline (^RPrMeOx), No. YNM035 (according to GSP1)

Butyronitrile: 27.6 g (0.399 mol, 1.2 eq)

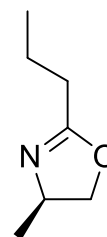
(R)-(-)-2-Amino-1-propanol: 25 g (0.33 mol, 1 eq)

ZnAc₂·(H₂O)₂: 1.8 g (0.0083 mol, 0.025 eq)

Bp: 36°C (10 mbar)

Yield: 19.3 g (0.152 mol, 46.3%) of a colorless liquid

$^1\text{H-NMR}$: $^1\text{H NMR}$ (300 MHz, Chloroform-*d*, 298K): δ =4.24 (dd, $^3J_{1,2}$ =7.8 Hz, $^2J_{1,3}$ =9.3 Hz,



1H, H¹), 4.13-4.01 (m, 1H, H²), 3.67 (dd, ³J_{3,2}=²J_{3,1}=7.8 Hz, 1H, H³), 2.17 (t, ³J_{4,5}=7.2 Hz, 2H, H⁴), 1.65-1.53 (m, 2H, H⁵), 1.18 (d, ²J_{6,2}=6.6 Hz, 3H, H⁶), 0.90 (t, ³J_{7,5}=7.2 Hz, 3H, H⁷).

(S)-2-propyl-4-methyl -2-oxazoline (^SPrMeOx), No. YNM036 (according to GSP1)

Butyronitrile: 27.6 g (0.399 mol, 1.2 eq)

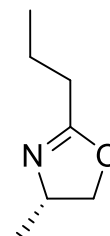
(S)-(+)-2-Amino-1-propanol: 25 g (0.33 mol, 1 eq)

ZnAc₂·(H₂O)₂: 1.8 g (0.0083 mol, 0.025 eq)

Bp: 39°C (10 mbar)

Yield: 23.4 g (0.184 mol, 55.3%) of a colorless liquid

¹H-NMR: ¹H NMR (300 MHz, Chloroform-*d*, 298K): δ=4.23 (dd, ³J_{1,2}=8.1, ²J_{1,3}=9.3 Hz, 1H, H¹), 4.13-4.01 (m, 1H, H²), 3.67 (dd, ³J_{3,2}=²J_{3,1}=7.5 Hz, 1H, H³), 2.17 (t, ³J_{4,5}=7.2 Hz, 2H, H⁴), 1.65-1.53 (m, 2H, H⁵), 1.18 (d, ²J_{6,2}=6.6 Hz, 3H, H⁶), 0.90 (t, ³J_{7,5}=7.2 Hz, 3H, H⁷).



(RS)-2-propyl-4-methyl -2-oxazoline (^{RS}PrMeOx), No. YNM052 (according to GSP1)

Butyronitrile: 27.6 g (0.399 mol, 1.2 eq)

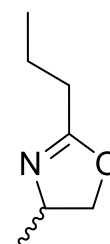
DL-2-Amino-1-propanol: 25 g (0.33 mol, 1 eq)

ZnAc₂·(H₂O)₂: 1.8 g (0.0083 mol, 0.025 eq)

Bp: 43°C (14.4 mbar)

Yield: 22.3 g (0.175 mol, 52.6%) of a colorless liquid

¹H-NMR: ¹H NMR (300 MHz, Chloroform-*d*, 298K): δ=4.24 (dd, ³J_{1,2}=²J_{1,3}=9.3 Hz, 1H, H¹), 4.13-4.01 (m, 1H, H²), 3.67 (dd, ³J_{3,2}=²J_{3,1}=7.8 Hz, 1H, H³), 2.17 (t, ³J_{4,5}=6.9 Hz, 2H, H⁴), 1.65-1.53 (m, 2H, H⁵), 1.18 (d, ²J_{6,2}=6.3 Hz, 3H, H⁶), 0.90 (t, ³J_{7,5}=7.5 Hz, 3H, H⁷).



7.3.2 Polymer synthesis, LCROP of 2-oxazolines

7.3.2.1 Homopolymers, general synthetic procedure, GSP 2

The polymerization and workup procedures were carried out similar to Lübtow *et al.* as described previously¹⁵². Briefly, 1 eq of initiator methyl trifluoromethylsulfonate (MeOTf) was added to a dried and argon flushed flask and dissolved in the respective amount of solvent sulfolane. The respective monomer PrMeOx or EtEtOx was added, and the reaction mixture was heated to 130°C for approximately 24-72 h. Reaction progress was controlled by ¹H-NMR spectroscopy. After complete consumption of the monomer, termination was carried out by addition of 3 eq of 1-Boc-piperazine (PipBoc) at 50°C for 4 hours. Subsequently, 1 eq of K₂CO₃

was added and the mixture was stirred at 50°C for 4 hours.

The product was purified using two methods. For method 1, the reaction mixture was dissolved in chloroform and washed with water for 3 times to remove the sulfolane. A waxy crude product was obtained after drying the organic phase under vacuum. Afterwards, the crude product was dissolved in methanol and precipitated from water to obtain a white precipitate. This white precipitate was collected by centrifugation and lyophilized. However, the method 1 was complicated and not able to remove the sulfolane residues completely, even after redispersing and precipitating in methanol and water for 3 times. For method 2, the reaction mixture was dissolved in ethanol and dialyzed against ethanol/water = 2/1 (v/v), followed by dialysis against water to remove the ethanol. The white suspension remained in the dialysis bag was recovered and lyophilized. The method 2 was convenient and removed the sulfolane completely, so that it was used further for the homopolymer purification. Dialysis bag: MWCO 1 kDa, cellulose acetate, Spectra/Por[®]7, Pre/treated RC tubing.

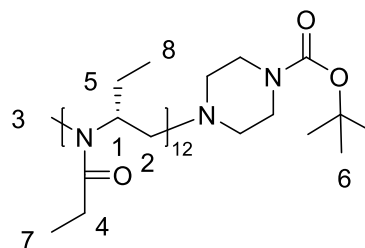
Me-^REtEtO_{x12}-PipBoc (H1), No. YNM039-aa (according to GSP2)

		M (g/mol)	eq	m (g)	n (mmol)
Monomer	^R EtEtOx	127.19	10	0.78	6.1(0)
Initiator	MeOTf	164.1	1	0.100	0.611
Terminator	1-Boc-piperazine	186.25	3	0.35	1.8(9)
Neutralizer	K ₂ CO ₃	138.21	1	0.092	0.66
Solvent	sulfolane	3 mL for polymerization and 1 mL for termination			

Yield 0.70 g (0.40 mmol, 77.4%)

SEC[#] (HFIP) M_n = 1.0 kg/mol; Đ = 1.05

¹H-NMR M_n = 1.7 kg/mol



Me-^REtEtO_{x21}-PipBoc (H2, p^REtEtOx), No. YNM039-b (according to GSP2)

		M (g/mol)	eq	m (g)	n (mmol)
Monomer	^R EtEtOx	127.19	20	0.83	6.5(3)
Initiator	MeOTf	164.1	1	0.054	0.33
Terminator	1-Boc-piperazine	186.25	3	0.18	0.99

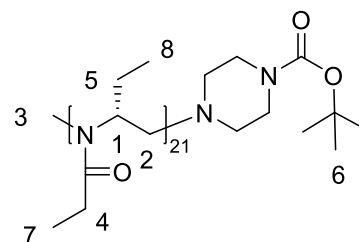
Neutralizer	K ₂ CO ₃	138.21	1	0.047	0.34
Solvent	sulfolane	3 mL for polymerization and 0.5 mL for termination			

Yield 0.62 g (0.22 mmol, 69.3%)

SEC[#] (HFIP) M_n=1.5 kg/mol; Đ=1.07

SEC^{##} (HFIP) M_n=1.3 kg/mol; Đ=1.09

¹H-NMR M_n=2.9 kg/mol



¹H-NMR (300 MHz, Chloroform-*d*, 298K): δ = 4.89-2.90 (br, 60H, H¹⁻²), 2.88-2.71 (br, 7H, H³), 2.57-2.11 (br, 41H, H⁴), 1.83-1.43 (br, 29H, H⁵), 1.40-1.33 (s, 9H, H⁶), 1.16-0.94 (br, 60H, H⁷), 0.93-0.51 (br, 55H, H⁸).

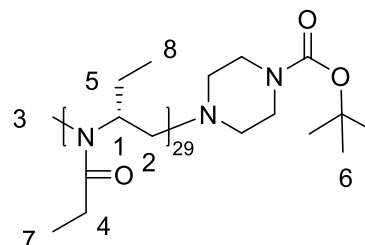
Me-R^{EtEtOx}₂₉-PipBoc (H3), No. YNM039-3 (according to GSP2)

		M (g/mol)	eq	m (g)	n (mmol)
Monomer	R ^{EtEtOx}	127.19	30	0.95	7.5(0)
Initiator	MeOTf	164.1	1	0.041	0.25
Terminator	1-Boc-piperazine	186.25	3	0.14	0.74
Neutralizer	K ₂ CO ₃	138.21	1	0.046	0.33
Solvent	sulfolane	3.5 mL for polymerization and 1.5 mL for termination			

Yield 0.85 g (0.22 mmol, 84.9%)

SEC[#] (HFIP) M_n=1.6 kg/mol; Đ=1.15

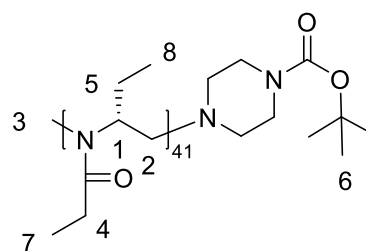
¹H-NMR M_n=3.9 kg/mol



Me-R^{EtEtOx}₄₁-PipBoc (H4), No. YNM039-4 (according to GSP2)

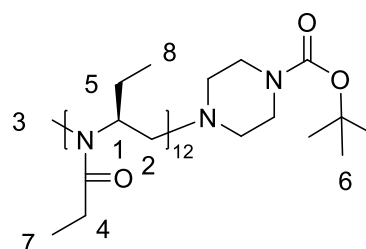
		M (g/mol)	eq	m (g)	n (mmol)
Monomer	R ^{EtEtOx}	127.19	40	0.93	7.2(9)
Initiator	MeOTf	164.1	1	0.030	0.18
Terminator	1-Boc-piperazine	186.25	3	0.11	0.59
Neutralizer	K ₂ CO ₃	138.21	2	0.041	0.30
Solvent	sulfolane	3.5 mL for polymerization and 1.5 mL for termination			

Yield 0.59 g (0.11 mmol, 61.0%)

SEC[#] (HFIP) $M_n = 2.0$ kg/mol; $\mathcal{D} = 1.18$ ¹H-NMR $M_n = 5.4$ kg/mol**Me^SEtEtOx₁₂-PipBoc (H5), No. YNM042-1 (according to GSP2)**

		M (g/mol)	eq	m (g)	n (mmol)
Monomer	^S EtEtOx	127.19	10	0.42	3.3(0)
Initiator	MeOTf	164.1	1	0.053	0.32
Terminator	1-Boc-piperazine	186.25	3	0.18	0.97
Neutralizer	K ₂ CO ₃	138.21	1	0.046	0.33
Solvent	sulfolane	1.5 mL for polymerization and 0.5 mL for termination			

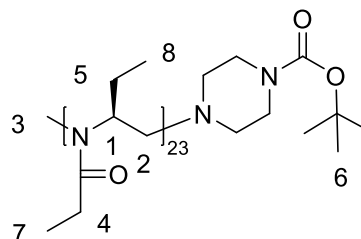
Yield 0.29 g (0.17 mmol, 59.9%)

SEC[#] (HFIP) $M_n = 0.9$ kg/mol; $\mathcal{D} = 1.13$ ¹H-NMR $M_n = 1.7$ kg/mol**Me^SEtEtOx₂₃-PipBoc (H6, p^SEtEtOx), No. YNM042-2d (according to GSP2)**

		M (g/mol)	eq	m (g)	n (mmol)
Monomer	^S EtEtOx	127.19	20	0.75	5.8(7)
Initiator	MeOTf	164.1	1	0.048	0.29
Terminator	1-Boc-piperazine	186.25	4	0.22	1.2(0)
Neutralizer	K ₂ CO ₃	138.21	1	0.041	0.29
Solvent	sulfolane	3 mL for polymerization and 0.5 mL for termination			

Yield 0.63 g (0.21 mmol, 83.2%)

SEC[#] (HFIP) $M_n = 1.1$ kg/mol; $\mathcal{D} = 1.22$ SEC^{##} (HFIP) $M_n = 1.0$ kg/mol; $\mathcal{D} = 1.16$

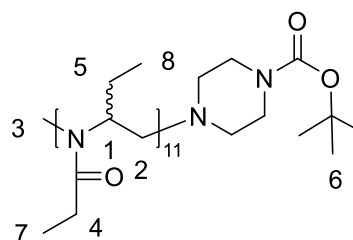
¹H-NMR $M_n = 3.1$ kg/mol

¹H-NMR (300 MHz, Chloroform-*d*, 298K): $\delta = 4.82$ -2.91 (br, 69H, H^{1-2}), 2.89-2.78 (br, 5H, H^3), 2.56-2.19 (br, 47H, H^4), 1.84-1.42 (br, 33H, H^5), 1.41-1.31 (s, 9H, H^6), 1.14-0.94 (br, 77H, H^7), 0.91-0.68 (br, 71H, H^8).

Me-^{RS}EtEtOx₁₁-PipBoc (H7), No. YNM043-1b (according to GSP2)

		M (g/mol)	eq	m (g)	n (mmol)
Monomer	^{RS} EtEtOx	127.19	10	1.49	11.7(0)
Initiator	MeOTf	164.1	1	0.192	1.17
Terminator	1-Boc-piperazine	186.25	3	0.67	3.5(9)
Neutralizer	K ₂ CO ₃	138.21	1	0.162	1.17
Solvent	sulfolane	6 mL for polymerization and 2 mL for termination			

Yield 1.13 g (0.71 mmol, 65.7%)

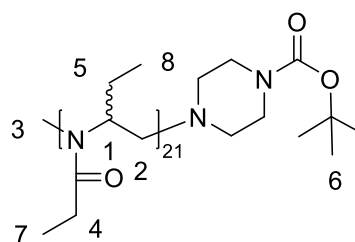
SEC[#] (HFIP) $M_n = 0.8$ kg/mol; $\mathcal{D} = 1.17$ ¹H-NMR $M_n = 1.6$ kg/mol

Me-^{RS}EtEtOx₂₁-PipBoc (H8, p^{RS}EtEtOx), No. YNM043-2a (according to GSP2)

		M (g/mol)	eq	m (g)	n (mmol)
Monomer	^{RS} EtEtOx	127.19	20	0.59	4.6(5)
Initiator	MeOTf	164.1	1	0.038	0.23
Terminator	1-Boc-piperazine	186.25	3	0.15	0.79
Neutralizer	K ₂ CO ₃	138.21	1	0.032	0.23
Solvent	sulfolane	3 mL for polymerization and 0.5 mL for termination			

Yield 0.37 g (0.13 mmol, 57.7%)

SEC[#] (HFIP) $M_n = 1.7$ kg/mol; $\mathcal{D} = 1.11$

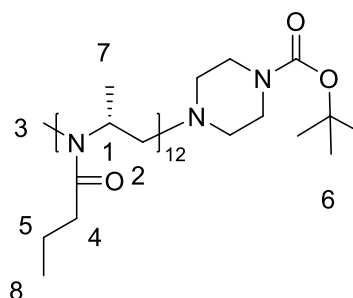
SEC^{##} (HFIP) $M_n = 1.2$ kg/mol; $\mathcal{D} = 1.13$ ¹H-NMR $M_n = 2.9$ kg/mol

¹H-NMR (300 MHz, Chloroform-*d*, 298K): $\delta = 4.78$ -2.89 (br, 63H, H^{1-2}), 2.87-2.76 (br, 5H, H^3), 2.62-2.14 (br, 43H, H^4), 1.82-1.41 (br, 38H, H^5), 1.41-1.32 (s, 9H, H^6), 1.17-0.94 (br, 60H, H^7), 0.93-0.56 (br, 57H, H^8).

Me-^RPrMeOx₁₂-PipBoc (H9), No. YNM040-1 (according to GSP2)

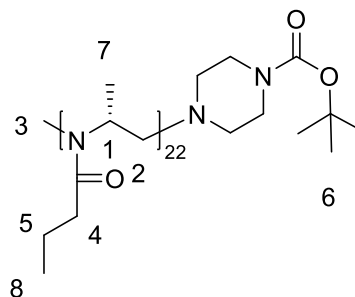
		M (g/mol)	eq	m (g)	n (mmol)
Monomer	^R PrMeOx	127.19	10	0.41	3.2(2)
Initiator	MeOTf	164.1	1	0.053	0.32
Terminator	1-Boc-piperazine	186.25	3	0.19	1.0(1)
Neutralizer	K ₂ CO ₃	138.21	1	0.048	0.34
Solvent	sulfolane	2 mL for polymerization and 0.7 mL for termination			

Yield 0.29 g (0.17 mmol, 60.2%)

SEC[#] (HFIP) $M_n = 1.2$ kg/mol; $\mathcal{D} = 1.05$ ¹H-NMR $M_n = 1.7$ kg/mol**Me-^RPrMeOx₂₂-PipBoc (H10, p^RPrMeOx), No. YNM040-2 (according to GSP2)**

		M (g/mol)	eq	m (g)	n (mmol)
Monomer	^R PrMeOx	127.19	20	0.94	7.3(9)
Initiator	MeOTf	164.1	1	0.060	0.37
Terminator	1-Boc-piperazine	186.25	3	0.21	1.1(1)
Neutralizer	K ₂ CO ₃	138.21	1	0.053	0.38
Solvent	sulfolane	3 mL for polymerization and 0.5 mL for termination			

Yield 0.77 g (0.26 mmol, 76.0%)

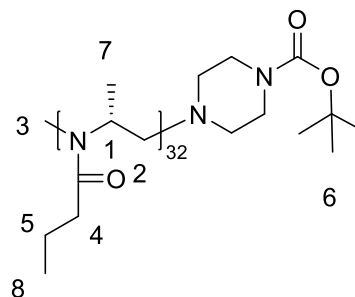
SEC[#] (HFIP) $M_n = 1.6 \text{ kg/mol}$; $\mathcal{D} = 1.07$ SEC^{##} (HFIP) $M_n = 1.3 \text{ kg/mol}$; $\mathcal{D} = 1.10$ ¹H-NMR $M_n = 3.0 \text{ kg/mol}$ 

¹H-NMR (300 MHz, Chloroform-*d*, 298K): $\delta = 4.89\text{-}2.91$ (br, 51H, H^{1-2}), $2.87\text{-}2.74$ (br, 4H, H^3), $2.55\text{-}2.02$ (br, 44H, H^4), $1.65\text{-}1.44$ (br, 39H, H^5), $1.43\text{-}1.36$ (s, 9H, H^6), $1.36\text{-}0.97$ (br, 61H, H^7), $0.96\text{-}0.79$ (br, 57H, H^8).

Me^RPrMeOx₃₂-PipBoc (H11), No. YNM040-3 (according to GSP2)

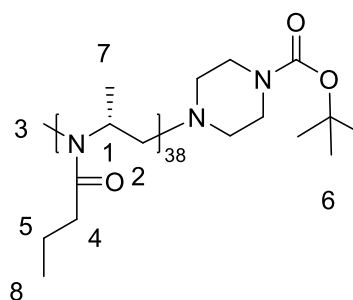
		M (g/mol)	eq	m (g)	n (mmol)
Monomer	^R PrMeOx	127.19	30	0.97	7.6(1)
Initiator	MeOTf	164.1	1	0.042	0.25
Terminator	1-Boc-piperazine	186.25	3	0.14	0.77
Neutralizer	K ₂ CO ₃	138.21	3	0.10	0.72
Solvent	sulfolane	3.5 mL for polymerization and 1.5 mL for termination			

Yield 0.81 g (0.19 mmol, 79.7%)

SEC[#] (HFIP) $M_n = 1.8 \text{ kg/mol}$; $\mathcal{D} = 1.11$ ¹H-NMR $M_n = 4.3 \text{ kg/mol}$ **Me^RPrMeOx₃₈-PipBoc (H12), No. YNM040-4 (according to GSP2)**

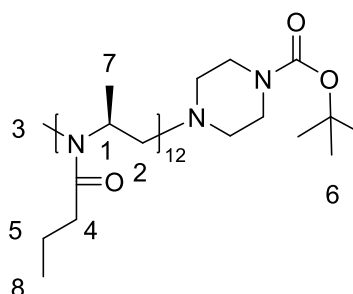
		M (g/mol)	eq	m (g)	n (mmol)
Monomer	^R PrMeOx	127.19	39	0.93	7.3(2)
Initiator	MeOTf	164.1	1	0.031	0.19
Terminator	1-Boc-piperazine	186.25	3	0.11	0.58
Neutralizer	K ₂ CO ₃	138.21	2	0.063	0.46
Solvent	sulfolane	3.5 mL for polymerization and 1.5 mL for termination			

Yield 0.77 g (0.15 mmol, 79.6%)

SEC[#] (HFIP) $M_n = 2.1$ kg/mol; $\mathcal{D} = 1.11$ ¹H-NMR $M_n = 5.0$ kg/mol**Me-^sPrMeOx₁₂-PipBoc (H13), No. YNM041-1 (according to GSP2)**

		M (g/mol)	eq	m (g)	n (mmol)
Monomer	^s PrMeOx	127.19	10	0.40	3.1(6)
Initiator	MeOTf	164.1	1	0.051	0.31
Terminator	1-Boc-piperazine	186.25	3	0.17	0.94
Neutralizer	K ₂ CO ₃	138.21	1	0.044	0.32
Solvent	sulfolane	1.5 mL for polymerization and 0.5 mL for termination			

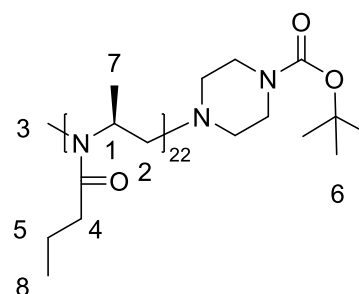
Yield 0.32 g (0.19 mmol, 69.9 %)

SEC[#] (HFIP) $M_n = 1.2$ kg/mol; $\mathcal{D} = 1.06$ ¹H-NMR $M_n = 1.7$ kg/mol**Me-^sPrMeOx₂₂-PipBoc (H14, p^sPrMeOx), No. YNM041-2 (according to GSP2)**

		M (g/mol)	eq	m (g)	n (mmol)
Monomer	^s PrMeOx	127.19	20	0.80	6.2(7)
Initiator	MeOTf	164.1	1	0.050	0.31
Terminator	1-Boc-piperazine	186.25	3	0.17	0.92
Neutralizer	K ₂ CO ₃	138.21	1	0.044	0.32
Solvent	sulfolane	3 mL for polymerization and 0.5 mL for termination			

Yield 0.74 g (0.25 mmol, 86.6%)

SEC[#] (HFIP) $M_n = 1.7$ kg/mol; $\mathcal{D} = 1.06$

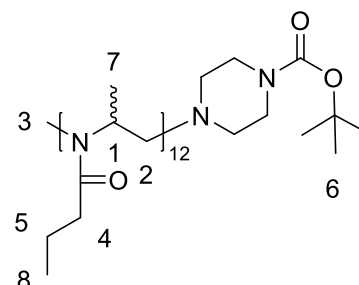
SEC[#] (HFIP) $M_n = 1.3$ kg/mol; $\mathcal{D} = 1.09$ ¹H-NMR $M_n = 3.0$ kg/mol

¹H-NMR (300 MHz, Chloroform-*d*, 298K): $\delta = 4.74$ - 2.99 (br, 58H, H^{1-2}), 2.85 - 2.75 (br, 4H, H^3), 2.56 - 2.01 (br, 44H, H^4), 1.64 - 1.45 (br, 43H, H^5), 1.43 - 1.36 (s, 9H, H^6), 1.35 - 0.98 (br, 57H, H^7), 0.96 - 0.73 (br, 57H, H^8).

Me-^{RS}PrMeOx₁₂-PipBoc (H15), No. YNM044-1b (according to GSP2)

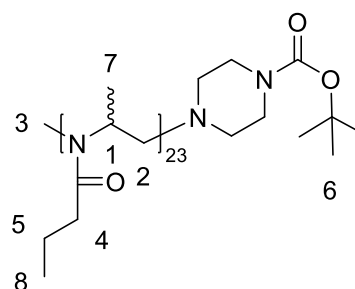
		M (g/mol)	eq	m (g)	n (mmol)
Monomer	^{RS} PrMeOx	127.19	10	1.47	11.5(9)
Initiator	MeOTf	164.1	1	0.190	1.16
Terminator	1-Boc-piperazine	186.25	3	0.66	3.5(3)
Neutralizer	K ₂ CO ₃	138.21	1	0.160	1.16
Solvent	sulfolane	6 mL for polymerization and 2 mL for termination			

Yield 1.32 g (0.76 mmol, 77.1 %)

SEC[#] (HFIP) $M_n = 1.1$ kg/mol; $\mathcal{D} = 1.02$ ¹H-NMR $M_n = 1.7$ kg/mol**Me-^{RS}PrMeOx₂₃-PipBoc (H16, p^{RS}PrMeOx), No. YNM044-2b (according to GSP2)**

		M (g/mol)	eq	m (g)	n (mmol)
Monomer	^{RS} PrMeOx	127.19	20	0.67	5.3(0)
Initiator	MeOTf	164.1	1	0.043	0.26
Terminator	1-Boc-piperazine	186.25	4	0.19	1.0(4)
Neutralizer	K ₂ CO ₃	138.21	1	0.037	0.26
Solvent	sulfolane	3 mL for polymerization and 0.5 mL for termination			

Yield	0.63 g (0.20 mmol, 87.1%)
SEC [#] (HFIP)	M _n = 1.4 kg/mol; Đ = 1.03
SEC ^{##} (HFIP)	M _n = 1.0 kg/mol; Đ = 1.11
¹ H-NMR	M _n = 3.1 kg/mol



¹H-NMR (300 MHz, Chloroform-*d*, 298K): δ = 4.79-2.91 (br, 55H, H^{1-2}), 2.88-2.77 (br, 5H, H^3), 2.43-2.07 (br, 47H, H^4), 1.65-1.46 (br, 45H, H^5), 1.42-1.35 (s, 9H, H^6), 1.32-0.97 (br, 61H, H^7), 0.93-0.80 (br, 71H, H^8).

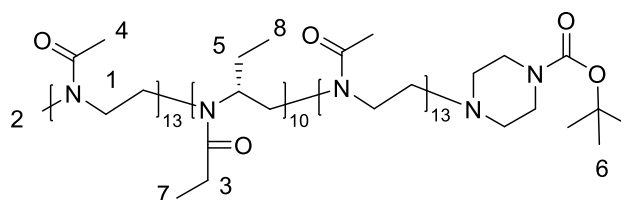
7.3.2.2 Triblock copolymer, general synthetic procedure, GSP 3

Briefly, 1 eq of initiator was added to a dried and argon flushed flask and dissolved in the respective amount of solvent. The monomer 2-methyl-2-oxazoline (MeOx) was added and the reaction mixture was heated to 100°C for approximately 2-3 h. Reaction progress was controlled by ¹H-NMR spectroscopy. After complete consumption of MeOx, the mixture was cooled to RT and the monomer EtEtOx or PrMeOx for the second block was added. The reaction mixture was heated to 130°C for 14-48 h. The procedure was repeated for the third block (MeOx) and termination was carried out by addition of 3 eq of 1-Boc-piperazine (PipBoc) at 50°C for 4 hours. Subsequently, 1 eq of K₂CO₃ was added and the mixture was stirred at 50°C for 4 hours. The crude product was transferred to a dialysis bag (MWCO 1 kDa, cellulose acetate) and dialyzed against Millipore water for 2 days. The solution was recovered from the bag and lyophilized.

Me-MeOx₁₃-^REtEtOx₁₀-MeOx₁₃-PipBoc (T1), No. YNM045-1 (according to GSP3)

		M (g/mol)	eq	m (g)	n (mmol)
Segment 1	MeOx	85.1	10	0.80	9.4(0)
Segment 2	^R EtEtOx	127.19	10	1.16	9.12
Segment 3	MeOx	85.1	10	0.77	9.0(5)
Initiator	MeOTf	164.1	1	0.15	0.91
Terminator	1-Boc-piperazine	186.25	3	0.52	2.8(0)
Neutralizer	K ₂ CO ₃	138.21	1	0.13	0.93
Solvent	sulfolane	13.5 mL for polymerization and 4 mL for termination			

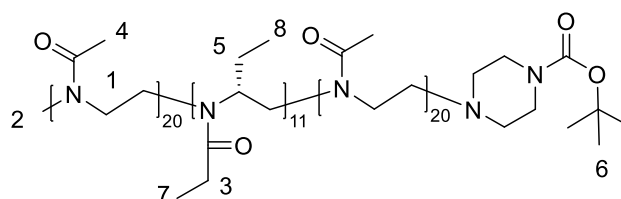
Yield	2.77 g (0.75 mmol, 95.2%)
SEC# (HFIP)	$M_n = 1.7$ kg/mol; $\mathcal{D} = 1.07$
$^1\text{H-NMR}$	$M_n = 3.7$ kg/mol



Me-MeOx₂₀-^REtEtOx₁₁-MeOx₂₀-PipBoc (T2), No. YNM047 (according to GSP3)

		M (g/mol)	eq	m (g)	n (mmol)
Segment 1	MeOx	85.1	20	0.69	8.1(1)
Segment 2	^R EtEtOx	127.19	10	0.52	4.0(6)
Segment 3	MeOx	85.1	20	0.68	8.0(4)
Initiator	MeOTf	164.1	1	0.066	0.40
Terminator	1-Boc-piperazine	186.25	3	0.21	1.1(4)
Neutralizer	K ₂ CO ₃	138.21	1	0.065	0.47
Solvent	sulfolane	8.5 mL for polymerization and 2.5 mL for termination			

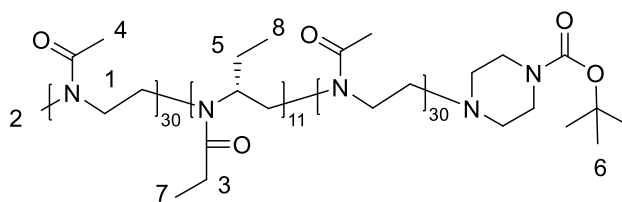
Yield	1.20 g (0.24 mmol, 60.6%)
SEC# (HFIP)	$M_n = 2.0$ kg/mol; $\mathcal{D} = 1.14$
$^1\text{H-NMR}$	$M_n = 5.0$ kg/mol



Me-MeOx₃₀-^REtEtOx₁₁-MeOx₃₀-PipBoc (T3), No. YNM048 (according to GSP3)

		M (g/mol)	eq	m (g)	n (mmol)
Segment 1	MeOx	85.1	28	0.78	9.1(4)
Segment 2	^R EtEtOx	127.19	10	0.39	3.0(5)
Segment 3	MeOx	85.1	28	0.77	9.0(8)
Initiator	MeOTf	164.1	1	0.053	0.32
Terminator	1-Boc-piperazine	186.25	3	0.21	1.1(2)
Neutralizer	K ₂ CO ₃	138.21	1	0.050	0.36
Solvent	sulfolane	10.5 mL for polymerization and 3.5 mL for termination			

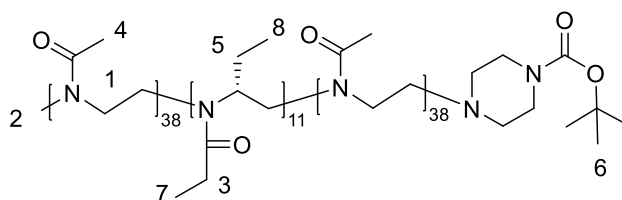
Yield	1.55 g (0.23 mmol, 77.4%)
SEC# (HFIP)	$M_n = 2.4$ kg/mol; $\mathcal{D} = 1.14$
$^1\text{H-NMR}$	$M_n = 6.7$ kg/mol



Me-MeOx₃₈-^REtEtOx₁₁-MeOx₃₈-PipBoc (T4), No. YNM053 (according to GSP3)

		M (g/mol)	eq	m (g)	n (mmol)
Segment 1	MeOx	85.1	40	1.15	13.4(8)
Segment 2	^R EtEtOx	127.19	10	0.43	3.3(6)
Segment 3	MeOx	85.1	40	1.15	13.4(7)
Initiator	MeOTf	164.1	1	0.055	0.34
Terminator	1-Boc-piperazine	186.25	3	0.20	1.0(5)
Neutralizer	K ₂ CO ₃	138.21	1	0.052	0.37
Solvent	sulfolane	13.5 mL for polymerization and 4 mL for termination			

Yield	2.50 g (0.31 mmol, 89.6%)
SEC# (HFIP)	$M_n = 4.5$ kg/mol; $\mathcal{D} = 1.15$
$^1\text{H-NMR}$	$M_n = 8.1$ kg/mol



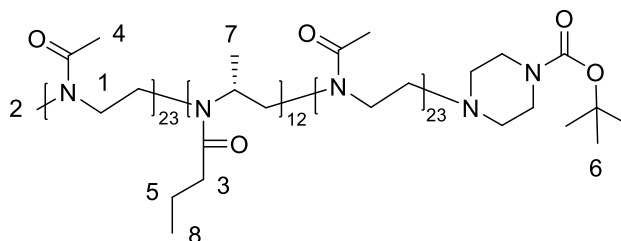
Me-MeOx₄₃-^REtEtOx₁₀-MeOx₄₃-PipBoc (T5), No. YNM054 (according to GSP3)

		M (g/mol)	eq	m (g)	n (mmol)
Segment 1	MeOx	85.1	50	1.64	19.2(7)
Segment 2	^R EtEtOx	127.19	10	0.49	3.8(3)
Segment 3	MeOx	85.1	50	1.64	19.2(4)
Initiator	MeOTf	164.1	1	0.063	0.39
Terminator	1-Boc-piperazine	186.25	3	0.22	1.1(8)
Neutralizer	K ₂ CO ₃	138.21	1	0.072	0.52

7 Experimental

Terminator	1-Boc-piperazine	186.25	3	0.18	0.94
Neutralizer	K ₂ CO ₃	138.21	1	0.040	0.29
Solvent	sulfolane	7.5 mL for polymerization and 2.5 mL for termination			

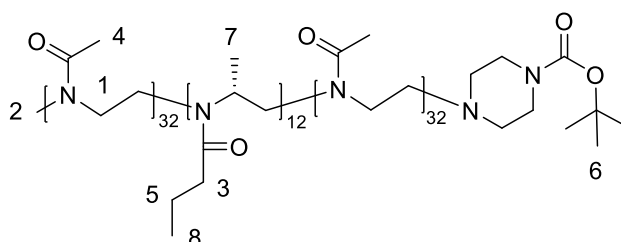
Yield	1.05 g (0.19 mmol, 75.0%)
SEC [#] (HFIP)	M _n = 2.7 kg/mol; Đ = 1.09
¹ H-NMR	M _n = 5.6 kg/mol



Me-MeO_{x32}-^RPrMeO_{x12}-MeO_{x32}-PipBoc (T8), No. YNM062 (according to GSP3)

		M (g/mol)	eq	m (g)	n (mmol)
Segment 1	MeOx	85.1	30	0.78	9.1(4)
Segment 2	^R PrMeOx	127.19	10	0.39	3.0(5)
Segment 3	MeOx	85.1	30	0.78	9.1(4)
Initiator	MeOTf	164.1	1	0.050	0.30
Terminator	1-Boc-piperazine	186.25	3	0.17	0.91
Neutralizer	K ₂ CO ₃	138.21	1	0.042	0.30
Solvent	sulfolane	10.5 mL for polymerization and 3.5 mL for termination			

Yield	1.57 g (0.22 mmol, 78.4%)
SEC [#] (HFIP)	M _n = 3.6 kg/mol; Đ = 1.12
¹ H-NMR	M _n = 7.2 kg/mol

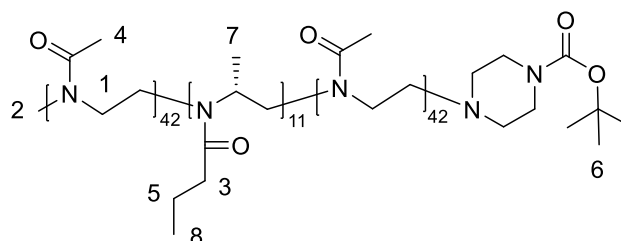


Me-MeO_{x42}-^RPrMeO_{x11}-MeO_{x42}-PipBoc (T9), No. YNM055 (according to GSP3)

		M (g/mol)	eq	m (g)	n (mmol)
Segment 1	MeOx	85.1	40	1.07	12.5(6)
Segment 2	^R PrMeOx	127.19	10	0.39	3.0(7)
Segment 3	MeOx	85.1	40	1.07	12.5(7)

Initiator	MeOTf	164.1	1	0.052	0.31
Terminator	1-Boc-piperazine	186.25	4	0.22	1.1(8)
Neutralizer	K ₂ CO ₃	138.21	1	0.044	0.32
Solvent	sulfolane	13.5 mL for polymerization and 4.5 mL for termination			

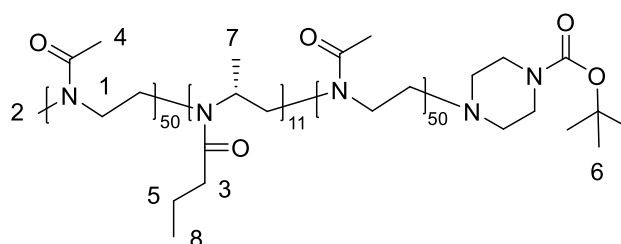
Yield	2.38 g (0.27 mmol, 91.9%)
SEC# (HFIP)	M _n = 4.1 kg/mol; Đ = 1.16
¹ H-NMR	M _n = 8.7 kg/mol



Me-MeOx₅₀-^RPrMeOx₁₁-MeOx₅₀-PipBoc (T10), No. YNM056 (according to GSP3)

		M (g/mol)	eq	m (g)	n (mmol)
Segment 1	MeOx	85.1	50	1.53	18.0(3)
Segment 2	^R PrMeOx	127.19	10	0.46	3.6(0)
Segment 3	MeOx	85.1	50	1.53	18.0(1)
Initiator	MeOTf	164.1	1	0.059	0.36
Terminator	1-Boc-piperazine	186.25	3	0.22	1.1(7)
Neutralizer	K ₂ CO ₃	138.21	1	0.050	0.36
Solvent	sulfolane	16.5 mL for polymerization and 5.5 mL for termination			

Yield	3.45 g (0.342 mmol, 95.9%)
SEC# (HFIP)	M _n = 4.8 kg/mol; Đ = 1.17
¹ H-NMR	M _n = 10.1 kg/mol



Me-MeOx₃₅-^REtEtOx₂₀-MeOx₃₅-PipBoc (T21, A-p^REtEtOx-A), No. YNM067 (according to GSP3)

		M (g/mol)	eq	m (g)	n (mmol)
Segment 1	MeOx	85.1	35	0.64	7.5(0)

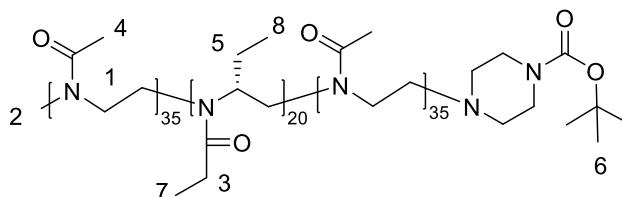
7 Experimental

Segment 2	^R EtEtOx	127.19	20	0.55	4.2(9)
Segment 3	MeOx	85.1	35	0.64	7.5(1)
Initiator	MeOTf	164.1	1	0.035	0.21
Terminator	1-Boc-piperazine	186.25	4	0.13	0.71
Neutralizer	K ₂ CO ₃	138.21	1	0.030	0.21
Solvent	sulfolane	9 mL for polymerization and 2.5 mL for termination			

Yield 1.48 g
(0.17 mmol, 79.5%)

SEC (HFIP) M_n = 4.4 kg/mol; Đ = 1.13

¹H-NMR M_n = 8.7 kg/mol



¹H-NMR (300 MHz, Chloroform-*d*, 298K): δ = 3.55-3.23 (br, 280H, H¹), 3.01-2.97 (br, 5H, H²), 2.57-2.20 (br, 41H, H³), 2.18-1.96 (br, 208H, H⁴), 1.77-1.43 (br, 33H, H⁵), 1.41-1.37 (s, 9H, H⁶), 1.16-0.94 (br, 60H, H⁷), 0.94-0.54 (br, 60H, H⁸).

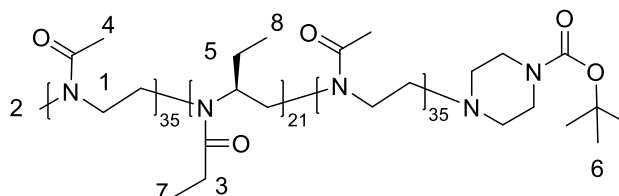
Me-MeOx₃₅-^SEtEtOx₂₁-MeOx₃₅-PipBoc (T22, A-p^SEtEtOx-A), No. YNM068 (according to GSP3)

		M (g/mol)	eq	m (g)	n (mmol)
Segment 1	MeOx	85.1	35	0.64	7.5(0)
Segment 2	^S EtEtOx	127.19	20	0.54	4.2(8)
Segment 3	MeOx	85.1	35	0.64	7.4(7)
Initiator	MeOTf	164.1	1	0.035	0.21
Terminator	1-Boc-piperazine	186.25	3	0.14	0.72
Neutralizer	K ₂ CO ₃	138.21	1	0.030	0.21
Solvent	sulfolane	9 mL for polymerization and 2.5 mL for termination			

Yield 1.16 g
(0.13 mmol, 62.5%)

SEC (HFIP) M_n = 4.2 kg/mol; Đ = 1.17

¹H-NMR M_n = 8.8 kg/mol



¹H-NMR (300 MHz, Chloroform-*d*, 298K): δ = 3.52-3.26 (br, 287H, H¹), 3.00-2.95 (br, 4H, H²), 2.58-2.17 (br, 48H, H³), 2.15-1.99 (br, 211H, H⁴), 1.74-1.43 (br, 29H, H⁵), 1.41-1.36 (s,

9H, H^6), 1.15-0.94 (br, 64H, H^7), 0.94-0.61 (br, 63H, H^8).

Me-MeOx₃₅-^{RS}EtEtOx₂₀-MeOx₃₅-PipBoc (T23, A-p^{RS}EtEtOx-A), No. YNM063 (according to GSP3)

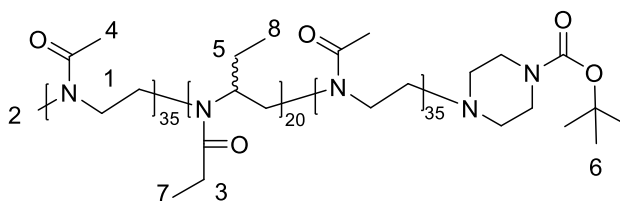
		M (g/mol)	eq	m (g)	n (mmol)
Segment 1	MeOx	85.1	35	0.74	8.6(7)
Segment 2	^{RS} EtEtOx	127.19	20	0.63	4.9(5)
Segment 3	MeOx	85.1	35	0.74	8.6(9)
Initiator	MeOTf	164.1	1	0.041	0.25
Terminator	1-Boc-piperazine	186.25	4	0.17	0.91
Neutralizer	K ₂ CO ₃	138.21	1	0.034	0.25
Solvent	sulfolane	9 mL for polymerization and 2.5 mL for termination			

Yield 1.65 g
(0.19 mmol, 76.5%)

SEC (HFIP) $M_n=4.2$ kg/mol; \mathcal{D}
=1.16

¹H-NMR $M_n=8.7$ kg/mol

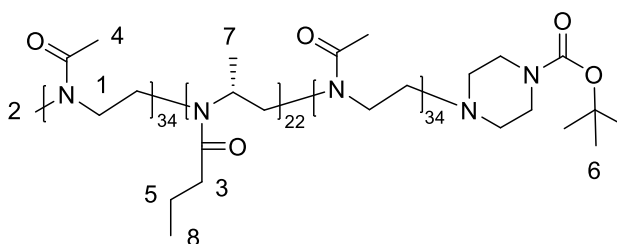
¹H-NMR (300 MHz, Chloroform-*d*, 298K): δ = 3.56-3.22 (br, 280H, H^1), 3.01-2.95 (br, 5H, H^2), 2.63-2.19 (br, 44H, H^3), 2.18-1.98 (br, 207H, H^4), 1.77-1.42 (br, 29H, H^5), 1.41-1.37 (s, 9H, H^6), 1.16-0.95 (br, 59H, H^7), 0.95-0.63 (br, 61H, H^8).



Me-MeOx₃₄-^RPrMeOx₂₂-MeOx₃₄-PipBoc (T24, A-p^RPrMeOx-A), No. YNM065 (according to GSP3)

		M (g/mol)	eq	m (g)	n (mmol)
Segment 1	MeOx	85.1	35	0.61	7.1(3)
Segment 2	^R PrMeOx	127.19	20	0.52	4.0(7)
Segment 3	MeOx	85.1	35	0.60	7.1(0)
Initiator	MeOTf	164.1	1	0.033	0.20
Terminator	1-Boc-piperazine	186.25	3.5	0.11	0.62
Neutralizer	K ₂ CO ₃	138.21	1	0.028	0.20
Solvent	sulfolane	9 mL for polymerization and 2.5 mL for termination			

Yield 1.26 g
(0.14 mmol, 70.9%)
SEC (HFIP) $M_n = 4.2$ kg/mol; $\mathcal{D} = 1.15$
 $^1\text{H-NMR}$ $M_n = 8.8$ kg/mol

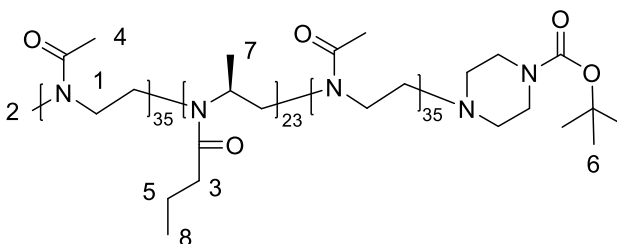


$^1\text{H-NMR}$ (300 MHz, Chloroform-*d*, 298K): $\delta = 3.55\text{-}3.24$ (br, 272H, H^1), 3.02-2.96 (br, 4H, H^2), 2.50-2.19 (br, 38H, H^3), 2.19-1.94 (br, 205H, H^4), 1.67-1.44 (br, 45H, H^5), 1.43-1.37 (s, 9H, H^6), 1.36-1.00 (br, 73H, H^7), 0.97-0.72 (br, 66H, H^8).

Me-MeOx₃₅-^SPrMeOx₂₃-MeOx₃₅-PipBoc (T25, A-p^SPrMeOx-A), No. YNM066 (according to GSP3)

		M (g/mol)	eq	m (g)	n (mmol)
Segment 1	MeOx	85.1	35	0.69	8.0(5)
Segment 2	^S PrMeOx	127.19	20	0.59	4.6(1)
Segment 3	MeOx	85.1	35	0.69	8.0(6)
Initiator	MeOTf	164.1	1	0.038	0.23
Terminator	1-Boc-piperazine	186.25	3.5	0.15	0.79
Neutralizer	K ₂ CO ₃	138.21	1	0.032	0.23
Solvent	sulfolane	9 mL for polymerization and 2.5 mL for termination			

Yield 1.39 g
(0.15 mmol, 69.3%)
SEC (HFIP) $M_n = 4.1$ kg/mol; $\mathcal{D} = 1.15$
 $^1\text{H-NMR}$ $M_n = 9.1$ kg/mol



$^1\text{H-NMR}$ (300 MHz, Chloroform-*d*, 298K): $\delta = 3.57\text{-}3.24$ (br, 283H, H^1), 3.01-2.96 (br, 4H, H^2), 2.54-2.19 (br, 40H, H^3), 2.19-1.95 (br, 210H, H^4), 1.66-1.45 (br, 47H, H^5), 1.43-1.37 (s, 9H, H^6), 1.37-0.99 (br, 77H, H^7), 0.96-0.73 (br, 69H, H^8).

Me-MeOx₃₄-^{RS}PrMeOx₂₂-MeOx₃₄-PipBoc (T26, A-p^{RS}PrMeOx-A), No. YNM064 (according to GSP3)

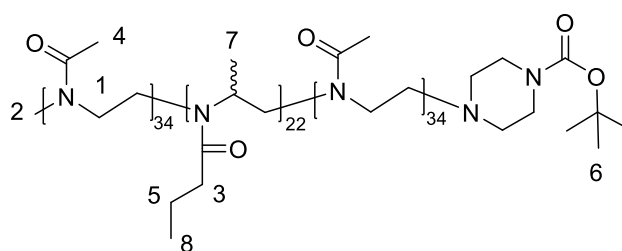
	M (g/mol)	eq	m (g)	n (mmol)
--	-----------	----	-------	----------

Segment 1	MeOx	85.1	35	0.71	8.3(5)
Segment 2	^{RS} PrMeOx	127.19	20	0.61	4.7(8)
Segment 3	MeOx	85.1	35	0.71	8.3(5)
Initiator	MeOTf	164.1	1	0.039	0.24
Terminator	1-Boc-piperazine	186.25	3.5	0.15	0.83
Neutralizer	K ₂ CO ₃	138.21	1	0.033	0.24
Solvent	sulfolane	9 mL for polymerization and 2.5 mL for termination			

Yield 1.70 g
(0.19 mmol, 81.9%)

SEC (HFIP) M_n = 4.2 kg/mol; Đ = 1.18

¹H-NMR M_n = 8.8 kg/mol



¹H-NMR (300 MHz, Chloroform-*d*, 298K): δ = 3.55-3.21 (br, 280H, *H*¹), 3.03-2.96 (br, 5H, *H*²), 2.54-2.17 (br, 36H, *H*³), 2.16-1.98 (br, 206H, *H*⁴), 1.66-1.43 (br, 44H, *H*⁵), 1.42-1.36 (s, 9H, *H*⁶), 1.34-0.97 (br, 66H, *H*⁷), 0.96-0.75 (br, 69H, *H*⁸).

Bibliography

1. Nguyen, L. A.; He, H.; Pham-Huy, C., Chiral Drugs: An Overview. *Int. J. Biomed. Sci.* **2006**, *2* (2), 85-100.
2. Hirose, D.; Isobe, A.; Quiñó E.; Freire, F.; Maeda, K., Three-state switchable chiral stationary phase based on helicity control of an optically active poly (phenylacetylene) derivative by using metal cations in the solid state. *J. Am. Chem. Soc.* **2019**, *141* (21), 8592-8598.
3. Abyaneh, H. S.; Vakili, M. R.; Lavasanifar, A., The effect of polymerization method in stereo-active block copolymers on the stability of polymeric micelles and their drug release profile. *Pharm. Res.* **2014**, *31* (6), 1485-1500.
4. Mochida, Y.; Cabral, H.; Miura, Y.; Albertini, F.; Fukushima, S.; Osada, K.; Nishiyama, N.; Kataoka, K., Bundled assembly of helical nanostructures in polymeric micelles loaded with platinum drugs enhancing therapeutic efficiency against pancreatic tumor. *ACS nano* **2014**, *8* (7), 6724-6738.
5. Ding, J.; Li, C.; Zhang, Y.; Xu, W.; Wang, J.; Chen, X., Chirality-mediated polypeptide micelles for regulated drug delivery. *Acta biomaterialia* **2015**, *11*, 346-355.
6. Abyaneh, H. S.; Vakili, M. R.; Shafaati, A.; Lavasanifar, A., Block Copolymer Stereoregularity and Its Impact on Polymeric Micellar Nanodrug Delivery. *Mol. Pharm.* **2017**, *14* (8), 2487-2502.
7. Luxenhofer, R.; Han, Y. C.; Schulz, A.; Tong, J.; He, Z. J.; Kabanov, A. V.; Jordan, R., Poly(2-oxazoline)s as Polymer Therapeutics. *Macromol. Rapid Commun.* **2012**, *33* (19), 1613-1631.
8. Glassner, M.; Vergaelen, M.; Hoogenboom, R., Poly (2 - oxazoline) s: A comprehensive overview of polymer structures and their physical properties. *Polym. Int.* **2018**, *67* (1), 32-45.
9. Lorson, T.; Lübtow, M. M.; Wegener, E.; Haider, M. S.; Borova, S.; Nahm, D.; Jordan, R.; Sokolski-Papkov, M.; Kabanov, A. V.; Luxenhofer, R., Poly(2-oxazoline)s based biomaterials: A comprehensive and critical update. *Biomaterials* **2018**, *178*, 204-280.
10. Witte, H.; Seeliger, W., Cyclische Imidsäureester aus Nitrilen und Aminoalkoholen. *Liebigs Ann. Chem.* **1974**, 996-1009.
11. Seeliger, W.; Aufderhaar, E.; Diepers, W.; Feinauer, R.; Nehring, R.; Thier, W.; Hellmann, H., Neuere Synthesen und Reaktionen cyclischer Imidsäureester. *Angew. Chem.* **1966**, *78* (20), 913-927.
12. Hansen, J. F.; Cooper, C. S., Preparation and alkylation of a new chiral oxazoline from L-serine. *J. Org. Chem.* **1976**, *41* (19), 3219-3220.
13. Rossegger, E.; Schenk, V.; Wiesbrock, F., Design strategies for functionalized poly (2-oxazoline) s and derived materials. *Polymers* **2013**, *5* (3), 956-1011.
14. Bodner, T.; Ellmaier, L.; Schenk, V.; Albering, J.; Wiesbrock, F., Delocalized π -electrons in 2-oxazoline rings resulting in negatively charged nitrogen atoms: revealing the selectivity during the initiation of cationic ring-opening polymerizations. *Polym. Int.* **2011**, *60* (8), 1173-1179.
15. Aoi, K.; Okada, M., Polymerization of oxazolines. *Prog. Polym. Sci.* **1996**, *21* (1), 151-208.
16. Saegusa, T.; Kobayash.S; Ishiguro, M., New Route to optically-active linear poly(propylenimine). *Macromolecules* **1974**, *7* (6), 958-959.

17. Saegusa, T.; Hirao, T.; Ito, Y., Polymerization of (4S, 5R)-4-Carbomethoxy-5-methyl-2-oxazoline. *Macromolecules* **1975**, *8* (1), 87-87.
18. Bloksma, M. M.; Hendrix, M.; Schubert, U. S.; Hoogenboom, R., Ordered Chiral Structures in the Crystals of Main-Chain Chiral Poly(2-oxazoline)s. *Macromolecules* **2010**, *43* (10), 4654-4659.
19. Bloksma, M. M.; Rogers, S.; Schubert, U. S.; Hoogenboom, R., Secondary structure formation of main-chain chiral poly(2-oxazoline)s in solution. *Soft Matter* **2010**, *6* (5), 994-1003.
20. Bloksma, M. M.; Rogers, S.; Schubert, U. S.; Hoogenboom, R., Main-Chain Chiral Poly(2-oxazoline)s: Influence of Alkyl Side-chain on Secondary Structure Formation in Solution. *J. Polym. Sci. Pol. Chem.* **2011**, *49* (13), 2790-2801.
21. Bloksma, M. M.; Schubert, U. S.; Hoogenboom, R., Main-chain chiral copoly(2-oxazoline)s. *Polym. Chem.* **2011**, *2* (1), 203-208.
22. Bloksma, M. M.; Hoepfener, S.; D'Haese, C.; Kempe, K.; Mansfeld, U.; Paulus, R. M.; Gohy, J. F.; Schubert, U. S.; Hoogenboom, R., Self-assembly of chiral block and gradient copolymers. *Soft Matter* **2012**, *8* (1), 165-172.
23. Luxenhofer, R.; Huber, S.; Hytry, J.; Tong, J.; Kabanov, A. V.; Jordan, R., Chiral and Water-Soluble Poly(2-oxazoline)s. *J. Polym. Sci. Pol. Chem.* **2013**, *51* (3), 732-738.
24. Bott, K.; Schmidt, P. Neue, optisch aktive Polymere für die chromatographische Racemattrennung, European Patent. DE3418525A1;EP0161547A2;EP0161547A3;EP0161547B1, 1985.
25. Bruschi, M. L., 2 - Modification of drug release. In *Strategies to modify the drug release from pharmaceutical systems*, Bruschi, M. L., Ed. Woodhead Publishing: 2015; pp 15-28.
26. Duncan, R.; Vicent, M. J., Polymer therapeutics-prospects for 21st century: the end of the beginning. *Advanced drug delivery reviews* **2013**, *65* (1), 60-70.
27. Moradi Kashkooli, F.; Soltani, M.; Souri, M., Controlled anti-cancer drug release through advanced nano-drug delivery systems: Static and dynamic targeting strategies. *J. Controlled Release* **2020**, *327*, 316-349.
28. Guimarães, D.; Cavaco-Paulo, A.; Nogueira, E., Design of liposomes as drug delivery system for therapeutic applications. *Int. J. Pharm.* **2021**, *601*, 120571.
29. Vigata, M.; Meinert, C.; Hutmacher, D. W.; Bock, N., Hydrogels as drug delivery systems: A review of current characterization and evaluation techniques. *Pharmaceutics* **2020**, *12* (12), 1188.
30. Idrees, H.; Zaidi, S. Z. J.; Sabir, A.; Khan, R. U.; Zhang, X.; Hassan, S. U., A Review of Biodegradable Natural Polymer-Based Nanoparticles for Drug Delivery Applications. *Nanomaterials (Basel)* **2020**, *10* (10).
31. Restani, R. B.; Silva, A. S.; Pires, R. F.; Cabral, R.; Correia, I. J.; Casimiro, T.; Bonifácio, V. D.; Aguiar - Ricardo, A., Nano - in - Micro POxylated Polyurea Dendrimers and Chitosan Dry Powder Formulations for Pulmonary Delivery. *Particle & Particle Systems Characterization* **2016**, *33* (11), 851-858.
32. Sung, Y. K.; Kim, S. W., Recent advances in polymeric drug delivery systems. *Biomaterials Research* **2020**, *24* (1), 12.
33. Sinha, V. R.; Bansal, K.; Kaushik, R.; Kumria, R.; Trehan, A., Poly- ϵ -caprolactone microspheres and nanospheres: an overview. *Int. J. Pharm.* **2004**, *278* (1), 1-23.
34. Knop, K.; Hoogenboom, R.; Fischer, D.; Schubert, U. S., Poly (ethylene glycol) in drug delivery: pros and cons as well as potential alternatives. *Angew. Chem. Int. Ed.* **2010**, *49* (36), 6288-6308.
35. Peng, P.; Chen, Z.; Wang, M.; Wen, B.; Deng, X., Polysaccharide-modified liposomes and their application in cancer research. *Chem. Biol. Drug Des.* **2023**, *101* (4), 998-1011.

36. Madau, M.; Morandi, G.; Rihouey, C.; Lapinte, V.; Oulyadi, H.; Cerf, D. L.; Dulong, V.; Picton, L., A mild and straightforward one-pot hyaluronic acid functionalization through termination of poly-(2-alkyl-2-oxazoline). *Polymer* **2021**, 124059.
37. Qi, X.; Wei, W.; Li, J.; Zuo, G.; Pan, X.; Su, T.; Zhang, J.; Dong, W., Salecan-based pH-sensitive hydrogels for insulin delivery. *Mol. Pharm.* **2017**, *14* (2), 431-440.
38. Sayed, E.; Haj-Ahmad, R.; Ruparelia, K.; Arshad, M. S.; Chang, M. W.; Ahmad, Z., Porous Inorganic Drug Delivery Systems—a Review. *AAPS PharmSciTech* **2017**, *18* (5), 1507-1525.
39. Avramović, N.; Mandić, B.; Savić-Radojević, A.; Simić, T., Polymeric nanocarriers of drug delivery systems in cancer therapy. *Pharmaceutics* **2020**, *12* (4), 298.
40. Vlachopoulos, A.; Karlioti, G.; Balla, E.; Daniilidis, V.; Kalamas, T.; Stefanidou, M.; Bikiaris, N. D.; Christodoulou, E.; Koumentakou, I.; Karavas, E., Poly (lactic acid)-based microparticles for drug delivery applications: An overview of recent advances. *Pharmaceutics* **2022**, *14* (2), 359.
41. Martinho, N.; Damg é C.; Reis, C. P., Recent advances in drug delivery systems. *Journal of biomaterials and nanobiotechnology* **2011**, *2* (05), 510.
42. Prajapati, S. K.; Jain, A.; Jain, A.; Jain, S., Biodegradable polymers and constructs: A novel approach in drug delivery. *Eur. Polym. J.* **2019**, *120*, 109191.
43. Singh, N.; Son, S.; An, J.; Kim, I.; Choi, M.; Kong, N.; Tao, W.; Kim, J. S., Nanoscale porous organic polymers for drug delivery and advanced cancer theranostics. *Chem. Soc. Rev.* **2021**, *50* (23), 12883-12896.
44. Sponchioni, M.; Capasso Palmiero, U.; Moscatelli, D., Thermo-responsive polymers: Applications of smart materials in drug delivery and tissue engineering. *Mater. Sci. Eng. C Mater. Biol. Appl.* **2019**, *102*, 589-605.
45. Ding, H.; Tan, P.; Fu, S.; Tian, X.; Zhang, H.; Ma, X.; Gu, Z.; Luo, K., Preparation and application of pH-responsive drug delivery systems. *J. Controlled Release* **2022**, *348*, 206-238.
46. Tan, L.; Yu, X.; Wan, P.; Yang, K., Biodegradable materials for bone repairs: a review. *Journal of Materials Science & Technology* **2013**, *29* (6), 503-513.
47. Tyler, B.; Gullotti, D.; Mangraviti, A.; Utsuki, T.; Brem, H., Polylactic acid (PLA) controlled delivery carriers for biomedical applications. *Advanced Drug Delivery Reviews* **2016**, *107*, 163-175.
48. Xu, Y.; Kim, C. S.; Saylor, D. M.; Koo, D., Polymer degradation and drug delivery in PLGA-based drug-polymer applications: A review of experiments and theories. *Journal of biomedical materials research part B: applied biomaterials* **2017**, *105* (6), 1692-1716.
49. Xu, J.; Bai, Y.; Li, X.; Wei, Z.; Sun, L.; Yu, H.; Xu, H., Porous Core/Dense Shell PLA Microspheres Embedded with High Drug Loading of Bupivacaine Crystals for Injectable Prolonged Release. *AAPS PharmSciTech* **2021**, *22* (1), 27.
50. Gref, R.; Minamitake, Y.; Peracchia, M. T.; Trubetskoy, V.; Torchilin, V.; Langer, R., Biodegradable long-circulating polymeric nanospheres. *Science* **1994**, *263* (5153), 1600-1603.
51. Pasut, G.; Veronese, F. M., PEG conjugates in clinical development or use as anticancer agents: an overview. *Advanced drug delivery reviews* **2009**, *61* (13), 1177-1188.
52. Reddy, K. R.; Modi, M. W.; Pedder, S., Use of peginterferon alfa-2a (40 KD)(Pegasys®) for the treatment of hepatitis C. *Advanced Drug Delivery Reviews* **2002**, *54* (4), 571-586.
53. Barril, G.; Quiroga, J.; Sanz, P.; Rodríguez - Salvanes, F.; Selgas, R.; Carreno, V., Pegylated interferon - α 2a kinetics during experimental haemodialysis: impact of permeability and pore size of dialysers. *Aliment. Pharmacol. Ther.* **2004**, *20* (1), 37-44.
54. Loquai, C.; Nashan, D.; Hensen, P.; Luger, T. A.; Grabbe, S.; Sunderkötter, C.; Schiller, M., Safety of pegylated interferon-alpha-2a in adjuvant therapy of intermediate and high-risk melanomas. *Eur. J. Dermatol.* **2008**, *18* (1), 29-35.

55. Lipton, J. H.; Khoroshko, N.; Golenkov, A.; Abdulkadyrov, K.; Nair, K.; Raghunadharao, D.; Brummendorf, T.; Yoo, K.; Bergstrom, B., Phase II, randomized, multicenter, comparative study of peginterferon- α -2a (40 kD)(Pegasys®) versus interferon α -2a (Roferon®-A) in patients with treatment-naïve, chronic-phase chronic myelogenous leukemia. *Leuk. Lymphoma* **2007**, *48* (3), 497-505.
56. Li, X.; Sun, H.; Li, H.; Hu, C.; Luo, Y.; Shi, X.; Pich, A., Multi - responsive biodegradable cationic nanogels for highly efficient treatment of tumors. *Adv. Funct. Mater.* **2021**, *31* (26), 2100227.
57. Medina, D. D.; Mastai, Y., Chiral Polymers and Polymeric Particles for Enantioselective Crystallization. *Isr. J. Chem.* **2018**, *58* (12), 1330-1337.
58. Feng, K.; Wang, S. Z.; Ma, H. R.; Chen, Y. J., Chirality plays critical roles in enhancing the aqueous solubility of nocathiacin I by block copolymer micelles. *J. Pharm. Pharmacol.* **2013**, *65* (1), 64-71.
59. Radwan, M. A.; Aboul-Enein, H. Y., In vitro release and stereoselective disposition of flurbiprofen loaded to poly (D,L-lactide-co-glycolide) nanoparticles in rats. *Chirality* **2004**, *16* (2), 119-125.
60. Hu, J. L.; Tang, J. H.; Qiu, X. Y.; Han, Y. D.; Liu, Q.; Chen, X. S.; Jing, X. B., Effects of stereoregularity of multiblock copoly(rac-lactide)s on stereocomplex microparticles and their insulin delivery. *Macromol. Biosci.* **2005**, *5* (12), 1193-1199.
61. Nguyen, H. V. T.; Jiang, Y.; Mohapatra, S.; Wang, W.; Barnes, J. C.; Oldenhuis, N. J.; Chen, K. K.; Axelrod, S.; Huang, Z.; Chen, Q.; Golder, M. R.; Young, K.; Suvlu, D.; Shen, Y.; Willard, A. P.; Hore, M. J. A.; Gómez-Bombarelli, R.; Johnson, J. A., Bottlebrush polymers with flexible enantiomeric side chains display differential biological properties. *Nat. Chem.* **2022**, *14* (1), 85-93.
62. Tomalia, D.; Sheetz, D., Homopolymerization of 2-alkyl-and 2-aryl-2-oxazolines. *Journal of Polymer Science Part A - 1: Polymer Chemistry* **1966**, *4* (9), 2253-2265.
63. Kagiya, T.; Narisawa, S.; Maeda, T.; Fukui, K., Ring-opening polymerization of 2-substituted 2-oxazolines. *Journal of Polymer Science Part B: Polymer Letters* **1966**, *4* (7), 441-445.
64. Bassiri, T.; Levy, A.; Litt, M., Polymerization of cyclic imino ethers. I. Oxazolines. *Journal of Polymer Science Part B: Polymer Letters* **1967**, *5* (9), 871-879.
65. Hoogenboom, R., Poly (2 - oxazoline) s: a polymer class with numerous potential applications. *Angew. Chem. Int. Ed.* **2009**, *48* (43), 7978-7994.
66. Kobayashi, S., Ethylenimine polymers. *Prog. Polym. Sci.* **1990**, *15* (5), 751-823.
67. Guillerm, B.; Monge, S.; Lapinte, V.; Robin, J. J., How to modulate the chemical structure of polyoxazolines by appropriate functionalization. *Macromol. Rapid Commun.* **2012**, *33* (19), 1600-1612.
68. Haider, M. S.; Ahmad, T.; Yang, M.; Hu, C.; Hahn, L.; Stahlhut, P.; Groll, J.; Luxenhofer, R., Tuning the thermogelation and rheology of poly (2-oxazoline)/poly (2-oxazine) s based thermosensitive hydrogels for 3D bioprinting. *Gels* **2021**, *7* (3), 78.
69. Ali, M. W.; Cheng, S.; Si, J.; Siddiq, M.; Ye, X., Synthesis and characterization of degradable hyperbranched poly (2-ethyl-2-oxazoline). *J. Polym. Sci., Part A: Polym. Chem.* **2019**, *57* (19), 2030-2037.
70. Ali, M. W.; Muhammad, Z.; Jia, Q.; Li, L.; Saleem, M.; Siddiq, M.; Chen, Y., Synthesis of cyclic poly (2-ethyl-2-oxazoline) with a degradable disulfide bond. *Polym. Chem.* **2020**, *11* (25), 4164-4171.
71. Floyd, T. G.; Hakkinen, S.; Hall, S. C.; Dalgliesh, R. M.; Lehnen, A.-C.; Hartlieb, M.; Perrier, S., Cationic bottlebrush copolymers from partially hydrolyzed poly (oxazoline) s. *Macromolecules* **2021**, *54* (20), 9461-9473.

72. Alvaradejo, G. G.; Nguyen, H. V. T.; Harvey, P.; Gallagher, N. M.; Le, D.; Ottaviani, M. F.; Jasanoff, A.; Delaittre, G.; Johnson, J. A., Polyoxazoline-Based Bottlebrush and Brush-Arm Star Polymers via ROMP: Syntheses and Applications as Organic Radical Contrast Agents. *ACS Macro Letters* **2019**, *8* (4), 473-478.
73. Kim, K.-M.; Ouchi, Y.; Chujo, Y., Synthesis of organic-inorganic star-shaped polyoxazolines using octafunctional silsesquioxane as an initiator. *Polym. Bull.* **2003**, *49* (5), 341-348.
74. Blokhin, A. N.; Dudkina, M. M.; Tenkovtsev, A. V., Ionic Ring-Opening Polymerization for the Synthesis of Star-Shaped Polymers. *Polymer Science, Series C* **2022**, *64* (2), 161-175.
75. Portier, É.; Azemar, F.; Benkhaled, B. T.; Bardeau, J.-F.; FayF.; R̄hel, K.; Lapinte, V.; Linossier, I., Poly (oxazoline) for the design of amphiphilic silicone coatings. *Prog. Org. Coat.* **2021**, *153*, 106116.
76. Wylie, R. A.; Miller, B.; Connal, L. A.; Qiao, G., Oligomeric Poly (Oxazoline) as Potential Lithium Battery Electrolytes. *J. Electrochem. Soc.* **2022**, *169* (6), 060533.
77. Nam, S.; Seo, J.; Woo, S.; Kim, W. H.; Kim, H.; Bradley, D. D.; Kim, Y., Inverted polymer fullerene solar cells exceeding 10% efficiency with poly (2-ethyl-2-oxazoline) nanodots on electron-collecting buffer layers. *Nature communications* **2015**, *6* (1), 8929.
78. Viegas, T. X.; Bentley, M. D.; Harris, J. M.; Fang, Z.; Yoon, K.; Dizman, B.; Weimer, R.; Mero, A.; Pasut, G.; Veronese, F. M., Polyoxazoline: Chemistry, Properties, and Applications in Drug Delivery. *Bioconjugate Chem.* **2011**, *22* (5), 976-986.
79. Nemati Mahand, S.; Aliakbarzadeh, S.; Moghaddam, A.; Salehi Moghaddam, A.; Kruppke, B.; Nasrollahzadeh, M.; Khonakdar, H. A., Polyoxazoline: A review article from polymerization to smart behaviors and biomedical applications. *Eur. Polym. J.* **2022**, *178*, 111484.
80. Meyers, A.; Knaus, G.; Kamata, K.; Ford, M. E., Asymmetric synthesis of R and S. alpha.-alkylalkanoic acids from metalation and alkylation of chiral 2-oxazolines. *J. Am. Chem. Soc.* **1976**, *98* (2), 567-576.
81. Roush, D. M.; Patel, M. M., A Mild Procedure for the Preparation of 2-oxazolines. *Synth. Commun.* **1985**, *15* (8), 675-679.
82. Yang, M.; Haider, M. S.; Forster, S.; Hu, C.; Luxenhofer, R., Synthesis and Investigation of Chiral Poly(2,4-disubstituted-2-oxazoline)-Based Triblock Copolymers, Their Self-Assembly, and Formulation with Chiral and Achiral Drugs. *Macromolecules* **2022**, *55* (14), 6176-6190.
83. Wenker, H., Syntheses from Ethanolamine. V. Synthesis of Δ^2 -Oxazoline and of 2,2'- Δ^2 -Dioxazoline. *J. Am. Chem. Soc.* **1938**, *60* (9), 2152-2153.
84. Franco, F.; Muchowski, J. M., A convenient laboratory synthesis of 2-oxazoline. *J. Heterocycl. Chem.* **1980**, *17* (7), 1613-1613.
85. Ito, Y.; Inubushi, Y.; Zenbayashi, M.; Tomita, S.; Saegusa, T., Synthetic reactions by complex catalysts. XXXI. Novel and versatile method of heterocycle synthesis. *J. Am. Chem. Soc.* **1973**, *95* (13), 4447-4448.
86. Taubmann, C.; Luxenhofer, R.; Cesana, S.; Jordan, R., First aldehyde-functionalized poly(2-oxazoline)s for chemoselective ligation. *Macromol. Biosci.* **2005**, *5* (7), 603-612.
87. Dargaville, T. R.; Lava, K.; Verbraeken, B.; Hoogenboom, R., Unexpected Switching of the Photogelation Chemistry When Cross-Linking Poly(2-oxazoline) Copolymers. *Macromolecules* **2016**, *49* (13), 4774-4783.
88. Dworak, A.; Trzebicka, B.; Kowalczyk, A.; Tsvetanov, C.; Rangelov, S., Polyoxazolines — mechanism of synthesis and solution properties. *Polimery* **2014**, *59* (1), 88-94.

89. Fijten, M. W.; Hoogenboom, R.; Schubert, U. S., Initiator effect on the cationic ring - opening copolymerization of 2 - ethyl - 2 - oxazoline and 2 - phenyl - 2 - oxazoline. *J. Polym. Sci., Part A: Polym. Chem.* **2008**, *46* (14), 4804-4816.
90. Hoogenboom, R.; Paulus, R. M.; Fijten, M. W.; Schubert, U. S., Concentration effects in the cationic ring - opening polymerization of 2 - ethyl - 2 - oxazoline in N, N - dimethylacetamide. *J. Polym. Sci., Part A: Polym. Chem.* **2005**, *43* (7), 1487-1497.
91. Dworak, A., The role of cationic and covalent active centers in the polymerization of 2 - methyl - 2 - oxazoline initiated with benzyl bromide. *Macromol. Chem. Phys.* **1998**, *199* (9), 1843-1849.
92. Hoogenboom, R.; Fijten, M. W. M.; Schubert, U. S., Parallel kinetic investigation of 2-oxazoline polymerizations with different initiators as basis for designed copolymer synthesis. *J. Polym. Sci. Pol. Chem.* **2004**, *42* (8), 1830-1840.
93. Miyamoto, M.; Aoi, K.; Saegusa, T., Mechanisms of ring-opening polymerization of 2-(perfluoroalkyl)-2-oxazolines initiated by sulfonates: a novel covalent-type electrophilic polymerization. *Macromolecules* **1988**, *21* (6), 1880-1883.
94. Miyamoto, M.; Aoi, K.; Saegusa, T., Novel covalent-type electrophilic polymerization of 2-(perfluoroalkyl)-2-oxazolines initiated by sulfonates. *Macromolecules* **1991**, *24* (1), 11-16.
95. Verbraeken, B.; Monnery, B. D.; Lava, K.; Hoogenboom, R., The chemistry of poly (2-oxazoline) s. *Eur. Polym. J.* **2017**, *88*, 451-469.
96. Kobayashi, S.; Masuda, E.; Shoda, S.; Shimano, Y., Synthesis of acryl-and methacryl-type macromonomers and telechelics by utilizing living polymerization of 2-oxazolines. *Macromolecules* **1989**, *22* (7), 2878-2884.
97. Nuyken, O.; Maier, G.; Gross, A.; Fischer, H., Systematic investigations on the reactivity of oxazolinium salts. *Macromol. Chem. Phys.* **1996**, *197* (1), 83-95.
98. Kozma, G. T.; Shimizu, T.; Ishida, T.; Szebeni, J., Anti-PEG antibodies: Properties, formation, testing and role in adverse immune reactions to PEGylated nano-biopharmaceuticals. *Advanced drug delivery reviews* **2020**, *154*, 163-175.
99. Hoang Thi, T. T.; Pilkington, E. H.; Nguyen, D. H.; Lee, J. S.; Park, K. D.; Truong, N. P., The importance of poly (ethylene glycol) alternatives for overcoming PEG immunogenicity in drug delivery and bioconjugation. *Polymers* **2020**, *12* (2), 298.
100. Ishida, T.; Harada, M.; Wang, X. Y.; Ichihara, M.; Irimura, K.; Kiwada, H., Accelerated blood clearance of PEGylated liposomes following preceding liposome injection: effects of lipid dose and PEG surface-density and chain length of the first-dose liposomes. *J. Controlled Release* **2005**, *105* (3), 305-317.
101. Mima, Y.; Hashimoto, Y.; Shimizu, T.; Kiwada, H.; Ishida, T., Anti-PEG IgM is a major contributor to the accelerated blood clearance of polyethylene glycol-conjugated protein. *Mol. Pharm.* **2015**, *12* (7), 2429-2435.
102. Zalipsky, S.; Hansen, C. B.; Oaks, J. M.; Allen, T. M., Evaluation of blood clearance rates and biodistribution of poly (2 - oxazoline) - grafted liposomes. *J. Pharm. Sci.* **1996**, *85* (2), 133-137.
103. Woodle, M. C.; Engbers, C. M.; Zalipsky, S., New amphipatic polymer-lipid conjugates forming long-circulating reticuloendothelial system-evading liposomes. *Bioconjugate Chem.* **1994**, *5* (6), 493-496.
104. Konradi, R.; Pidhatika, B.; Mühlebach, A.; Textor, M., Poly-2-methyl-2-oxazoline: a peptide-like polymer for protein-repellent surfaces. *Langmuir* **2008**, *24* (3), 613-616.
105. Zhang, N.; Pompe, T.; Amin, I.; Luxenhofer, R.; Werner, C.; Jordan, R., Tailored Poly(2-oxazoline) Polymer Brushes to Control Protein Adsorption and Cell Adhesion. *Macromol. Biosci.* **2012**, *12* (7), 926-936.

106. Barz, M.; Luxenhofer, R.; Zentel, R.; Vicent, M. J., Overcoming the PEG-addiction: well-defined alternatives to PEG, from structure–property relationships to better defined therapeutics. *Polym. Chem.* **2011**, *2* (9), 1900-1918.
107. Grube, M.; Leiske, M. N.; Schubert, U. S.; Nischang, I., POx as an alternative to PEG? A hydrodynamic and light scattering study. *Macromolecules* **2018**, *51* (5), 1905-1916.
108. Pidhatika, B.; Mödler, J.; Vogel, V.; Konradi, R., Nonfouling surface coatings based on poly (2-methyl-2-oxazoline). *Chimia* **2008**, *62* (4), 264-269.
109. Gubarev, A. S.; Monnery, B. D.; Lezov, A. A.; Sedlacek, O.; Tsvetkov, N. V.; Hoogenboom, R.; Filippov, S. K., Conformational properties of biocompatible poly (2-ethyl-2-oxazoline) s in phosphate buffered saline. *Polym. Chem.* **2018**, *9* (17), 2232-2237.
110. Luxenhofer, R.; Sahay, G.; Schulz, A.; Alakhova, D.; Bronich, T. K.; Jordan, R.; Kabanov, A. V., Structure-property relationship in cytotoxicity and cell uptake of poly(2-oxazoline) amphiphiles. *J. Controlled Release* **2011**, *153* (1), 73-82.
111. Mansfield, E. D.; Victor, R.; Kowalczyk, R. M.; Grillo, I.; Hoogenboom, R.; Sillence, K.; Hole, P.; Williams, A. C.; Khutoryanskiy, V. V., Side chain variations radically alter the diffusion of poly (2-alkyl-2-oxazoline) functionalised nanoparticles through a mucosal barrier. *Biomater. Sci.* **2016**, *4* (9), 1318-1327.
112. Schmitz, M.; Kuhlmann, M.; Reimann, O.; Hackenberger, C. P.; Groll, J. r., Side-chain cysteine-functionalized poly (2-oxazoline) s for multiple peptide conjugation by native chemical ligation. *Biomacromolecules* **2015**, *16* (4), 1088-1094.
113. Luxenhofer, R.; López-García, M.; Frank, A.; Kessler, H.; Jordan, R., First poly (2-oxazoline)-peptide conjugate for targeted radionuclide cancer therapy. *PMSE Prepr* **2006**, *95*, 283-284.
114. Tong, J.; Luxenhofer, R.; Yi, X. A.; Jordan, R.; Kabanov, A. V., Protein Modification with Amphiphilic Block Copoly(2-oxazoline)s as a New Platform for Enhanced Cellular Delivery. *Mol. Pharm.* **2010**, *7* (4), 984-992.
115. Oudin, A.; Chauvin, J.; Gibot, L.; Rols, M.-P.; Balor, S.; Goudounèche, D.; Payré B.; Lonetti, B.; Vicendo, P.; Mingotaud, A.-F., Amphiphilic polymers based on polyoxazoline as relevant nanovectors for photodynamic therapy. *J. Mater. Chem. B* **2019**, *7* (32), 4973-4982.
116. Waschinski, C. J.; Tiller, J. C., Poly (oxazoline) s with telechelic antimicrobial functions. *Biomacromolecules* **2005**, *6* (1), 235-243.
117. Hahn, L.; Lübtow, M. M.; Lorson, T.; Schmitt, F.; Appelt-Menzel, A.; Schobert, R.; Luxenhofer, R., Investigating the Influence of Aromatic Moieties on the Formulation of Hydrophobic Natural Products and Drugs in Poly(2-oxazoline)-Based Amphiphiles. *Biomacromolecules* **2018**, *19* (7), 3119-3128.
118. Zahoranova, A.; Mrlik, M.; Tomanova, K.; Kronek, J.; Luxenhofer, R., ABA and BAB Triblock Copolymers Based on 2-Methyl-2-oxazoline and 2-n-Propyl-2-oxazoline: Synthesis and Thermoresponsive Behavior in Water. *Macromol. Chem. Phys.* **2017**, *218* (13).
119. Warne, N. M.; Finnegan, J. R.; Feeney, O. M.; Kempe, K., Using 2-isopropyl-2-oxazine to explore the effect of monomer distribution and polymer architecture on the thermoresponsive behavior of copolymers. *Journal of Polymer Science* **2021**, *59* (22), 2783-2796.
120. Cesana, S.; Auernheimer, J.; Jordan, R.; Kessler, H.; Nuyken, O., First Poly(2-oxazoline)s with Pendant Amino Groups. *Macromol. Chem. Phys.* **2006**, *207* (2), 183-192.
121. Biondi, O.; Motta, S.; Mosesso, P., Low molecular weight polyethylene glycol induces chromosome aberrations in Chinese hamster cells cultured in vitro. *Mutagenesis* **2002**, *17* (3), 261-264.
122. Bauer, M.; Lautenschlaeger, C.; Kempe, K.; Tauhardt, L.; Schubert, U. S.; Fischer, D., Poly (2 - ethyl - 2 - oxazoline) as Alternative for the Stealth Polymer Poly (ethylene glycol): Comparison of in vitro Cytotoxicity and Hemocompatibility. *Macromol. Biosci.* **2012**, *12* (7), 986-998.

123. Bauer, M.; Schroeder, S.; Tauhardt, L.; Kempe, K.; Schubert, U. S.; Fischer, D., In vitro hemocompatibility and cytotoxicity study of poly (2-methyl-2-oxazoline) for biomedical applications. *J. Polym. Sci., Part A: Polym. Chem.* **2013**, *51* (8), 1816-1821.
124. Kroneková, Z.; Mikulec, M.; Petrenčíková, N.; Paulovičová, E.; Paulovičová, L.; Jančinová, V.; Nosál', R.; Reddy, P. S.; Shimoga, G. D.; Chorvát Jr, D., Ex vivo and in vitro studies on the cytotoxicity and immunomodulative properties of poly (2-isopropenyl-2-oxazoline) as a new type of biomedical polymer. *Macromol. Biosci.* **2016**, *16* (8), 1200-1211.
125. Kronek, J.; Paulovičová, E.; Paulovičová, L.; Kroneková, Z.; Lustoň, J., Immunomodulatory efficiency of poly (2-oxazolines). *J. Mater. Sci. Mater. Med.* **2012**, *23* (6), 1457-1464.
126. Kronek, J.; Kroneková, Z.; Lustoň, J.; Paulovičová, E.; Paulovičová, L.; Mendrek, B., In vitro bio-immunological and cytotoxicity studies of poly(2-oxazolines). *J. Mater. Sci. Mater. Med.* **2011**, *22* (7), 1725-1734.
127. Kronek, J.; Lustoň, J.; Kroneková, Z.; Paulovičová, E.; Farkaš, P.; Petrenčíková, N.; Paulovičová, L.; Janigová, I., Synthesis and bioimmunological efficiency of poly(2-oxazolines) containing a free amino group. *J. Mater. Sci. Mater. Med.* **2010**, *21* (3), 879-886.
128. Le, Y.; Scott, M. D., Immunocamouflage: the biophysical basis of immunoprotection by grafted methoxypoly (ethylene glycol)(mPEG). *Acta biomaterialia* **2010**, *6* (7), 2631-2641.
129. Scott, M. D.; Murad, K. L.; Koumpouras, F.; Talbot, M.; Eaton, J. W., Chemical camouflage of antigenic determinants: stealth erythrocytes. *Proceedings of the national academy of sciences* **1997**, *94* (14), 7566-7571.
130. Murad, K. L.; Gosselin, E. J.; Eaton, J. W.; Scott, M. D., Stealth cells: prevention of major histocompatibility complex class II-mediated T-cell activation by cell surface modification. *Blood, The Journal of the American Society of Hematology* **1999**, *94* (6), 2135-2141.
131. Kylvik-Price, D. L.; Li, L.; Scott, M. D., Comparative efficacy of blood cell immunocamouflage by membrane grafting of methoxypoly (ethylene glycol) and polyethyloxazoline. *Biomaterials* **2014**, *35* (1), 412-422.
132. Goddard, P.; Hutchinson, L. E.; Brown, J.; Brookman, L. J., Soluble polymeric carriers for drug delivery. Part 2. Preparation and in vivo behaviour of N-acylthylenimine copolymers. *J. Controlled Release* **1989**, *10* (1), 5-16.
133. Gaertner, F. C.; Luxenhofer, R.; Blechert, B.; Jordan, R.; Essler, M., Synthesis, biodistribution and excretion of radiolabeled poly(2-alkyl-2-oxazoline)s. *J. Controlled Release* **2007**, *119* (3), 291-300.
134. Wyffels, L.; Verbrugghen, T.; Monnery, B. D.; Glassner, M.; Stroobants, S.; Hoogenboom, R.; Staelens, S., μ PET imaging of the pharmacokinetic behavior of medium and high molar mass ^{89}Zr -labeled poly (2-ethyl-2-oxazoline) in comparison to poly (ethylene glycol). *J. Controlled Release* **2016**, *235*, 63-71.
135. Simon, L.; Marcotte, N.; Devoisselle, J. M.; Begu, S.; Lapinte, V., Recent advances and prospects in nano drug delivery systems using lipopolyoxazolines. *Int. J. Pharm.* **2020**, *585*, 119536.
136. de Melo-Diogo, D.; Costa, E. C.; Alves, C. G.; Lima-Sousa, R.; Ferreira, P.; Louro, R. O.; Correia, I. J., POxylated graphene oxide nanomaterials for combination chemo-phototherapy of breast cancer cells. *Eur. J. Pharm. Biopharm.* **2018**, *131*, 162-169.
137. Restani, R. B.; Pires, R. F.; Tolmatcheva, A.; Cabral, R.; Baptista, P. V.; Fernandes, A. R.; Casimiro, T.; Bonifácio, V. D.; Aguiar - Ricardo, A., POxylated Dendrimer - Based Nano - in - Micro Dry Powder Formulations for Inhalation Chemotherapy. *ChemistryOpen* **2018**, *7* (10), 772-779.

138. Haas, D.; Hauptstein, N.; Dirauf, M.; Driessen, M. D.; Ruopp, M.; Schubert, U. S.; Lüthmann, T.; Meinel, L., Chemo-Enzymatic PEGylation/POxylation of Murine Interleukin-4. *Bioconjugate Chem.* **2022**, *33* (1), 97-104.
139. Moreadith, R. W.; Viegas, T. X.; Bentley, M. D.; Harris, J. M.; Fang, Z.; Yoon, K.; Dizman, B.; Weimer, R.; Rae, B. P.; Li, X.; Rader, C.; Standaert, D.; Olanow, W., Clinical development of a poly(2-oxazoline) (POZ) polymer therapeutic for the treatment of Parkinson's disease – Proof of concept of POZ as a versatile polymer platform for drug development in multiple therapeutic indications. *Eur. Polym. J.* **2017**, *88*, 524-552.
140. Bludau, H.; Czapar, A. E.; Pitek, A. S.; Shukla, S.; Jordan, R.; Steinmetz, N. F., POxylation as an alternative stealth coating for biomedical applications. *Eur. Polym. J.* **2017**, *88*, 679-688.
141. Tauhardt, L.; Kempe, K.; Gottschaldt, M.; Schubert, U. S., Poly (2-oxazoline) functionalized surfaces: from modification to application. *Chem. Soc. Rev.* **2013**, *42* (20), 7998-8011.
142. Fam, S. Y.; Chee, C. F.; Yong, C. Y.; Ho, K. L.; Mariatulqabtiah, A. R.; Tan, W. S., Stealth coating of nanoparticles in drug-delivery systems. *Nanomaterials* **2020**, *10* (4), 787.
143. McGary Jr., C. W., Degradation of poly(ethylene oxide). *Journal of Polymer Science* **1960**, *46* (147), 51-57.
144. Kumar, V.; Kalonia, D. S., Removal of peroxides in polyethylene glycols by vacuum drying: Implications in the stability of biotech and pharmaceutical formulations. *AAPS PharmSciTech* **2017**, *7* (3), 62.
145. Van Kuringen, H. P. C.; Lenoir, J.; Adriaens, E.; Bender, J.; De Geest, B. G.; Hoogenboom, R., Partial Hydrolysis of Poly(2-ethyl-2-oxazoline) and Potential Implications for Biomedical Applications? *Macromol. Biosci.* **2012**, *12* (8), 1114-1123.
146. Konradi, R.; Acikgoz, C.; Textor, M., Polyoxazolines for nonfouling surface coatings—a direct comparison to the gold standard PEG. *Macromol. Rapid Commun.* **2012**, *33* (19), 1663-1676.
147. Ulbricht, J.; Jordan, R.; Luxenhofer, R., On the biodegradability of polyethylene glycol, polypeptoids and poly(2-oxazoline)s. *Biomaterials* **2014**, *35* (17), 4848-4861.
148. Hermes, R.; Mathias, L., A new chiral peptide analog: Synthesis and characterization of poly [4 (S)-2-propyl-4-methoxycarbonyl-2-oxazoline]. *Journal of Polymer Science Part C: Polymer Letters* **1987**, *25* (4), 161-167.
149. Chengpei, W.; Guang, Y.; Caiyuan, P., Synthesis and ring-opening polymerization of optically active 4(S)-2-methyl-4-methoxycarbonyl-2-oxazoline. *Journal of University of Science and Technology of China* **1991**, *21* (2), 198-204.
150. Oh, Y. S.; Yamazaki, T.; Goodman, M., Syntheses and circular dichroism (CD) spectra of optically active polyoxazolines and their model compounds. *Macromolecules* **1992**, *25* (23), 6322-6331.
151. Lambert, R. F.; Thompson, G.; Kristofferson, C. E., Formation of 2-Propyl-5-methyl- and 2-Propyl-4-methyl- Δ^2 -oxazolines from the Thermal Decomposition of Phosphoric Amides Derived from 1-Amino-2-propyl and 2-Amino-1-propyl Butyrates. *J. Org. Chem.* **1964**, *29* (10), 3116-3118.
152. Lübtow, M. M.; Hahn, L.; Haider, M. S.; Luxenhofer, R., Drug Specificity, Synergy and Antagonism in Ultrahigh Capacity Poly(2-oxazoline)/Poly(2-oxazine) based Formulations. *J. Am. Chem. Soc.* **2017**, *139* (32), 10980-10983.
153. Hoogenboom, R.; Schlaad, H., Thermoresponsive poly (2-oxazoline) s, polypeptoids, and polypeptides. *Polym. Chem.* **2017**, *8* (1), 24-40.
154. Lorson, T.; Jaksch, S.; Lübtow, M. M.; Jungst, T.; Groll, J.; Luhmann, T.; Luxenhofer, R., A Thermogelling Supramolecular Hydrogel with Sponge-Like Morphology as a Cytocompatible Bioink. *Biomacromolecules* **2017**, *18* (7), 2161-2171.

155. Bloksma, M. M.; Paulus, R. M.; van Kuringen, H. P. C.; van der Woerd, F.; Lambermont-Thijs, H. M. L.; Schubert, U. S.; Hoogenboom, R., Thermoresponsive poly(2-oxazine)s. *Macromol. Rapid Commun.* **2012**, *33* (1), 92-96.
156. Christova, D.; Velichkova, R.; Loos, W.; Goethals, E. J.; Prez, F. D., New thermo-responsive polymer materials based on poly(2-ethyl-2-oxazoline) segments. *Polymer* **2003**, *44* (8), 2255-2261.
157. Hoogenboom, R.; Thijs, H. M. L.; Jochems, M.; van Lankvelt, B. M.; Fijten, M. W. M.; Schubert, U. S., Tuning the LCST of poly(2-oxazoline)s by varying composition and molecular weight: alternatives to poly(N-isopropylacrylamide)? *Chem. Commun.* **2008**, (44), 5758-5760.
158. Pérez-Trujillo, M.; Monteagudo, E.; Parella, T., ¹³C NMR spectroscopy for the differentiation of enantiomers using chiral solvating agents. *Anal. Chem.* **2013**, *85* (22), 10887-10894.
159. Wacker, A.; Weigand, J. E.; Akabayov, S. R.; Altincekic, N.; Bains, J. K.; Banijamali, E.; Binas, O.; Castillo-Martinez, J.; Cetiner, E.; Ceylan, B., Secondary structure determination of conserved SARS-CoV-2 RNA elements by NMR spectroscopy. *Nucleic Acids Res.* **2020**, *48* (22), 12415-12435.
160. Cavalli, A.; Salvatella, X.; Dobson, C. M.; Vendruscolo, M., Protein structure determination from NMR chemical shifts. *Proceedings of the National Academy of Sciences* **2007**, *104* (23), 9615-9620.
161. Hoogenboom, R.; Fijten, M. W. M.; Thijs, H. M. L.; Van Lankvelt, B. M.; Schubert, U. S., Microwave-assisted synthesis and properties of a series of poly(2-alkyl-2-oxazoline)s. *Des. Monomers Polym.* **2005**, *8* (6), 659-671.
162. Jing, C.; Suzuki, Y.; Matsumoto, A., Thermal decomposition of methacrylate polymers containing tert-butoxycarbonyl moiety. *Polym. Degrad. Stab.* **2019**, *166*, 145-154.
163. Lübtow, M. M.; Kessler, L.; Appelt-Menzel, A.; Lorson, T.; Gangloff, N.; Kirsch, M.; Dahms, S.; Luxenhofer, R., More Is Sometimes Less: Curcumin and Paclitaxel Formulations Using Poly(2-oxazoline) and Poly(2-oxazine)-Based Amphiphiles Bearing Linear and Branched C9 Side Chains. *Macromol. Biosci.* **2018**, *18* (11), 1800155.
164. Wiesbrock, F.; Hoogenboom, R.; Leenen, M.; van Nispen, S.; van der Loop, M.; Abeln, C. H.; van den Berg, A. M. J.; Schubert, U. S., Microwave-assisted synthesis of a 4(2)-membered library of diblock copoly(2-oxazoline)s and chain-extended homo poly(2-oxazoline)s and their thermal characterization. *Macromolecules* **2005**, *38* (19), 7957-7966.
165. Rettler, E. F. J.; Kranenburg, J. M.; Lambermont - Thijs, H. M.; Hoogenboom, R.; Schubert, U. S., Thermal, mechanical, and surface properties of poly (2-N-alkyl-2-oxazoline) s. *Macromol. Chem. Phys.* **2010**, *211* (22), 2443-2448.
166. Singh, M. K.; Singh, A., Chapter 9 - Thermal characterization of materials using differential scanning calorimeter. In *Characterization of polymers and fibres*, Singh, M. K.; Singh, A., Eds. Woodhead Publishing: 2022; pp 201-222.
167. Shrivastava, A., 1 - Introduction to Plastics Engineering. In *Introduction to Plastics Engineering*, Shrivastava, A., Ed. William Andrew Publishing: 2018; pp 1-16.
168. Haider, M. S.; Lübtow, M. M.; Endres, S.; Forster, S.; Flegler, V. J.; Böttcher, B.; Aseyev, V. O.; Pöppler, A.-C.; Luxenhofer, R., Think beyond the core: The impact of the hydrophilic corona on the drug solubilization using polymer micelles. *ACS Appl. Mater. Inter.* **2020**, *12* (22), 24531-24543.
169. Güner, P. T.; Miko, A.; Schweinberger, F. F.; Demirel, A. L., Self-assembled poly (2-ethyl-2-oxazoline) fibers in aqueous solutions. *Polym. Chem.* **2012**, *3* (2), 322-324.
170. Eliel, E. L.; Wilen, S. H., *Stereochemistry of organic compounds*. John Wiley & Sons: 1994.

171. Parrish, J. R.; Blout, E. R., Spectroscopic studies of random chain and α - helical polypeptides in hexafluoroisopropanol. *Biopolymers* **1971**, *10* (9), 1491-1512.
172. Wang, Y.; Fang, H. X.; Tranca, I.; Qu, H.; Wang, X. C.; Markvoort, A. J.; Tian, Z. Q.; Cao, X. Y., Elucidation of the origin of chiral amplification in discrete molecular polyhedra. *Nature Communications* **2018**, *9*.
173. Lübtow, M. M.; Nelke, L. C.; Seifert, J.; Kuhnemundt, J.; Sahay, G.; Dandekar, G.; Nietzer, S. L.; Luxenhofer, R., Drug induced micellization into ultra-high capacity and stable curcumin nanoformulations: Physico-chemical characterization and evaluation in 2D and 3D in vitro models. *J. Controlled Release* **2019**, *303*, 162-180.
174. Lübtow, M. M.; Haider, M. S.; Kirsch, M.; Klisch, S.; Luxenhofer, R., Like Dissolves Like? A Comprehensive Evaluation of Partial Solubility Parameters to Predict Polymer-Drug Compatibility in Ultrahigh Drug-Loaded Polymer Micelles. *Biomacromolecules* **2019**, *20* (8), 3041-3056.
175. Jordan, M. A.; Wilson, L., Microtubules as a target for anticancer drugs. *Nat. Rev. Cancer* **2004**, *4* (4), 253-265.
176. Ma, P.; Mumper, R. J., Paclitaxel nano-delivery systems: a comprehensive review. *Journal of nanomedicine & nanotechnology* **2013**, *4* (2), 1000164.
177. Aggarwal, B. B.; Kumar, A.; Bharti, A. C., Anticancer potential of curcumin: preclinical and clinical studies. *Anticancer Res.* **2003**, *23* (1/A), 363-398.
178. Das, U. N., Molecular Mechanisms of Action of Curcumin and Its Relevance to Some Clinical Conditions. In *Curcumin for Neurological and Psychiatric Disorders*, Elsevier: 2019; pp 325-332.
179. Jagannathan, R.; Abraham, P. M.; Poddar, P., Temperature-dependent spectroscopic evidences of curcumin in aqueous medium: a mechanistic study of its solubility and stability. *J. Phys. Chem. B* **2012**, *116* (50), 14533-14540.
180. Baell, J.; Walters, M. A., Chemistry: Chemical con artists foil drug discovery. *Nature News* **2014**, *513* (7519), 481.
181. Baell, J. B., Feeling nature's PAINS: natural products, natural product drugs, and pan assay interference compounds (PAINS). *J. Nat. Prod.* **2016**, *79* (3), 616-628.
182. Alavi, M.; Nokhodchi, A., Micro- and nanoformulations of paclitaxel based on micelles, liposomes, cubosomes, and lipid nanoparticles: Recent advances and challenges. *Drug Discovery Today* **2021**.
183. Stohs, S. J.; Chen, O.; Ray, S. D.; Ji, J.; Bucci, L. R.; Preuss, H. G., Highly bioavailable forms of curcumin and promising avenues for curcumin-based research and application: A review. *Molecules* **2020**, *25* (6), 1397.
184. Jamwal, R., Bioavailable curcumin formulations: A review of pharmacokinetic studies in healthy volunteers. *Journal of Integrative Medicine* **2018**, *16* (6), 367-374.
185. He, Z. J.; Wan, X. M.; Schulz, A.; Bludau, H.; Dobrovolskaia, M. A.; Stern, S. T.; Montgomery, S. A.; Yuan, H.; Li, Z. B.; Alakhova, D.; Sokolsky, M.; Darr, D. B.; Perou, C. M.; Jordan, R.; Luxenhofer, R.; Kabanov, A. V., A high capacity polymeric micelle of paclitaxel: Implication of high dose drug therapy to safety and in vivo anti-cancer activity. *Biomaterials* **2016**, *101*, 296-309.
186. Lübtow, M. M.; Oerter, S.; Quader, S.; Jeanclos, E.; Cubukova, A.; Krafft, M.; Haider, M. S.; Schulte, C.; Meier, L.; Rist, M.; Sampetean, O.; Kinoh, H.; Gohla, A.; Kataoka, K.; Appelt-Menzel, A.; Luxenhofer, R., In Vitro Blood-Brain Barrier Permeability and Cytotoxicity of an Atorvastatin-Loaded Nanoformulation Against Glioblastoma in 2D and 3D Models. *Mol. Pharm.* **2020**, *17* (6), 1835-1847.
187. Luxenhofer, R.; Schulz, A.; Roques, C.; Li, S.; Bronich, T. K.; Batrakova, E. V.; Jordan, R.; Kabanov, A. V., Doubly amphiphilic poly(2-oxazoline)s as high-capacity delivery systems for hydrophobic drugs. *Biomaterials* **2010**, *31* (18), 4972-4979.

188. Marzo, A.; Heftmann, E., Enantioselective analytical methods in pharmacokinetics with specific reference to genetic polymorphic metabolism. *J. Biochem. Bioph. Methods* **2002**, *54* (1-3), 57-70.
189. Jamali, F., Pharmacokinetics of enantiomers of chiral non-steroidal anti-inflammatory drugs. *Eur. J. Drug Metab. Pharmacokinet.* **1988**, *13* (1), 1-9.
190. Yalkowsky, S. H.; Dannenfelser, R. M., Aquasol database of aqueous solubility. *College of Pharmacy, University of Arizona, Tucson, AZ* **1992**, 189.
191. Lim, C.; Ramsey, J. D.; Hwang, D.; Teixeira, S. C. M.; Poon, C.-D.; Strauss, J. D.; Rosen, E. P.; Sokolsky-Papkov, M.; Kabanov, A. V., Drug-Dependent Morphological Transitions in Spherical and Worm-Like Polymeric Micelles Define Stability and Pharmacological Performance of Micellar Drugs. *Small* **2022**, *18* (4), 2103552.
192. Sarp, G.; Yilmaz, E., A flower-like hybrid material composed of Fe₃O₄, graphene oxide and CdSe nanodots for magnetic solid phase extraction of ibuprofen prior to its quantification by HPLC detection. *Microchim. Acta* **2019**, 186 (11).
193. Magiera, S.; Piwowarczyk, A.; Wegrzyn, A., A study of the enantiospecific degradation of ibuprofen in model aqueous samples using LLME-HPLC- DAD. *Anal. Methods* **2016**, *8* (43), 7789-7799.
194. Ingram, M. J.; Moynihan, H. A.; Powell, M. W.; Rostron, C., Synthesis and hydrolytic behaviour of glycerol-1,2-diibuprofenate-3-nitrate, a putative pro-drug of ibuprofen and glycerol-1-nitrate. *J. Pharm. Pharmacol.* **2001**, *53* (3), 345-350.
195. Kalyanasundaram, K.; Thomas, J. K., Environmental effects on vibronic band intensities in pyrene monomer fluorescence and their application in studies of micellar systems. *J. Am. Chem. Soc.* **1977**, *99* (7), 2039-2044.

Affidavit

I hereby confirm that my thesis entitled “Synthesis, solubility and optical activity of chiral poly(2,4-disubstituted-2-oxazoline)s” is the result of my own work. I did not receive any help or support from commercial consultants. All sources and / or materials applied are listed and specified in the thesis.

Furthermore, I confirm that this thesis has not yet been submitted as part of another examination process neither in identical nor in similar form.

Place, Date

Signature

Eidesstattliche Erklärung

Hiermit erkläre ich an Eides statt, die Dissertation „Synthese, Löslichkeit und optische Aktivität von chiralen Poly(2,4-disubstituierten-2-oxazolin)en“ eigenständig, d.h. insbesondere selbstständig und ohne Hilfe eines kommerziellen Promotionsberaters, angefertigt und keine anderen als die von mir angegebenen Quellen und Hilfsmittel verwendet zu haben.

Ich erkläre außerdem, dass die Dissertation weder in gleicher noch in ähnlicher Form bereits in einem anderen Prüfungsverfahren vorgelegen hat.

Ort, Datum

Unterschrift

Curriculum Vitae

PERSONAL INFORMATION:

Birth Date: January 3, 1992

Citizenship: P. R. China

Gender: Female

ACADEMIC EDUCATION:

Since 10/2017

Doctoral thesis

Julius-Maximilians-Universität Würzburg, Würzburg, Germany

Graduate School of Science and Technology (GSST)

Focus: Polymer chemistry

Supervisor: Prof. Dr. Robert Luxenhofer

Thesis topic: "Synthesis, solubility and optical activity of chiral poly(2,4-disubstituted-2-oxazoline)s"

09/2014 - 03/2017

Master

Donghua University, Shanghai, China

College of Material Science and Engineering

Focus: Chemistry

Supervisor: Prof. Dr. Zhilong Chen

Master thesis topic: "Preparation and targeted delivery of TPGS nanoparticle loaded with verteporfin and functionalized with tLyp-1 peptide in photodynamic therapy"

09/2010 - 06/2014

Bachelor

Zhejiang A & F University, Zhejiang, China

School of Engineering

Focus: Polymer material and engineering

Supervisor: Jiewang Ye

Bachelor thesis topic: "Size effect of silk fibroin peptide chains in growth process"

SCIENTIFIC ACTIVITY & AWARDS:

- 11/2018 6th GALENUS-Workshop 2018 - Development & Translation of Bioresponsive Drug Delivery Systems and Medical Devices
- 05/2019 5th Euro BioMAT 2019 - European Symposium and Exhibition on Biomaterials and Related Areas (Poster)
- 02/2020 CRS Local Chapter Meeting 2020 - Delivery and Formulation of Biologics (Poster)
- 05/2020 Explain My Research: Drug Delivery & Precision Medicine, 2020 (virtual)
- 09/2020 1st Virtual European Polymer Conference, 2020 (virtual)
- 07/2022 Ophthalmological Conference, Oculoplasty - Cornea - Glaucoma, the University Eye Clinic in Würzburg

Signature